PRELIMINARY SEISMIC TESTS TO DETECT THE PRESENCE OF AIR IN A SEMI-CONFINED AQUIFER

by

Richard D. Miller
Don W. Steeples
Randie L. Grantham
Mubarik Ali
Dean A. Keiswetter
Joe M. Anderson
John M. Healey
Brett C. Bennett
Fabian T. Wirnkar

of the

Kansas Geological Survey
The University of Kansas,
Lawrence, Kansas 44047

A PRELIMINARY REPORT TO THE
U.S. ENVIRONMENTAL PROTECTION AGENCY
ENVIRONMENTAL MONITORING SYSTEMS LABORATORY
LAS VEGAS, NEVADA

June 1, 1990

Open-file Report 90-16

INTRODUCTION

Shallow seismic reflection has been used in a variety of geologic and hydrologic settings to detect, delineate, and differentiate subsurface targets. Detailed information about properties of subsurface materials has generally come from extensive drilling programs. In resent years, the use of seismic reflection has become an increasingly popular way to study the shallow (less than 30 m) subsurface (Doornenbal and Helbig, 1983; Hunter et al., 1984; Steeples and Miller, 1990). This report describes attempts to seismically detect the presence of air injected under pressure into a shallow semi-confined aquifer in an alluvial setting.

Seismic detection of confined air (gas) in the subsurface could potentially have application to a variety of engineering, hydrologic, and petroleum problems. Some of these problems include: methane plums associated with landfills, preferential flow in hydrocarbon reserves (permeability mapping), and quantification of hydrologic characteristics. Injection of gas into a normally fluid-filled solid matrix (cemented or uncemented) could seismically appear as:

1) a delay in apparent arrival time of reflections from interfaces beneath the gas-filled layer (indicative of a decrease in the apparent average velocity above the reflecting interface),
2) direct reflection from the top of the trapped gas,
3) reflection amplitude anomaly (bright spot) associated with the gas confining layer (in this case the base of the clay),
4) reduction in apparent velocity of non-reflection seismic energy (i.e., lower surface waves or refractions),
5) changes in phase or frequency of seismic energy with travel paths that intersect or come in contact with the confined air volume, or
6) any of multiple combinations of the above.

PRELIMINARY AIR INJECTION STUDIES

Initial experiments to determine the feasibility of the injection process were carried out at two test sites within the Kansas River Valley near Lawrence, Kansas (Figure 1). Compressed air was injected into a shallow (20 ft) aquifer semi-confined by a relatively impermeable clay layer extending from about 23 ft to within 5-8 ft of the ground surface. The purpose of the initial injection experiments was to determine if a stable, relatively uniform volume of air could be generated and contained within several tens of feet of a shallow injection well.

Three wells were initially installed at each of the two sites (Figure 1). One was installed as an injection well; the other two were installed as monitor wells. The injection well was screened over an 8 ft interval beginning approximately 10 ft below the base of the clay. The monitor wells were screened over an 8 ft interval starting at the base of the clay and were at 90 degrees with respect to and 25 ft from the injection well. The well construction was designed to maximize the potential to identify and quantify draw-down, or in this case, push-down from the injection of air.

Preliminary injection of air at volume rates of between 20 cfm (at 90 psi) and 185 cfm (at 120 psi) resulted in total water evacuation of the monitor wells in less than 30 min. Stable air pressures of between approximately 10-13 psi were observed in both monitor wells less than 2 hours after commencing the injection of air regardless of the instantaneous input volume.

Interpolating water-level measurements between monitor wells and the injection well, before and after air injection, suggests a locally uniform subsurface model for the air/water contact beneath the confining clay layer. If interpolation between wells is valid in this case, a relatively large, locally well-confined volume of air can be generated and maintained over a period of time sufficient to investigate induced physical property changes with surface seismic techniques.

BACKGROUND INVESTIGATIONS

Extensive tests to determine critical near-surface characteristics and evaluation techniques were completed prior to initiation of the primary 6-weeks-long experiment (Appendix A). All significant geologic, hydrologic, and geophysical data for the study area were compiled and documented as background information over a 9-month period prior to the primary experiment.

The background geophysical work included several CDP lines and walkaway noise tests, comparing several different sources, receivers, and seismograph settings (analog filter and fixed gain). Also tested was the significance of subtle variations in the ground surface condition and the seismic importance of quantity and duration of air injection. These series of geophysical tests were designed and carried out to determine which physical conditions, properties, and acquisition parameters were most significant, and how each affected the recorded information.

Instantaneous air velocity is a critical parameter. Detection of injected air was not possible with low (20-50 cfm) velocity compressors used over extended periods of time. High velocity compressors (185 cfm) over much shorter times were capable of generating seismically detectable changes in the physical properties of the alluvial materials.

Consistency in source time break and wavelet characteristics is necessary to produce comparable sections (Appendix A). Drastic differences in arrival times and spectral characteristics can be observed on individual shot records from repeated projectile firings in the same shot hole. Each repeated projectile fired into a single hole creates different shot-hole conditions for the next projectile. Subtle changes in body-wave characteristics and arrival times can result from inconsistency in the acquisition techniques.

PRIMARY EXPERIMENT DESIGN

The intent of the primary experiment was to determine if by any seismic means it is possible to detect the presence of air injected into a semi-confined aquifer at this site. Long term (for the duration of the experiment) placement of receivers between the injection well and the two in-line monitor wells was necessary to maintain optimum consistency in comparative data sets (Figure 1). A series of tests shots (walkaway noise tests) recorded prior to beginning the injection of air were classified as "normal" for this site (Figures 2 and 3).

A 24-channel Input/Output DHR 2400 seismograph recorded all the data from this experiment on half-inch magnetic tape in modified SEG-Y format. The record length was 125 ms with a sampling interval of 0.25 ms. Analog-to-digital (A/D) conversion was 11 bits plus sign. The adjustable fixed-gain amplifiers have a factory noise specification of 120 nanovolts RMS.

Acquisition parameters were determined during a series of pre-injection tests performed the first day of the primary experiment. The parameters (and variations of) included analog low-cut filter settings (220 and 340 Hz at 24 dB/octave rolloff), projectile sources (.30-06 downhole gun and .50-caliber downhole gun), 48 geophone station locations (2-100 Hz L-40A geophones connected in series at each station location), and two source locations (each 30 inch holes, located 2 ft and 50 ft from the nearest geophone station). This group of field parameters and associated key variations were determined during preliminary testing.

Source-to-receiver offsets and receiver spacing were determined using the optimum window technique (Hunter et al ,1984). The walkaway spreads were designed to primarily target reflection from the bedrock/alluvial interface, with reflections from intra-alluvial interfaces a secondary priority. The optimum recording window for the bedrock reflection ranges between 14 to 90 ft. A receiver-station interval of 1 ft was necessary to maintain trace-to-trace coherency on the bedrock reflection. Data were acquired at two different source-to-nearest-receiver offsets (2 ft and 50 ft) in a series of off-line shotholes equally spaced from the first live receiver. The combined walkaway spread length for both shot locations is 96 ft with 96 source-to-receiver offsets ranging from 2 to 98 ft.

Consistency was the primary criteria during the recording procedure. Test holes, one at each source location, served as an amplifier calibration hole for various analog filter, source, and offset configurations. Each source, offset, and filter configuration was assigned a set of 24 amplification values. This set of amplification values was used each time the appropriate recording configuration was tested. Two shot holes, one for each source, were drilled equal distance from the first receiver station at both shot locations. The predetermined firing sequence maintained for all walkaways, was shot hole to shot hole consistent with respect to repeat shot number, analog filter setting, and source-to-nearest-receiver distance. Shot holes used for comparison walkaways throughout the 6-weeks-long test were drilled on an as-need basis to maintain consistent downhole conditions.

The receiver locations were established and the geophones were securely planted prior to beginning and for the duration of the primary experiment. The receivers, single 100-Hz Mark Products geophones with 14 cm spikes, characteristically attenuate energy below 100 Hz (6 dB/octave) while maintaining a flat response to energy at frequencies up to 1000 Hz. Two geophones in a one-foot perpendicular receiver array occupied each of the 48 receiver stations. The receiver stations were on one-foot centers allowing single walkaway spread lengths of 47 ft per shot location.

The design and configuration of the wells used for air injection and monitoring during the primary experiment were similar to previously described preliminary air injection studies. One injection well (2-1) and four monitor wells (2-2, 2-3, 2-4, and 1-3) were active during the primary experiment (Figure 1). A constant pressure of 75 psi was maintained at the injection well head throughout the 5 day injection period. Monitor wells 2-2, 2-3, and 2-4 detected the presence of the air approximately 20 minutes after the initiation of the air-injection process. Monitor well 1-3 located at site 1 never detected a variation in downhole pressure during the entire 6-weeks experiment. Monitor wells 2-2, 2-3, and 2-4 were eventually evacuated of water and stable pressures of approximately 13 psi were measured at the well heads within 2 hours of the initiation of injection process.

The air-injection process was terminated after 5 days of continuous operation. Upon termination of air injection, the injection well was capped and periodic monitoring of well head pressures continued. The same set of walkaway noise tests (consistent with pre-injection seismic recording conditions and parameters) were run at the time air injection was terminated (5 days) and then once a week (weather permitting) until either pre-injection pressures and/or velocities were observed. Walkaway noise tests were the only recording technique used during this primary experiment.

PRIMARY EXPERIMENT DATA RESULTS

Source-to-receiver offsets and the receiver station interval for walkaway-noise tests were chosen to maximize recorded reflection information from the alluvial/bedrock interface at a depth of approximately 60 ft. Non-reflection seismic energy was not directly considered during the initial selection of recording geometries.

Instability in the time-break system required subtle relative adjustment of entire field files. The time-break system consisted of a transducer attached to the gun source which utilized the recoil of the gun to initialize the recording system. Lack of consistent recoil, precision in the transducer, and consistent changes in shot-hole depths resulted in time break variability, in some cases of as much as 4 ms. To allow direct comparison of walkaways regardless of the recording configuration, time zero of each field file was adjusted using the arrival of the air wave at the first and last recorded station. All walkaways displayed and analyzed were adjusted for variations in the time-break system.

Shot static and dissimular downhole conditions associated with the different source locations inhibited combining simular sets of 48 channel walkaways-noise tests into a single 96-channel walkaway. Variabiilty in the near-surface conditions in an alluvial setting can drastically affect wavelet phase, frequency, first-break arrival time (due to localized velocity anomalies), and amplitude characteristics of seismic data. Walkaway-noise tests are grouped according to no only source and acquisition data but also source location as a result of this mismatch in seismic characteristics.

Walkaway-noise spreads collected prior to the injection of air (April 4, 1990) are considered "normal" for the test area (Figures 2 and 3). Several reflection events can be interpreted directly from unprocessed common shot gathers. Reflections can be traced to source-to-receiver offsets of less than 12 ft on .50-caliber walkaways. Reflection energy observed on the 50-caliber walkaways not present on comparable .30-06 walkaways are probably indicative of total source energy. Reflections on both the .50-caliber and .30-06 data sets are most easily identified at times greater than 50 ms and offsets greater than 25 ft. Reflection depths and NMO velocities cannot be accurately calculated for the reflection events. Inability to estimate reflector depths and velocities on data collected prior to the injection of air is due to a variable near-surface and/or dip on the bedrock surface and lack of longer offset traces.

It is not possible to correlate identifiable pre-injection to post-injection reflection energy (Figures 2 and 3). Reflection information, if present on field files after air injection cannot be confidently differentiated from coherent noise. Most of the coherent noise possesses an apparent linear slope approximately equivalent to the refraction arrivals (first breaks). Relative decrease in the NMO velocity and relative increase in arrival time of reflection events was anticipated to be the most probable seismic characteristics to vary as a result of the injection of air. Lack of correlatable reflection energy eliminates relative comparisons of the bedrock reflection arrival time and NMO velocity pre versus post air injection.

Quality non-reflection body wave information is present on the pre-injection walkaways (Figures 2 and 3). Refraction and direct wave energy interpreted as first breaks, can be represented classically as a two layer case. The apparent depth to the refracting interface (using non-reversed refraction data) is approximately 7 ft with a direct wave velocity of approximately 1300 ft/s and an apparent refraction velocity of approximately 7300 ft/s (Figures 4 and 5).

The apparent velocity of refracted energy from the top of the confining clay layer dropped by about 40 percent immediately after the termination of the air-injection process (Figures 4 and 5) (Table 1). After the initial drop in velocity, a gradual increase in the apparent refraction velocities was observed on walkaways acquired on approximately a weekly basis following termination of air injection. Six weeks after the termination of the air-injection process, 5-6 psi air pressure was measured at the well heads and the apparent refraction velocity had returned to within 20 percent of the normal apparent refraction velocity (Table 1).

Dominant frequency of body-wave energy decreased by 25 percent after air injection in comparison to before on both the .50 caliber and the .30-06 rifle data sets (Figures 6 and 7). The spikes on pre-air spectra at approximately 220 Hz and 190 Hz are interpreted as air-wave and body-wave energy, respectively. On post-air spectra relative increases in energy (with respect to the air wave) and decreases in frequency of body-waves are attributed to the presence of air in the subsurface. On post-air spectra, body waves represent the highest amplitude energy with dominant frequencies of approximately 140 Hz. The 220 Hz low-cut filter effectively attenuated most of the surface-wave energy. Spectra of seismograms acquired before the injection of air are significantly different in comparison to post-air injected spectra.

The presence of air in the subsurface altered wavelet characteristics and phase velocities of coherent seismic energy. Comparison of seismograms acquired before the injection of air to seismograms acquired after air injection discloses approximately 3,000 ft/s change in apparent linear velocities of energy recorded between the refractions and the air wave. Frequency and phase changes in seismic wavelets are most noticeable in the body-wave arrivals. The refraction wavelet possesses at least three complete cycles on pre-air files and less than two complete cycles on the post-air files (Figures 2 and 3). Changes in the wavelet phase are sufficiently great that phase-angle variations are not meaningful. The bandwidth and apparent phase velocity of linear events are sensitive to the presence of air in the subsurface.

After completing the monitoring of the subsurface air, all the well-head caps were removed releasing air still contained in the subsurface after more than 6 weeks. Well-head pressures were less than 6 psi at the time the caps were removed. Upon removal of the caps air mixed with sand and water blew out of the cased holes in excess of 10 ft in the air for more than 15 minutes. After a time period of approximately 25 minutes, only two wells (2-3 and 2-1) continued to discharge the air, sand, and water mix. This preferential discharge may be indicative of localized porosity, variablity in grain size, or problems related to the slots in the screened area of the casing.

DISCUSSION

Seismic energy is sensitive to the presence of gas in the subsurface. A gas bubble can be sustained in the subsurface at this site in excess of six weeks. Alteration of physical properties of materials at this site were detected as shallow as approximately 7 ft. From a classic wave theory point of view the contact between the top of the clay and sand/soil represents the refracting horizon responsible for the refraction arrivals altered by the presence of air in the subsurface. Alteration of the physical properties of the clay at the sand/soil interface by the injected air would require penetration of the nonpermiable, yet porous semi-confining clay layer by the injected air. Since the static water table is at approximately 20 ft, changes in material properties at 8 ft of depth cannot totally be the result of water-table pushdown (drawdown). The injected air must have altered pore space in the clay resulting in drastic changes in Lame constants.

CONCLUSION AND RECOMMENDATIONS

Gas injected into the subsurface does sufficiently alter the physical properties of materials at this site to allow detection with surface seismic techniques. Refraction phase velocities are sensitive to and require very little subjectivity detecting the presence of air in the subsurface. Reflection information identifiable on the pre-air data sets could not be confidently interpreted on post-air data sets. The presence of air at this site resulted in a 40 percent drop in apparent refraction velocities. Over a six-week period, the apparent refraction velocity returned to 80 percent of the normal apparent refraction velocity. Consistency in the acquisition phase of this experiment was essential to obtaining comparable pre- and post-air injection data sets.

To determine what part the moisture content of the clay is playing in the alteration of the compressional wave velocity of the clay, a neutron log needs to be acquired coincident with the walkaway noise tests. A second injection test should also include longer offset refraction fan shoots. Targeting refraction from the top of the clay, the base of the clay, and the bedrock surface. A second injection experiment targeting moisture content as the most likely cause of the variability in the apparent refraction velocity would resolve many of the unknowns generated by this study.

REFERENCES

Doornenbal, J. C., and Helbig, K., 1983, High-resolution reflection seismics on a tidal flat in the Dutch Delta-acquisition, processing, and interpretation: First Break, May, 9-20.

Hunter , J. A., Pullan, S. E., Burns, R. A., Gagne, R. M., and Good, R. L., 1984, Shallow seismic-reflection mapping of the overburden-bedrock interface with the engineering seismograph—some simple techniques: Geophysics, 49, 1381-1385.

Steeples, D. W., and Miller, R. D, 1990, Seismic-reflection methods applied to engineering, environmental, and ground-water problems: Soc. Explor. Geophys. volume on Environmental Geophysics, Stan Ward, ed., in press.

TABLE CAPTIONS

Table 1. Direct wave and apparent refraction velocities for both sources at various times before, during, and after the injection of air are recorded. The underlined values represent seismic data displayed in Figures 2, 3, 4, and 5. Lack of values on lines with no data indicated could be the result of either to much wind noise, airplane noise, or machanical problems with the source.

Table 2. Pressure values are classified according to data and well locations. Two well heads had working pressure gauges.

TABLE 1

	V_o		V_1		V_2	
	.30-06	.50	.30-06	.50	.30-06	.50
4/4	1250	1310	7050	7630	6910	7830
4/6	no data	1410	3750	3960	no data	
4/9	1210	1420	4010	4210	3790	3920
4/19	1290	no data	4560	no data	5110	no data
5/1	1250	1330	4420	5770	no data	5880
5/18	1380	1360	5230	5750	no data	5750
5/23	1220	1250	no data	6390	no data	7190

TABLE 2

PRESSURE

	Pressure	
Day	South	West
4/4	16	?
4/5	12	13
4/6	12	13
4/7	12	13
4/8	12	13
4/9	12	13
4/10	8	13
4/11	8	6
4/12	8	9
4/16	8	8
4/17	8	9
4/18	8	9
4/19	7	9
4/24	7	9
4/25	7	8
4/28	7	7
5/1	7	7
5/8	5	5
5/18	5	5
5/23	5	5

FIGURE CAPTIONS

Figure 1. Site map indicating significant surface geology, test sites, well orientations, and an average geologic cross-section generated from samples acquired during well installation.

Figure 2. .30-06 downhole walkaway-noise tests from two different source locations and collected at three different times.

Figure 3. .50-caliber downhole walkaway-noise tests from two different source locations and collected at three different times.

Figure 4. .30-06 downhole walkaway-noise tests as Figure 2 with interpretations of the direct and refracted arrivals. The apparent linear velocity of the first-break energy is identified with a line that correlates to either V_o, V_1, or V_2 which are defined in Table 1.

Figure 5. .50-caliber downhole walkaway-noise tests as Figure 3 with interpretations of the direct and refracted arrivals. The apparent linear velocity of the first-break energy is identified with a line that correlates to either V_o, V_1, or V_2 which are defined in Table 1.

Figure 6. A comparison of amplitude vs frequency spectrum for .30-06 downhole data before and after the injection of air.

Figure 7. A comparison of amplitude vs frequency spectrum for .50-caliber downhole data before and after the injection of air.

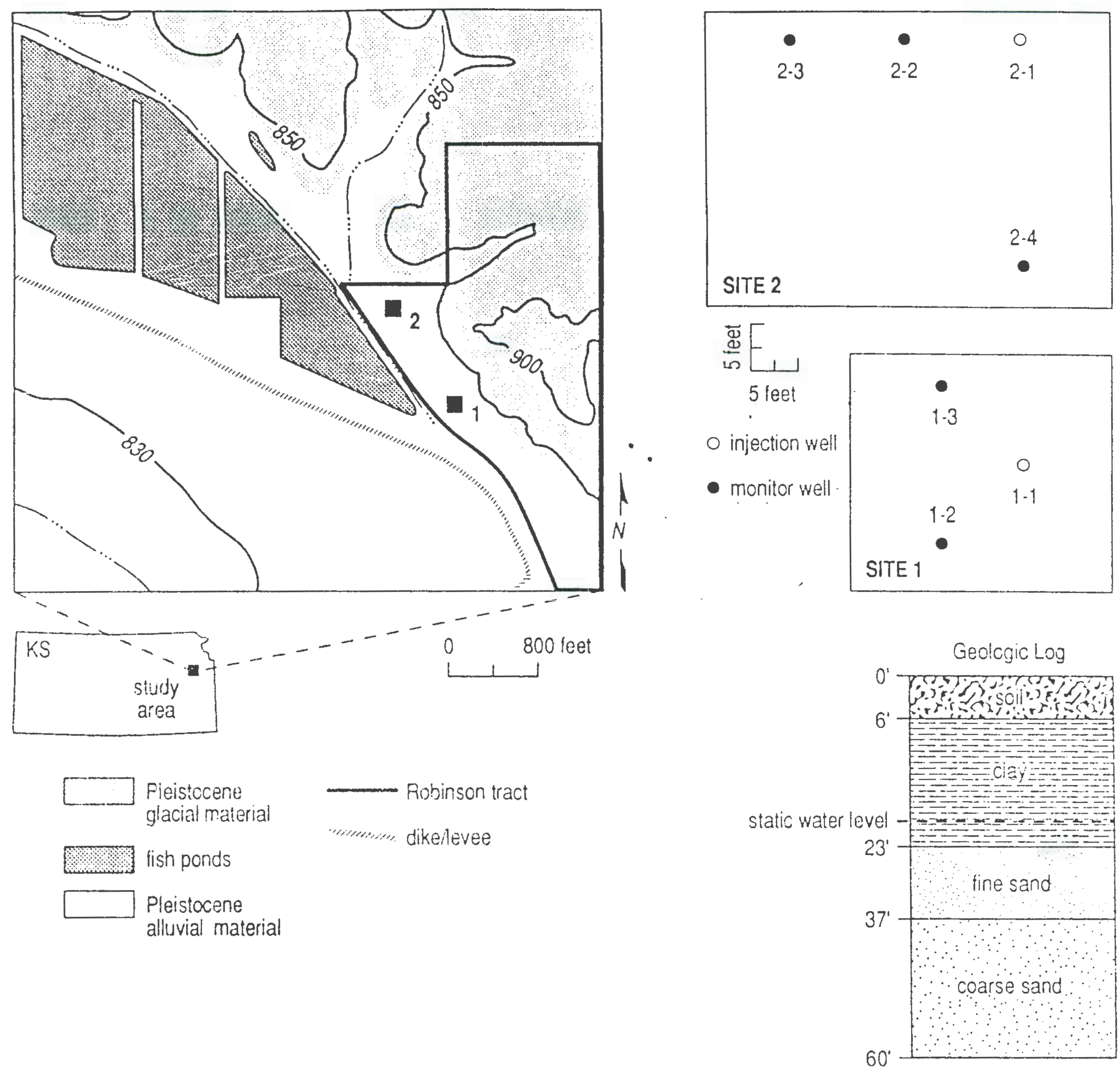
850
850
900
830
2
1
N
KS
study area
0
800 feet
Pleistocene glacial material
fish ponds
Pleistocene alluvial material
Robinson tract
dike/levee
2-3
2-2
2-1
2-4
SITE 2
5 feet
5 feet
injection well
monitor well
1-3
1-1
1-2
SITE 1
Geologic Log
0'
soil
6'
clay
static water level
23'
fine sand
37'
coarse sand
60'

Figure 1

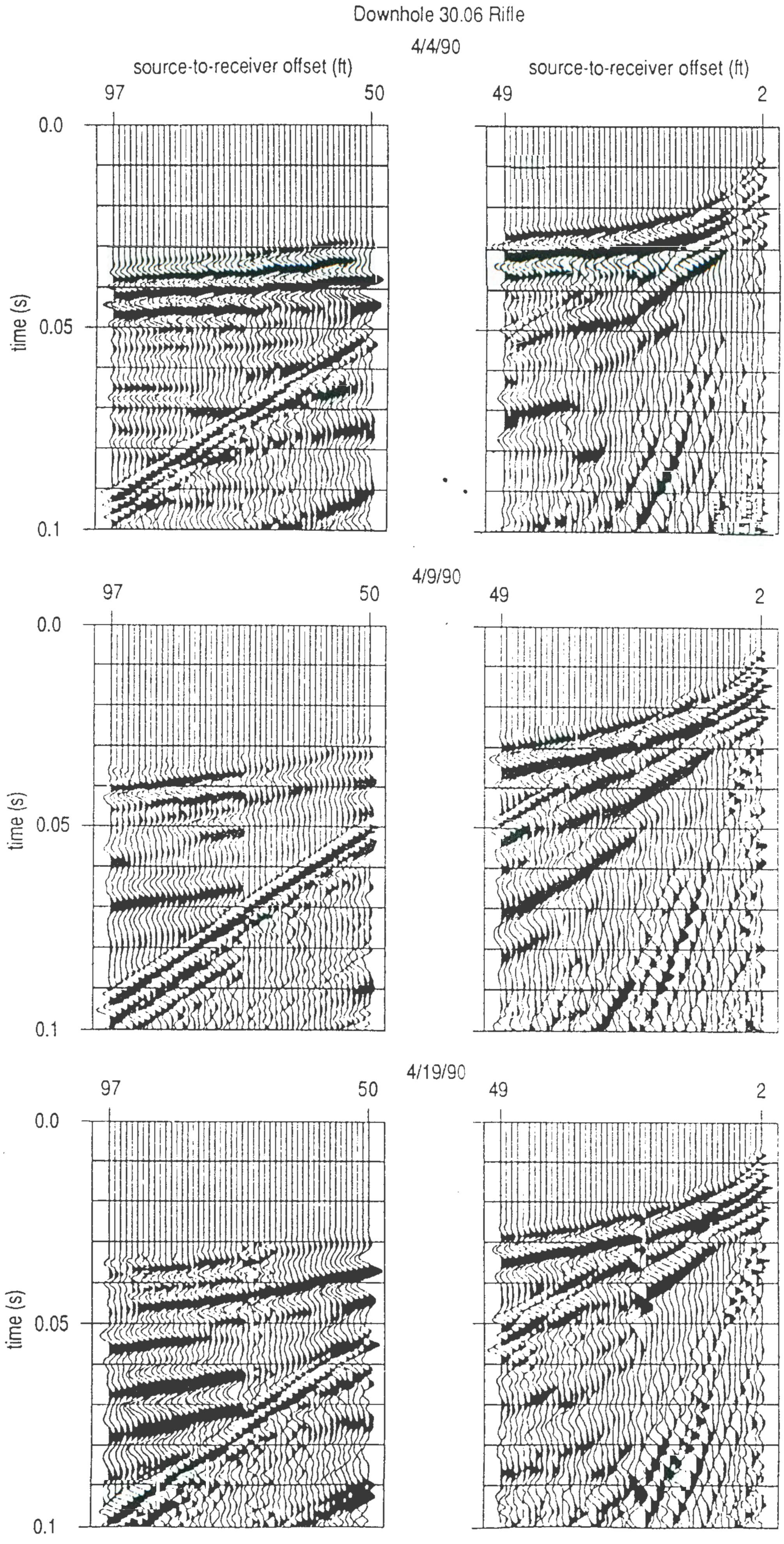
Downhole 30.06 Rifle
4/4/90
source-to-receiver offset (ft)
source-to-receiver offset (ft)
97
50
49
2
0.0
time (s)
0.05
0.1
4/9/90
97
50
49
2
0.0
time (s)
0.05
0.1
4/19/90
97
50
49
2
0.0
time (s)
0.05
0.1

Figure 2

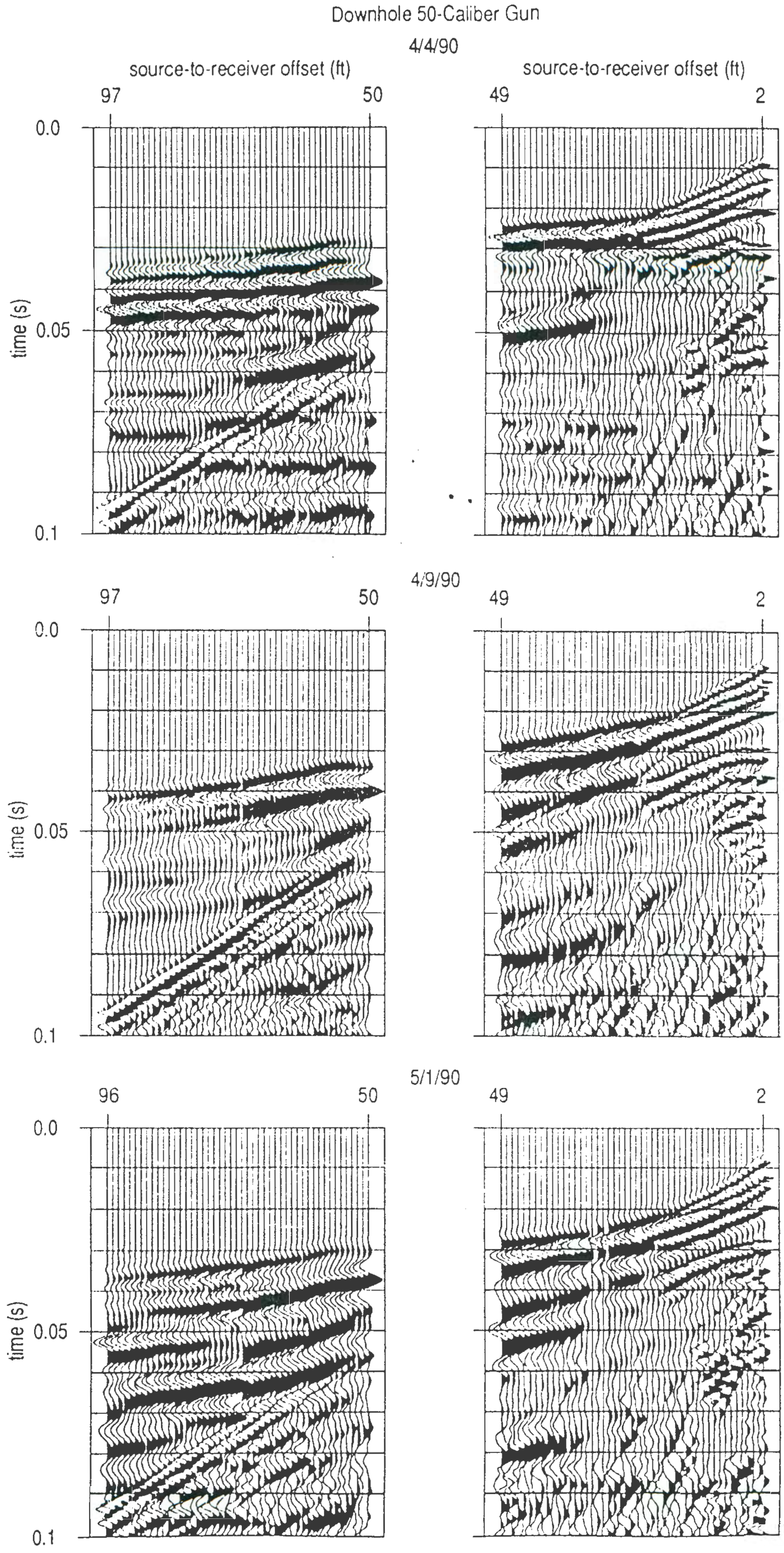
Downhole 50-Caliber Gun
4/4/90
source-to-receiver offset (ft)
source-to-receiver offset (ft)
97
50
49
2
0.0
time (s)
0.05
0.1
4/9/90
97
50
49
2
0.0
time (s)
0.05
0.1
5/1/90
96
50
49
2
0.0
time (s)
0.05
0.1

Figure 3

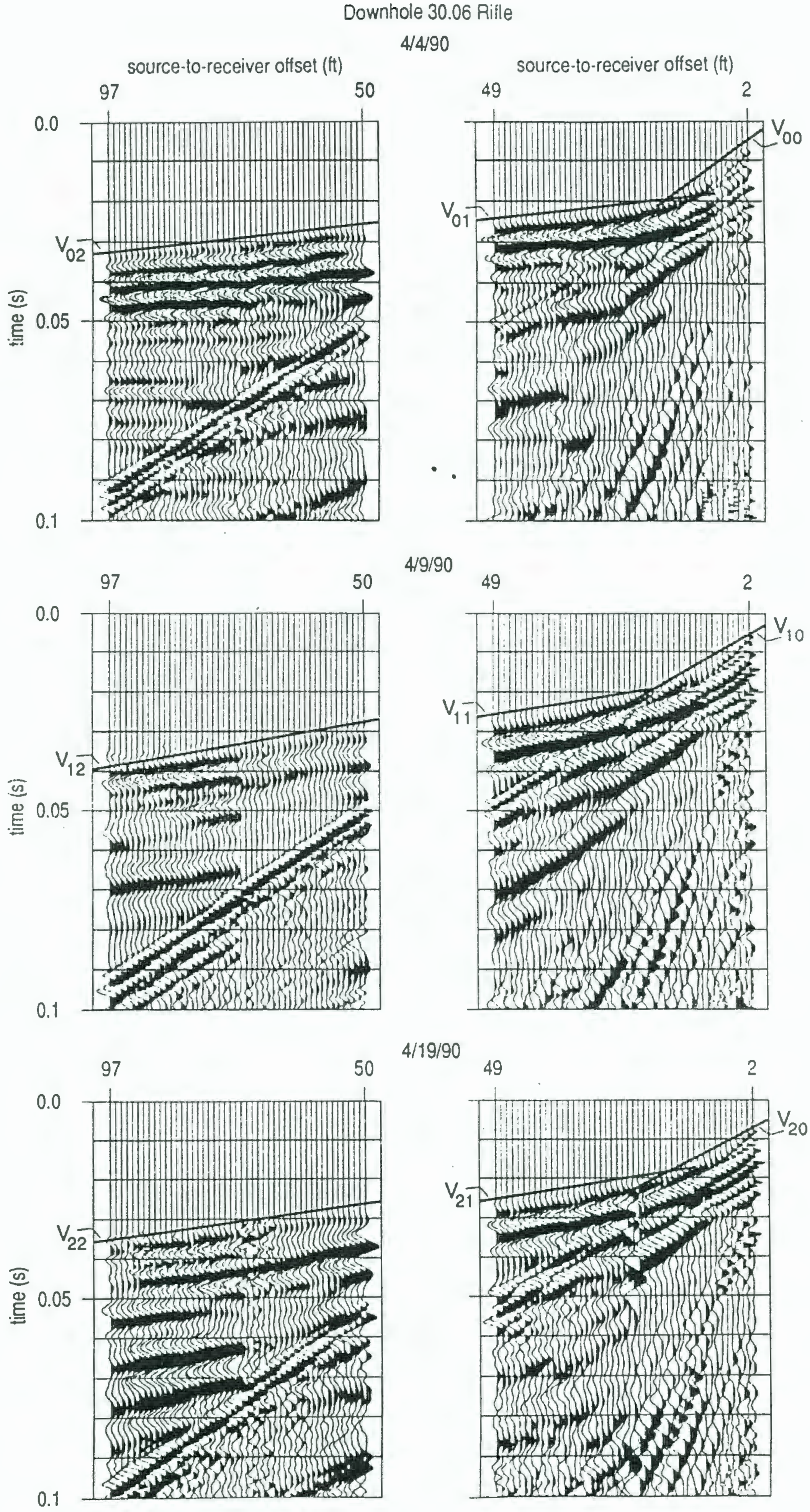
Downhole 30.06 Rifle
4/4/90
source-to-receiver offset (ft)
97
50
source-to-receiver offset (ft)
49
2
0.0
0.05
0.1
time (s)
V_{00}
V_{01}
V_{02}
4/9/90
V_{10}
V_{11}
V_{12}
4/19/90
V_{20}
V_{21}
V_{22}

Figure 4

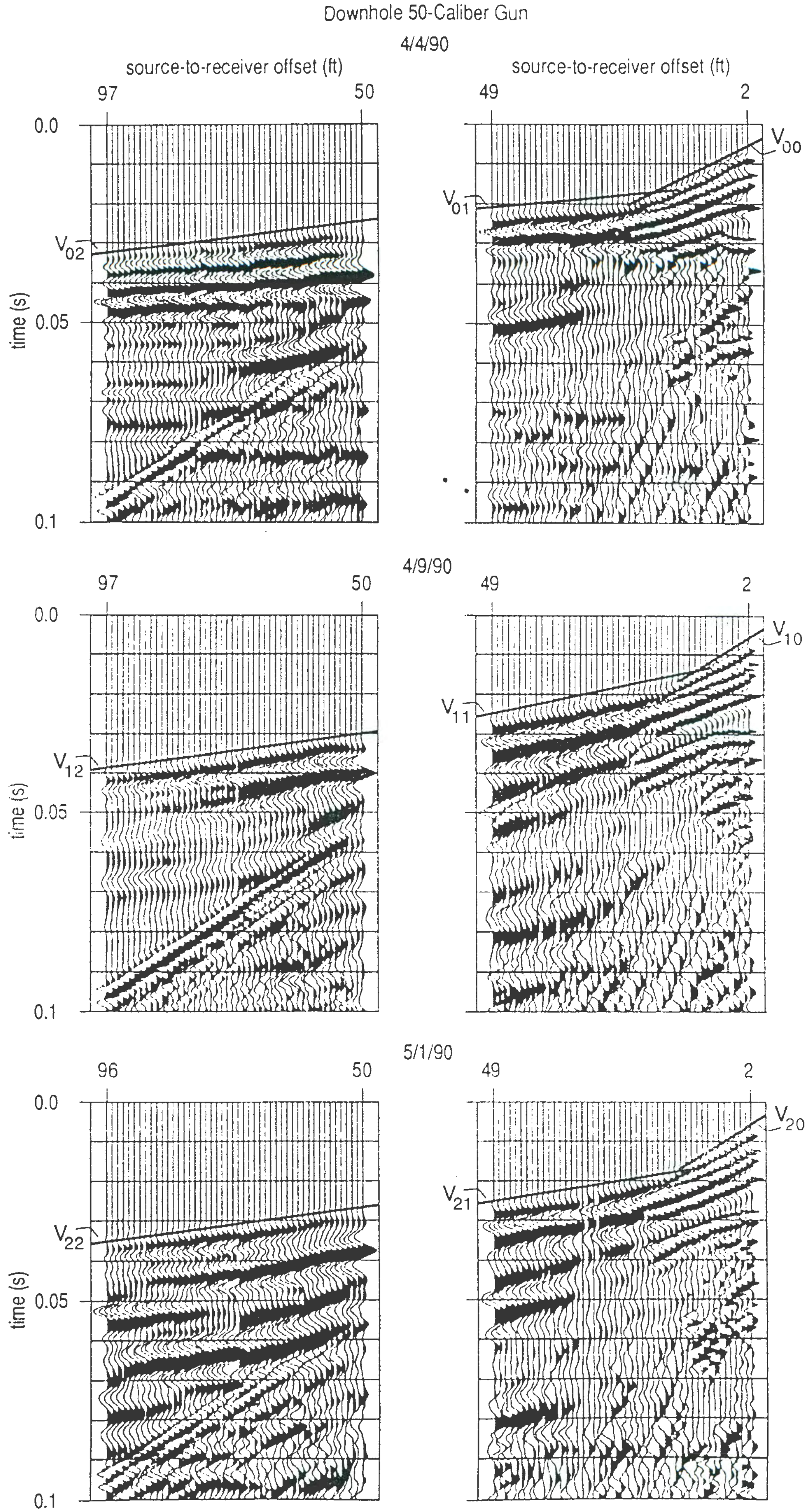
Downhole 50-Caliber Gun
4/4/90
source-to-receiver offset (ft)
source-to-receiver offset (ft)
97
50
49
2
0.0
0.05
0.1
time (s)
V00
V01
V02
4/9/90
97
50
49
2
0.0
0.05
0.1
time (s)
V10
V11
V12
5/1/90
96
50
49
2
0.0
0.05
0.1
time (s)
V20
V21
V22

Figure 5

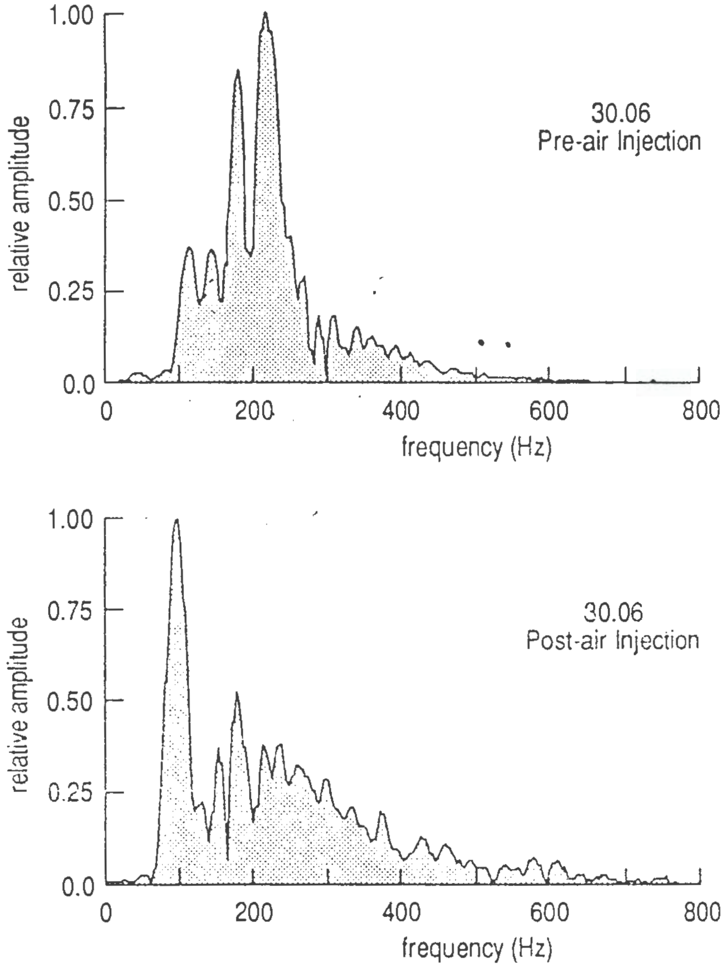
1.00
0.75
0.50
0.25
0.0
relative amplitude
30.06
Pre-air Injection
0
200
400
600
800
frequency (Hz)
1.00
0.75
0.50
0.25
0.0
relative amplitude
30.06
Post-air Injection
0
200
400
600
800
frequency (Hz)

Figure 6

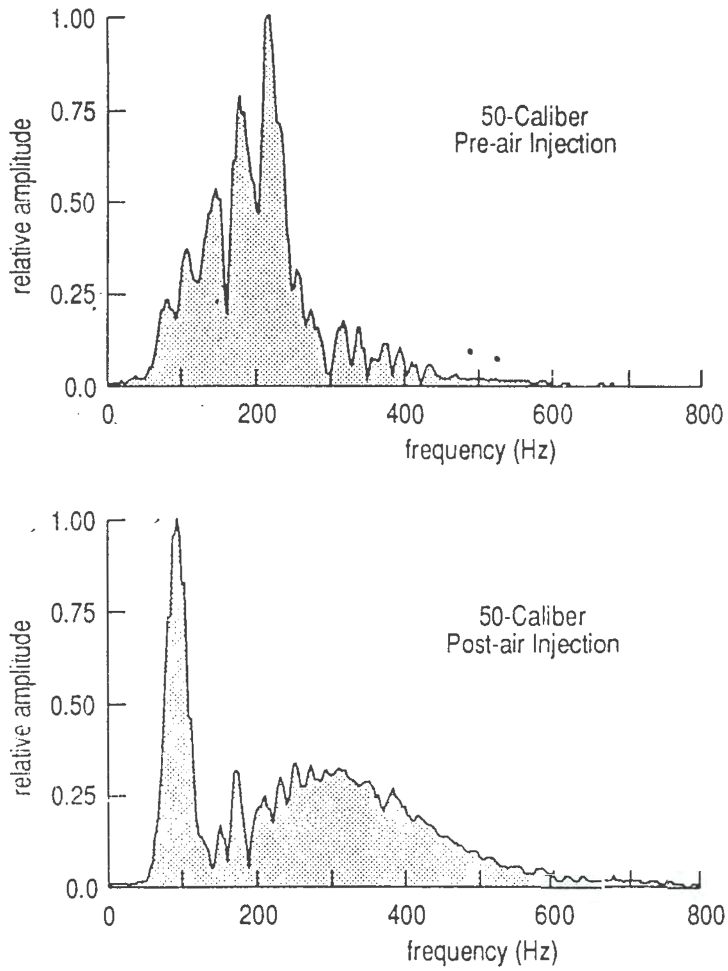

50-Caliber
Pre-air Injection
relative amplitude
1.00
0.75
0.50
0.25
0.0
0
200
400
600
800
frequency (Hz)
50-Caliber
Post-air Injection
relative amplitude
1.00
0.75
0.50
0.25
0.0
0
200
400
600
800
frequency (Hz)

Figure 7

APPENDIX A

FEASIBILITY OF USING SEISMIC REFLECTION TO DETECT GAS TRAPPED IN ALLUVIAL MATERIALS

by

Randie Lane Grantham

B.S. , University of Missouri-Rolla, 1987

Submitted to the Department of Geology and the Faculty of the Graduate School of the University of Kansas in partial fulfillment of the requirements for the degree of Master of Science.

Chairman

Committee Members

For the Department

Date thesis accepted

ABSTRACT

During the last nine months of 1989, several experiments were completed to determine the feasibility of using shallow seismic reflection techniques for detection of air contained in a semiconfined alluvial aquifer. Air was successfully injected and contained for up to three days in Newman terrace deposits on the Robinson tract in Douglas County, Kansas. On ten separate occasions, walkaway noise spreads were acquired to determine a suitable location and optimum recording parameters for seismic detection of air. Seismic data quality was found to vary with source type, source hole depth, source and receiver location, receiver plant, and date of acquisition. A 600 Hz intra-alluvial reflector was an additional product of one of these experiments.

Three combination air injection and seismic experiments were run on the Robinson tract. Seismic data were taken before and after air injection. Each set of data was scrutinized for any differences in arrival time, reflection occurrence, and spectral character. A maximum of 1 ms travel-time delay was found on a reflection in the third post-air data set. Experimental error for the same air injection experiment was 1.16 ms. Thus, detection of air contained in alluvial sand and gravel was not possible using seismic reflection techniques outside the limits of experimental error.

DEDICATION

This thesis is dedicated to my family for their love and support.

ACKNOWLEDGEMENTS

I would like to thank my committee for their contribution to this thesis. First of all, I would like to thank Don Steeples, my advisor, for giving me the opportunity to work at the Kansas Geological Survey and to work on a challenging project. More importantly, I would like to thank Don for his patience while I was pursuing conclusions. I would also like to thank my other committee members Don Sprowl and Wake Dort. Don Sprowl was a great source of support and guidance throughout my stay at the University of Kansas. Wake Dort gave me timely suggestions about the structure and content of this thesis.

Many others made major contributions toward completion of this thesis. Rick Miller did a good job in keeping me on tract. His tutoring in the field and in the lab was an immeasurable source of knowledge. Mubarik Ali, Joe Anderson, Brett Bennett, George Coyle, John Healey, Dean Keiswetter, Paul Myers, and Jianghai Xia, help with countless days and nights of data collection and equipment fabrication. Their help was indispensable. I would like to thank Pat Acker, Mimi Braverman, and Jennifer Simms for help and suggestions with the text and figures. I would also like to thank Dean Kettle of the Kansas Biological Survey for letting me pursue this study on the Robinson Tract. Finally, I would like to thank Evan Franseen, the Boneheads, and all of my other friends at the KGS for making my stay enjoyable.

TABLE OF CONTENTS

LIST OF FIGURES

LIST OF FIGURES (Cont'd)

LIST OF FIGURES (Cont'd)

LIST OF FIGURES (Cont'd)

LIST OF FIGURES (Cont'd)

INTRODUCTION AND BACKGROUND

Introduction and Overview

Reflection seismology has been used in the past decade to solve many near-surface, engineering, environmental, and ground water problems. Mapping of the bedrock beneath alluvium (Miller et al., 1989), shallow tunnel detection (Branham and Steeples, 1987), and shallow structural interpretation (Myers et al., 1987; Treadway et al., 1987) are a small sample of the application of this technique. In the shallowest application of seismic reflection published to date, Birkelo et al. (1987) showed that drawdown of the top of the saturated zone during a pumping test could be monitored by using seismic reflection techniques. This study was also the first to single out the water table as the target of a shallow reflection survey.

This thesis is a report on an experiment designed to extend the work of Birkelo et al. (1987) to a semiconfined aquifer at greater depth and investigate the acoustic detection of induced air pockets within the aquifer. Air was injected into and successfully contained in a semiconfined alluvial aquifer in December 1988. The purpose of the air injection experiment was to produce a "cone of compression" in the saturated zone similar to a cone of depression developed during a pumping test. Injection and containment were successful, but many questions about the shape and dimensions were left unanswered. It was the purpose of this study to determine the feasibility of using seismic reflection techniques to detect air trapped in alluvial material. The information gained from this study can be used to plan future studies of hazardous waste, geohydrological, and petroleum reservoir engineering experiments involving injected or emplaced gas.

Birkelo et al. (1987) showed that the top of the saturated zone could be imaged during a pumping test using reflection seismology. A change in seismic velocity was encountered between the wet and the dry sandy alluvium at their study location. This change in velocity created an acoustic impedance contrast that could be detected using reflection seismology. As the saturated zone dropped during the pumping test, the reflection from the the top of the saturated zone also dropped. His work was done at less than 4 m depth.

The question arose from Birkelo's work whether similar results could be attained by injecting air into alluvial material at a greater depth. In other words, can a change be seen between seismic data taken before and after air injection at depths greater than 10 m. If successful, air injection in coordination with seismic experiments could be used for many near-surface geologic experiments. Detection of methane within or near a landfill, shallow hydrocarbon detection, and another means of evaluating properties of alluvial materials are possible uses for this technique.

In order for this study to be successful, many questions not directly related to the injection of air and its detection by reflection seismology needed to be answered. First, a suitable seismic model was needed to establish the expected outcome of this experiment. Second, finding a proper location to inject and contain air, creating a proper well design, and developing specialized equipment to monitor injected air was necessary.

Finally, a proper seismic acquisition strategy was needed to increase the chance of successful imaging of an injected air pocket.

Following the successful completion of preliminary experiments, three combined air injection and seismic reflection studies were undertaken. Neither of the first two experiments produced evidence that an air pocket could be imaged using reflection seismology. The third experiment produced some evidence that the air might be affecting the seismic data. However, the changes were small.

Because the changes were small in the third experiment, a final set of seismic experiments were run to evaluate the experimental uncertainty in the seismic portion of the three combined air injection and seismic reflection studies. Finally, the results from the error analysis and all prior research were used to formulate conclusions about the feasibility of detection of air using reflection seismology.

Previous Studies

Most of the present knowledge about acquisition of shallow seismic reflection data has come from research done in the past 10 years. As early as 1979, shallow reflection surveys could retrieve reflection data from 20 m depth (Steeples, 1979). Later, Knapp and Steeples (1986 a,b) more precisely outlined the proper requirements for recording equipment and acquisition design techniques for shallow reflection surveys. Articles comparing energy, frequency, portability, and cost of shallow seismic sources completed the information needed to properly acquire shallow reflection data (Miller et al., 1986, 1989). This study's shallow reflection surveys were created through knowledge gained from each of the listed articles and the common-depth-point (CDP) stacking method (Mayne, 1962). The seismic data processing steps used in this study are discussed in great detail by Yilmaz (1987).

Although the water table and other intra-alluvial features have been targets for shallow reflection surveys, detection of an air pocket in the near-surface with seismic reflection methods has not been documented in the literature. Studies utilizing tomography and bright spot technology to explore gas and monitor steam injection during secondary oil recovery had similar goals but were done at a much greater depth in consolidated material (Justice et al., 1989; Bradley, 1985; Yu, 1985). In addition, several laboratory experiments have documented the dependence of rock properties on gas saturation (Domenico, 1976; Gregory, 1976), but, these experiments only addressed the change in specific rock properties of specific laboratory specimens under laboratory conditions and therefore may not apply in a field environment.

Geologic Setting

The site chosen for this experiment is located approximately 1.5 kilometers north of the Lawrence, Kansas, airport in the Kansas River valley. It is near Mud Creek on University of Kansas property known as the Robinson tract (Figure 1).

The near-surface lithology is consistent throughout the study tract, although two distinctly different depositional environments are responsible for its makeup. Most of the near-surface material in the

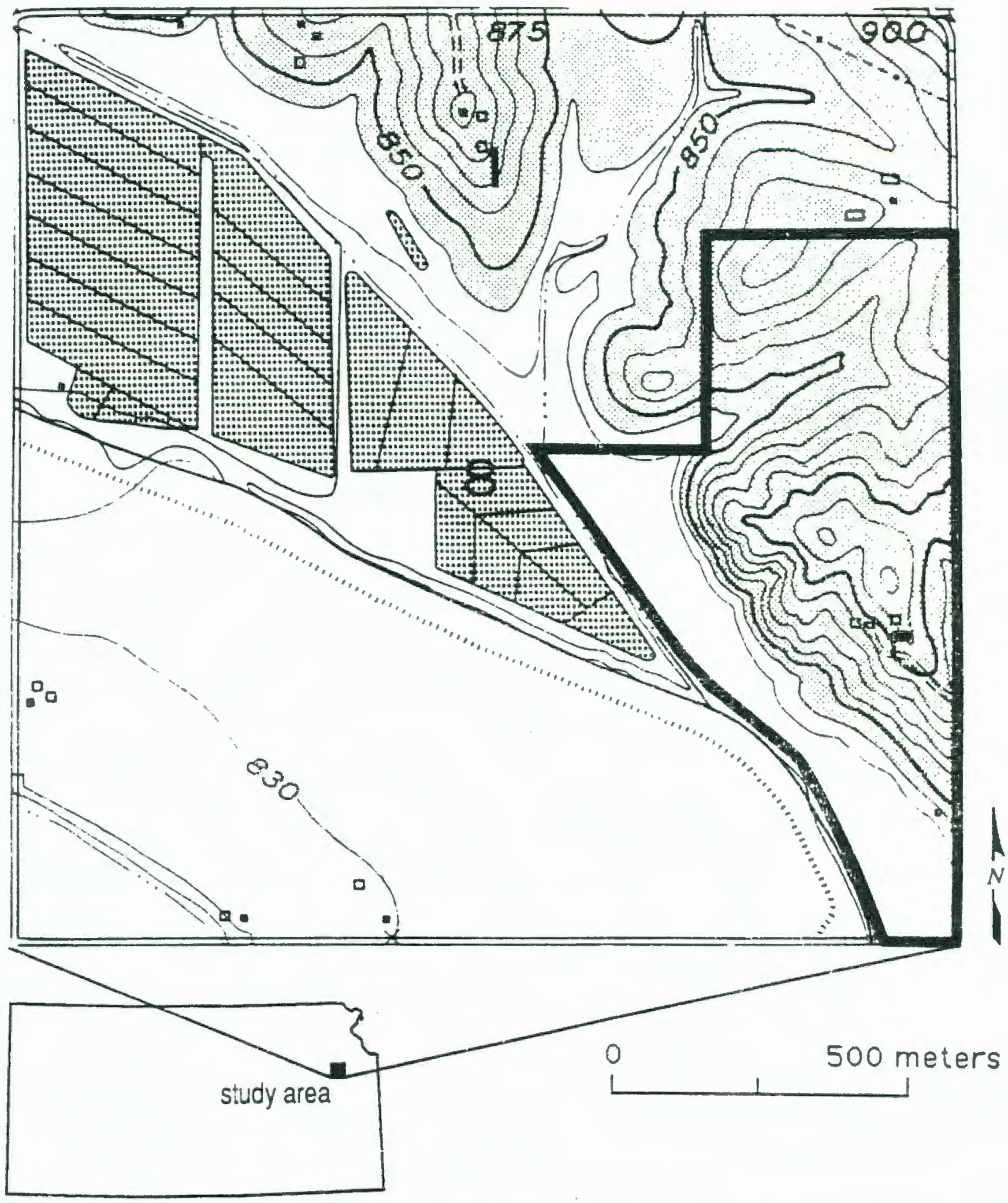

Figure 1. Robinson tract (section 8, township 12, range 20). Adapted from 10 minute Midland quadrangle map.

Legend

Pleistocene glacial material

Fish ponds

Pleistocene alluvial material

Robinson tract

northern and eastern parts of the tract is Pleistocene glacial deposits; in the southern and western parts of the tract are Pleistocene and Holocene alluvial deposits (Figure 1). A generalized cross section, adapted from Stewart et al. (1969), shows the stratigraphy of the Robinson tract (Figure 2).

As much as 90 feet (27 m) of glacial deposits overlies the Pennsylvanian age Haskell Limestone in some regions and the Vinland Shale Member of the Stranger Formation in others. The glacial deposits, which are early Kansan in age, grade from clay and fine-grained silt at the surface to sand and gravel near bedrock (Stewart et al., 1969).

As much as 80 feet (24 m) of fluvial deposits from the Kansas River and Mud Creek also overlie Pennsylvanian bedrock (Stewart et al., 1969). This fluvial material is part of the late Wisconsinan and younger Newman terrace deposits (Fader, 1974). The alluvium fines upward from cobbles and coarse-grained sand at the base to dark silty clay at the surface (Sorenson et al., 1986). Driller's notes and gamma ray logs (Figure 3) run in a well penetrating Newman terrace deposits in the southeastern tip of the Robinson tract (Figure 4) confirm a gradation from coarse-grained sand to clay. The clay, silt, sand, and gravel found in the terrace deposits are derived from Pennsylvanian bedrock and glacial deposits (Zeller et al., 1968).

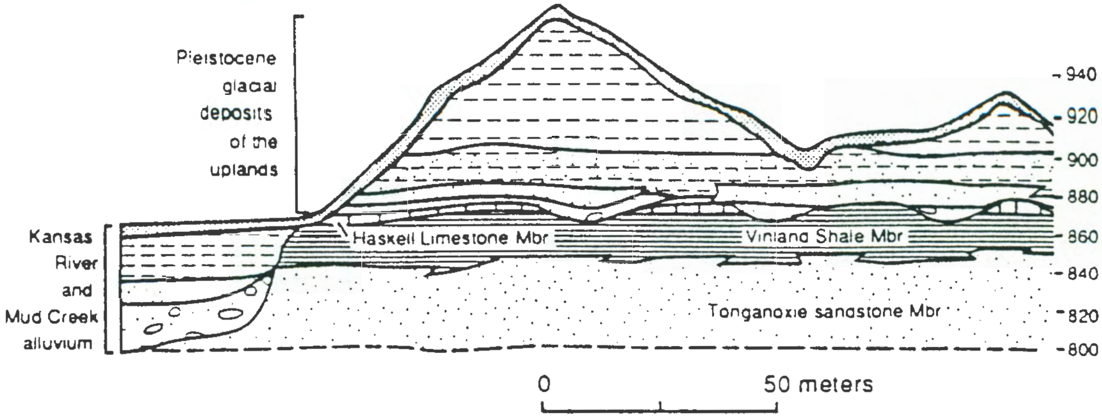

Alluvium - Pleistocene and Recent - Clay, silt, sand, and gravel, derived principally from Paleozoic rocks.

Glacial deposits - Pleistocene - Deposits which grade from clay and fine sand at the surface, to sand and gravel near bedrock.

LAWRENCE FORMATION

Haskell Limestone Member - Pennsylvanian - Bluish-gray, fine-grained limestone, witha locally developed oolitic facies at the top and base in which pelecypods and gastropods occur. The main part contains algal remains, fusilinids, and brachiopods.

STRANGER FORMATION

Vinland Shale Member - Pennsylvanian - Gray to greenish-gray, clayey, calcareous shale, sandy shale, and sandstone. A faunal zone containing abundant mollusks, particularly myalinid clams, characterizes the upper part of the Vinland Shale.

Tonganoxie Sandstone Member - Pennsylvanian - generally lenticular, massive, cross-bedded sandstone and more continuous sandy shale, containing several discontinuous coal beds.

Figure 2. Diagrammatic geologic cross section adapted from Stewart (et al., 1969). Formation descriptions taken from Zeller (1968).

GAMMA RAY AND DRILLER'S LOGS

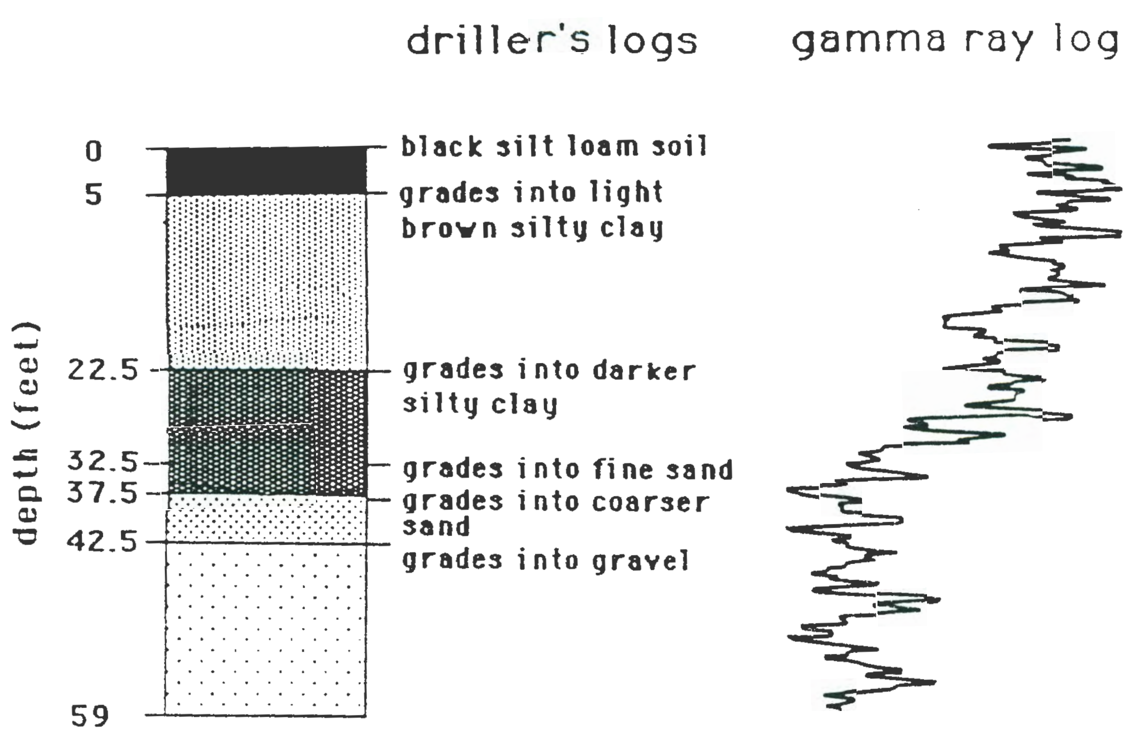

Figure 3. Driller's log and gamma ray log comparison.

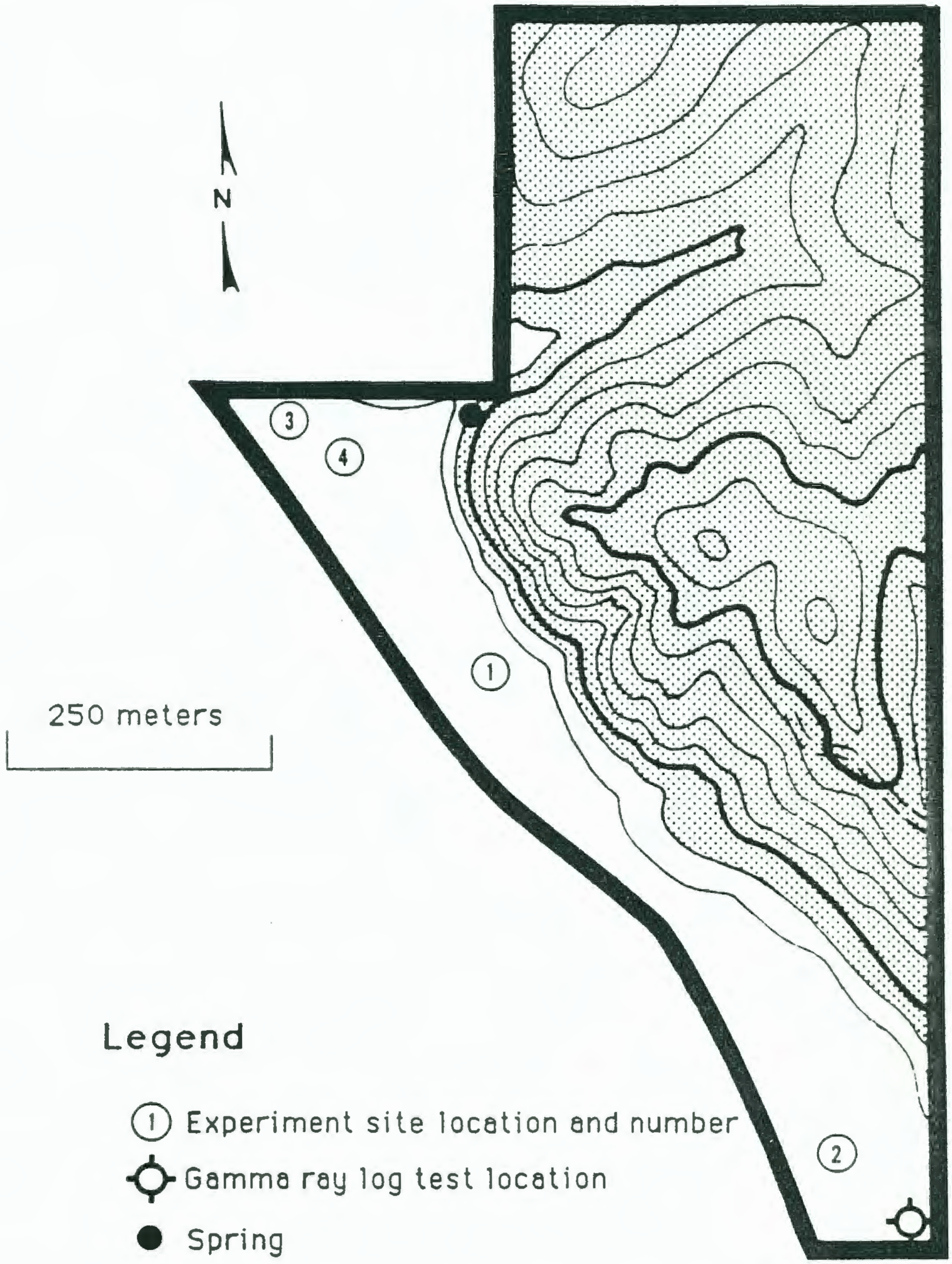

Figure 4. Experiment locations within Robinson tract. Map adapted from 10 minute Midland quadrangle map.

Seismic Model

A seismic model for imaging injected air was created using Birkelo et al.'s study (1987) and other unrelated work. Seismic characterization of the air injection experiment was indicated because it was expected that the injected air would change the seismic characteristics of the subsurface and that the replacement of water with air would decrease the P-wave velocity within the injection interval. Domenico (1976) and Gregory (1976) produced evidence from consolidated and unconsolidated laboratory sand samples that less than 5% gas saturation lowered compressional wave velocities by almost 75%. After the initial sudden drop in velocity, the curve flattens to almost no change of velocity with increased gas saturation. This decrease in velocity would result in a time delay in reflection events below the air pocket (Bradley, 1985) and would change the spectral characteristics of a reflection event found at the air containment interface (Birkelo et al., 1987). It is also possible that a drop in velocity along the containment interface might change the acoustic impedance enough to create a reflected event if one was not present before air injection (Domenico, 1976).

PRELIMINARY SEISMIC STUDIES

To design the proper seismic acquisition survey for the air injection experiments, it was necessary to pick the the proper seismic acquisition method and equipment. The following sections outline the seismic acquisition method and the seismic instrumentation used in this study and give one example of their successful implementation before the air injection tests at the Robinson tract.

Seismic Data Acquisition Methods

One of the seismic data acquisition methods used in this study is known as a walkaway noise spread, or "walkaway" for short. A walkaway is used to collect seismic data over a range of source-to-receiver offsets (distances). The source is fired in a fixed location; the receivers are planted at a linearly increasing distance away from the source. No receiver offset is repeated during acquisition.

A walkaway noise spread is collected in many stages. A number of geophones, equal to the number of channels on the seismograph, are planted at an increasing offset away from the source. These geophones are then connected to a cable that is connected to the seismograph. When the source is fired, the seismograph begins recording seismic information detected by the geophones. The seismograph quits recording seismic data after a set period of time (normally one-eighth of a second for this study). Each channel on the seismograph collects the seismic information corresponding to a unique geophone, and therefore a unique offset, on the walkaway. The seismic information is detected, filtered, and received by the seismograph in analog form but is converted to digital (A/D) data for storage on tape. A walkaway is extended by planting a new spread of geophones at one offset increment greater than was recorded on the previous shot. The repetition of this procedure is continued until a sufficient source-to-receiver offset is reached.

To retrieve the highest quality seismic data possible during acquisition, it is necessary to find the optimum source-to-receiver offsets and instrumental gain settings. Because there is a limited number of channels on a seismograph, it is necessary to find the offset that will produce the highest quality seismic information from a survey. Gains must be carefully selected for each channel so that desired seismic events will be high enough in amplitude to be recorded, but not so large that they are distorted. In addition to offset and gain changes, several different pre-A/D (analog to digital) filters are applied during walkaway testing to maximize the amount of desired seismic energy converted to digital data. Pre-A/D filters can be used to decrease the amplitude of unwanted seismic energy and to allow more lower-amplitude seismic energy not affected by the filter to be converted. Some testing may require additional parameter variation such as: source, receivers, arrays, offset interval, record length, sample interval, etc. for best experimental results. The information gained from walkaway noise spreads are often used to discover the best recording parameters for CDP seismic data acquisition.

Common-depth-point, or more precisely common-midpoint, data acquisition was also used during this study. The layout of the CDP seismic line is similar to the walkaway noise spread. However, CDP acquisition design incorporates a constant recording geometry that is repeatedly moved a distance equal to the station spacing (Figure 5). By keeping the recording geometry constant and by shifting the spread by one station interval before each shot, several traces with a common source-to-receiver midpoint (CDP) are collected. The number of traces with the same CDP location is known as the fold (Figure 5). Later, the common CDP traces may be stacked linearly by a computer into one trace to increase the amplitude of coherent reflected events from that location while decreasing the amplitude of incoherent noise.

Seismic Instrumentation

The seismograph used to record seismic data for this study was an Input/Output DHR 2400, which is a 24-channel fixed-gain system. This system has an 11-bit A/D converter plus 1 sign bit. Analog gains as well as high and low-cut analog filters may be used within the system before A/D conversion. The low-cut and high-cut filters used by the Kansas Geological Survey (KGS) reduce the amplitude of recorded energy 24 decibels (dB) per octave below and above their corner frequencies, respectively. For example, energy with a frequency of 55 hertz (Hz) would have a 24 dB drop in amplitude when using a 110 Hz corner frequency low-cut filter and 48 dB drop in amplitude when using a 220 Hz low-cut filter. Likewise, energy with the frequency of 440 Hz would drop 24 dB in amplitude when a 220 Hz high-cut filter is used.

END-ON RECORDING GEOMETRY

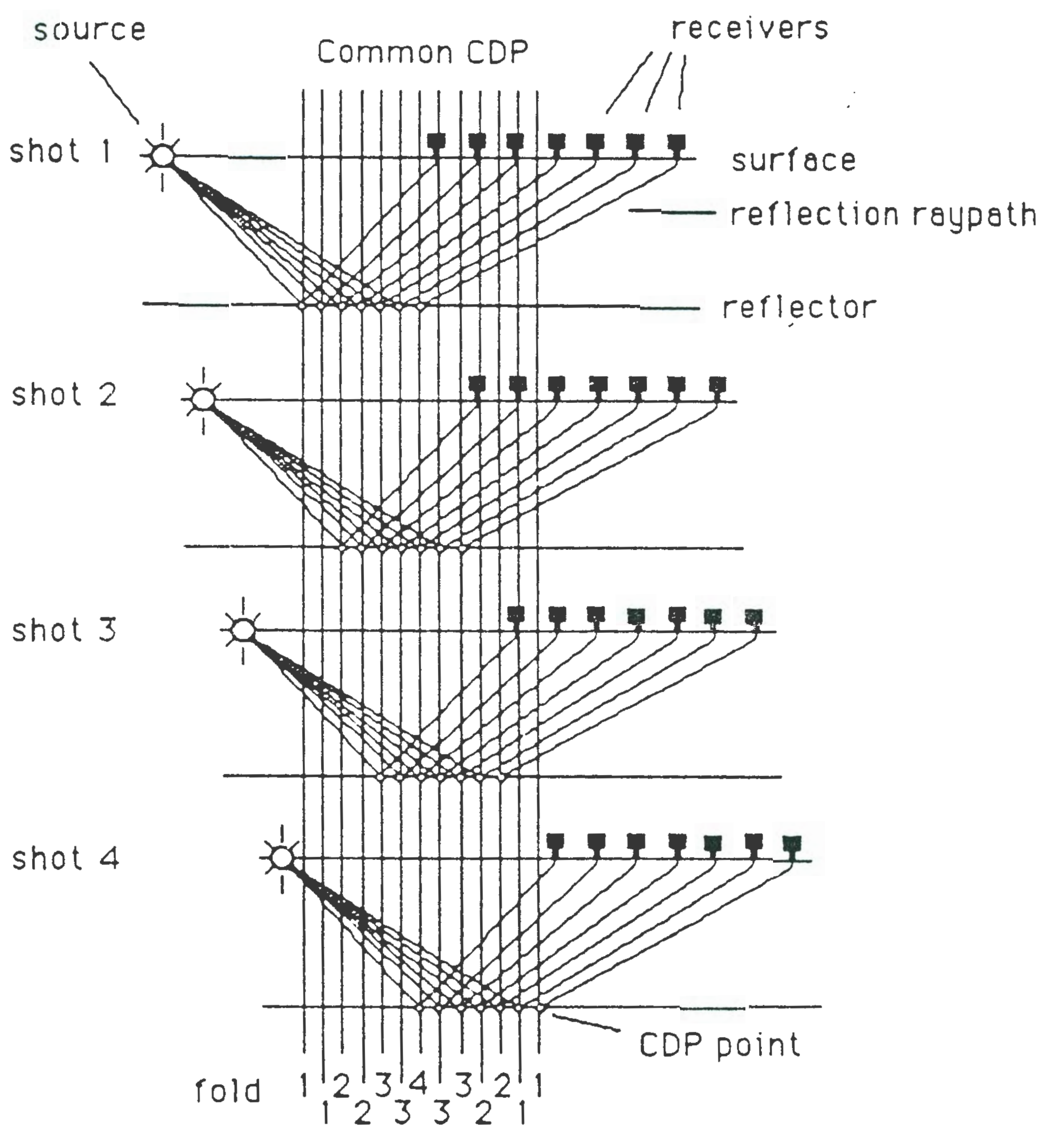

Figure 5. Representation of end-on geometry, CDP acquistion, and resulting fold.

Marks Products 40 Hz and 100 Hz natural frequency geophones were used as receivers for this study. Geophones respond best to seismic energy at or above their natural frequency. Below the natural frequency of the geophones, however, the amplitude of recorded energy drops off at 12 dB per octave. Thus the response of the geophone acts as a low-cut filter for frequencies below the natural frequency when acquiring seismic data.

A 30.06 rifle, a 50 caliber rifle, and a 20 lb (9.1 Kg) sledge hammer with steel plate were used as seismic sources for this study. The 30.06 rifle, utilizing a 180 grain bullet, was used both as a downhole source and a surface source. The 50 caliber rifle, utilizing a 750 grain bullet, was fired only downhole. Both of these sources are mounted to steel plates when fired downhole (Figure 6). When fired at the surface, the 30.06 rifle is placed in a large steel silencer to protect the shooter and to muffle the air-coupled wave. The amount of seismic energy released by the 30.06 rifle is significantly less than that of the 50 caliber rifle. As an alternative to projectile sources, a 3/4-inch (.02 m) steel plate was firmly placed in the soil and then struck with a 20 lb (9.1 Kg) sledge hammer to create seismic energy. The energy released from this source is less than that from the 50 caliber rifle but more than a surface 30.06 rifle shot (Miller, 1986).

Preliminary Testing

In December 1987, to follow up on the work done by Birkelo et al. (1987), several seismic tests were run at the Lawrence Ready Mix sand pit in North Lawrence. A reflection from the saturated zone may have been imaged during these tests (Figure 7). However, other more interesting

Kansas Geological Survey Rifle Sources

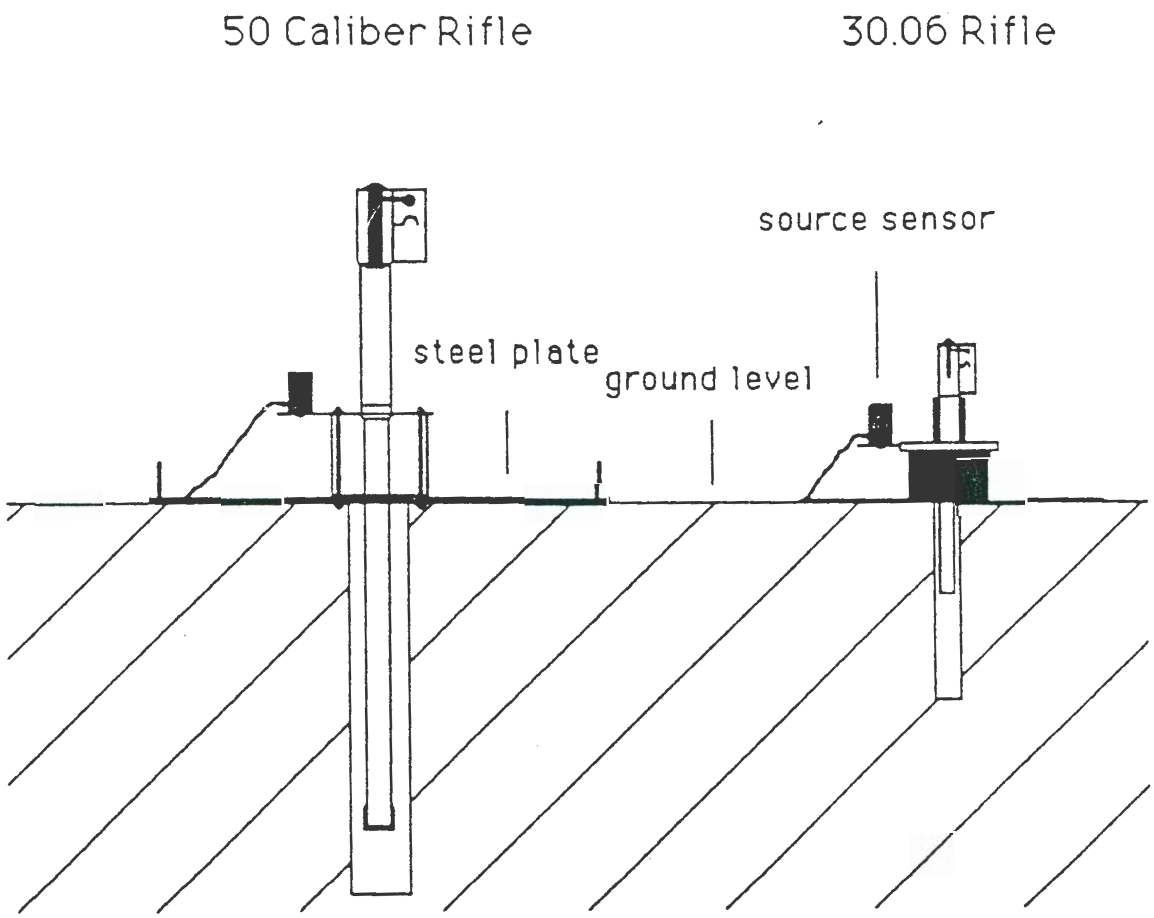

Figure 6. The diagrams above are the downhole versions of these rifle source.

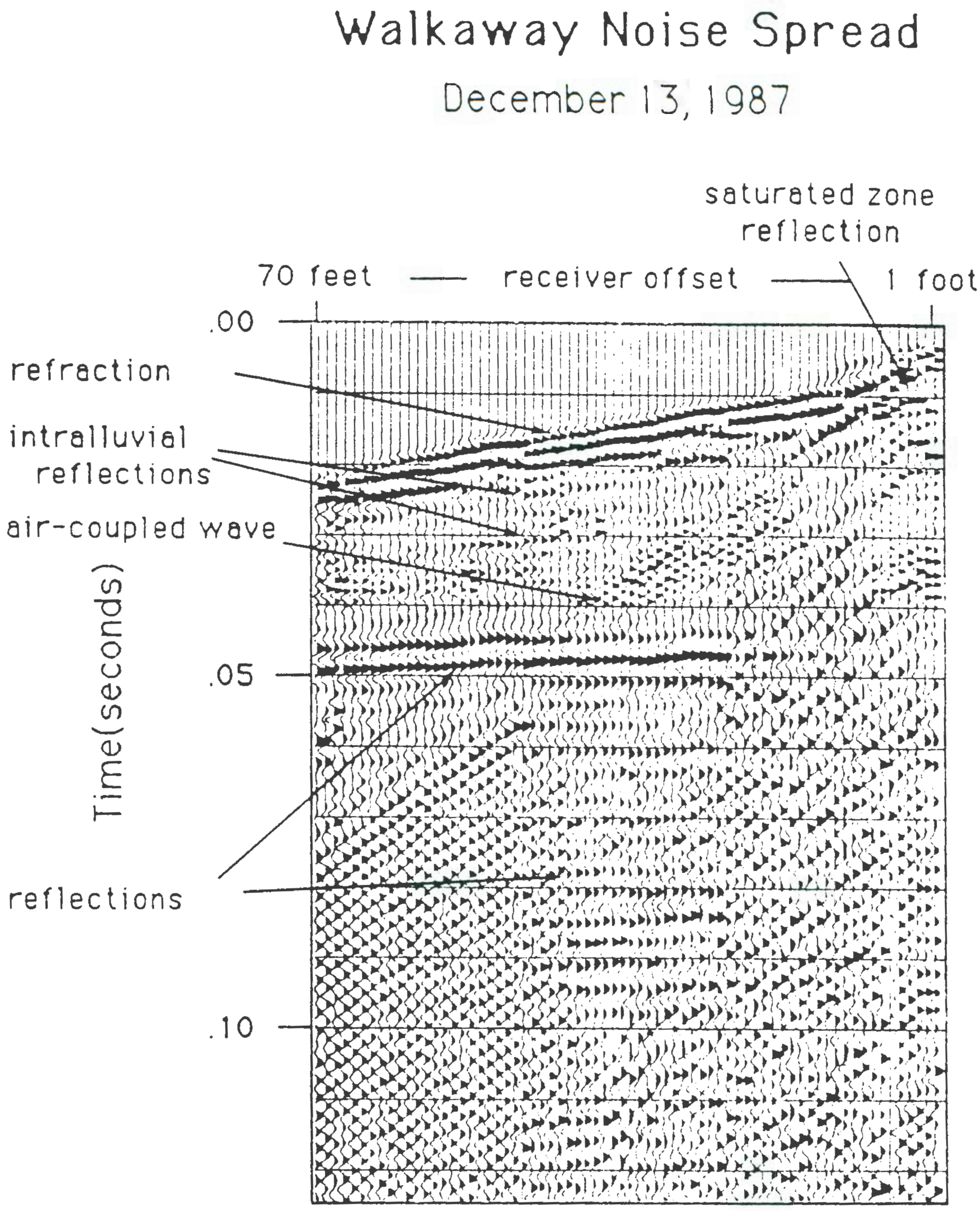

Figure 7. Walkaway noise spread from North Lawrence.

results were obtained during this work. Seismic data taken from this site during walkaway noise testing contained extremely high- frequency broad-bandwidth reflection information. Intra-alluvial reflection information with dominant frequencies of up to 590 Hz and a bedrock reflection with a dominant frequency of over 300 Hz were acquired (Figure 7). These data were some of the highest frequency information ever produced on land using seismic reflection techniques with a surface source and surface receivers. The intra-alluvial events seen on these walkaways are thought to be clay lenses within the sand.

Table 1 lists the parameters used to collect the walkaway data at this site. Extremely high 600 and 800 Hz low-cut filters were used. These filters allowed more high frequency seismic energy to be converted into digital data by lowering the amplitude of other seismic energy of lower frequency. In turn, this allowed larger gains on the amplifiers. Two 100 Hz geophones were grouped in series at each receiver location. In addition to the added low-cut filtering effect of the grouped geophones, the amplitude of the recorded signal is increased by linearly adding the voltage response of each single geophone to form a single summed voltage. Consistent signal tends to add constructively, whereas random noise tends to add destructively.

Later, in May 1988, CDP data were acquired at the sand pit. Although individual field files exhibited high-frequency reflected energy a brute-stacked section of the data showed a drop in frequency of the reflection data (Figure 8). The decrease in frequency was due to the averaging effect of stacking the data and to time break errors. Reflection information with

Recording Parameters

SEISMOGRAPH (DHR 2400):	PARAMETERS
LOW-CUT FILTERS (24 dB rolloff)	600/800 Hz
HIGH-CUT FILTERS (24 dB rolloff)	1000 Hz
ANTIALIAS HIGH-CUT FILTER (60 dB rolloff)	3000 Hz
NUMBER OF SAMPLES	500
SAMPLE RATE	1/4 ms
RECORD LENGTH	125 ms

SOURCE:	PARAMETERS
TYPE	downhole 30.06
SPACING	walkaway

RECEIVERS:	PARAMETERS
TYPE (natural frequency)	100 Hz Marks Products
SPACING	1' (.30 m)
ARRAYS (connected in series)	2 geophones (grouped)
RECORDING GEOMETRY	walkaway
SOURCE-NEAR-RECEIVER DISTANCE	1' (.30 m)
SOURCE-FAR-RECEIVER DISTANCE	71' (21.6 m)

WEATHER/SOIL CONDITIONS	PARAMETERS
WIND SPEED	0-10 mph (0-4.5 m/s)
WIND DIRECTION	not recorded
NEAR-SURFACE MATERIAL	packed sand
NEAR-SURFACE MOISTURE	dry
TEMPERATURE	40° F (4° C)

Table 1

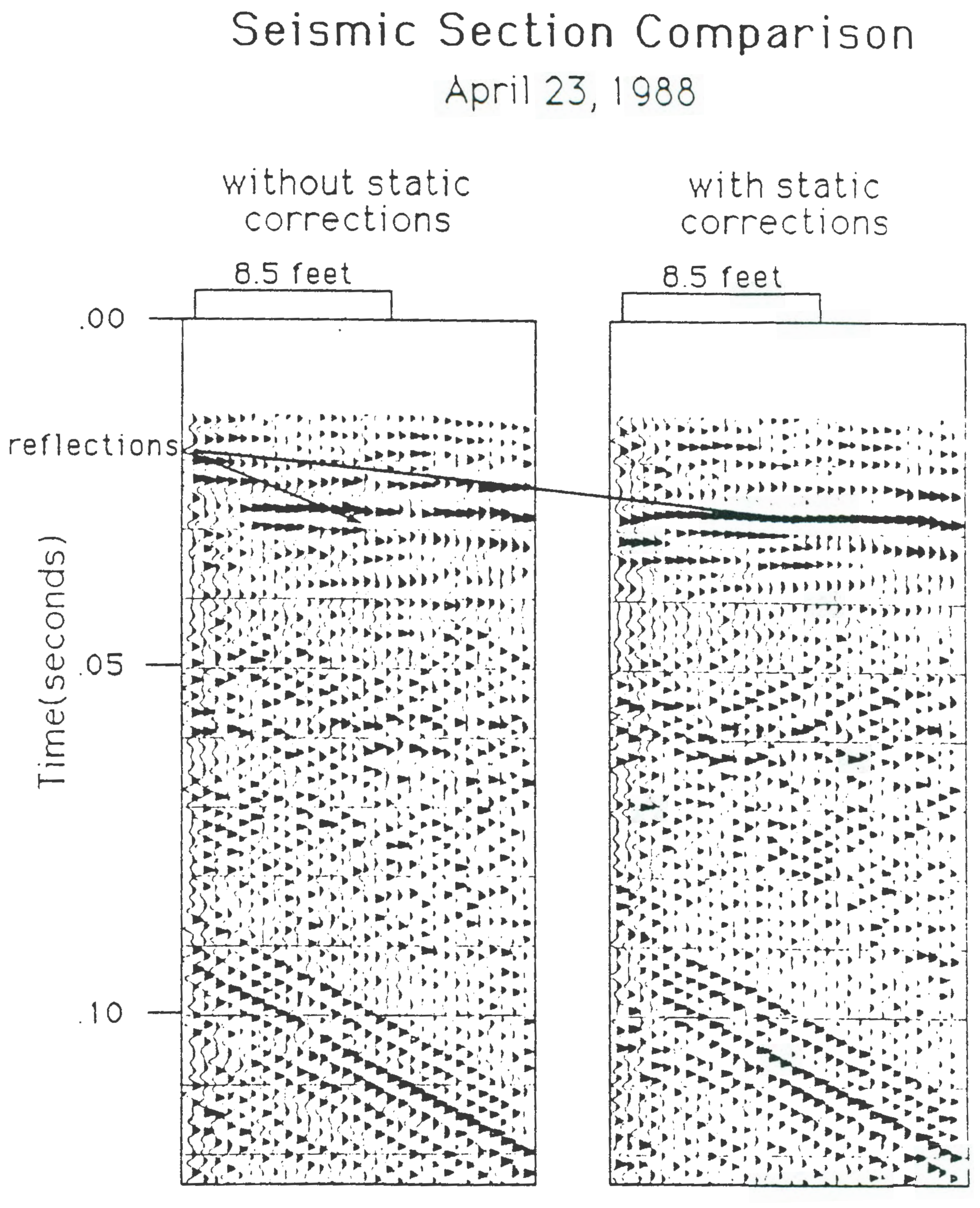

Figure 8. Comparison between high frequency reflected events stacked with and without static corrections.

a dominant frequency of 400 Hz, for instance, has a dominant period of 2.5 milliseconds (ms). Because the maximum sample rate of the DHR 2400 is 1/4 ms, there are only 10 samples imaging a 400 Hz waveform. An improper correction of even 1 sample before stacking would decrease the dominant frequency of the combined stacked waveform by 37 Hz. Consequently, automatic static corrections and residual static corrections were applied to this same data set before stacking. Static corrections are used to account for small inconsistencies in elevation of the source and receivers or in velocity. The static corrections increased reflector coherency, frequency, and amplitude of these data in the final stacked section (Figure 8). Table 2 shows the entire processing flow used to produce this section.

One unique feature of the sandpit site was the sand near the land surface. The Lawrence Ready Mix sand pit is continuously dredged for sand. Repeated movement by heavy machinery has compacted the sandy surficial material. Thus geophones were hard to plant and were not coupled well with the ground. During CDP data collection, as shots were fired near the line, geophones decreased their coupling to the ground as the sand broke up around them. Although the compacted sand near the surface was a problem during data collection, it may have also been a reason for the high data quality. Normally, geophones are planted in soil located just beneath the land surface. Soil is usually a good coupling medium and an easy environment in which to plant the geophones. However, soil attenuates seismic energy, especially high-frequency seismic energy. The fact that the soil layer was not present may have been a

Processing Flow

Processing Step	Description
1. Bad trace editing	Seismic traces of poor quality or dead dead during acquisition were removed.
2. First arrival mute	Mute of seismic energy above the first reflected event.
3. Air-coupled wave mute	Mute of main air-coupled wave event.
4. CDP sort	Seismic traces were sorted into gathers containing the same midpoints (common-depth points).
5. NMO correction	Shift applied to the CDP gathers to correct for the time differential due to different source to receiver offsets.
6. Automatic statics	Surface-consistent time shifts applied to CDP traces to correct for near-surface velocity anomalies at a shot or receiver.
7. Residual statics	Slight shifts applied to the CDP gathers to to correct anomalies not removed by Auts.
8. Frequency filter	A process used to reduce the amplitude of unwanted seismic energy while leaving the desired seismic energy alone.
9. Stack	A linear addition of samples from same CDP location into one trace to enhance the data.
10. AGC scaling	A step which boosts the amplitude of events occurring later in the seismic record.

Table 2

reason that such high-frequency reflection events were seen. An even more important factor is thought to be the presence of a shallow water table. The water table was at an approximate depth of 2.5 m at the sand pit. Saturated alluvium is less attenuative to seismic energy than dry alluvium.

In addition to the possible imaging of the water table at this site, techniques on how to acquire and process high-frequency broad-bandwidth seismic data were developed. The high-quality data collected at the sand pit became the standard by which future data sets in this study were compared. Because the sandpit was actively being dredged, the prospect of doing any major study at this site was questionable. The Robinson tract was picked as the location to continue seismic testing and begin air injection experiments.

INITIAL AIR INJECTION EXPERIMENTS AND WATER TESTING

A necessary step before the seismic portion of an air injection experiment was successful injection and containment of air. To succeed in For this portion of the study, to succeed a special monitoring apparatus had to be created to detect the movement of air away from an injection well. The following sections describe the monitoring apparatus, well design, and well placement used in all of the air injection experiments. In addition, the results of an inorganic chemical analysis of water samples taken before and after air injection at several sites in the Robinson tract.

Well design and Monitoring Apparatus

The air injection and monitor wells used in this study were cased with 2 inch (.05 m) diameter steel or plastic pipe. The first two wells drilled at site 1 were cased in plastic except for the final 5 feet (1.5 m) at the surface which was cased in steel. All of the other wells were cased exclusively with steel. Each pipe received slotted section (screen) at its base. The length of screen used varied from 5 feet (1.5 m) to 26 feet (7.9 m) in length from pipe to pipe. It was through the screen of the injection well that air was driven into the aquifer. Likewise, it was through the screen of the observation wells that air was allowed to enter from the aquifer for monitoring. The first two wells emplaced were rotary drilled to total depth. Later, wells were drilled to near the base of the clay at approximately 30 feet (9 m) and then driven the remainder of the distance to ensure a proper air cap by the clay. Drilling the well to total depth could create an avenue by which the air could escape from the aquifer. By driving the pipe through the last foot or so of clay, the remaining clay helps create a seal around the pipe. Also, to ensure an air seal at the top of the aquifer, 10 feet (3 m) of cement was poured around the well above the level of the clay/sand interface.

The water level within the observation wells was measured to within 6 inches (.2 m) using a geophone cable and a roll-along switch, two pieces of equipment normally used in seismic acquisition. Every 6 inches (.2 m) of the latter one third of the geophone cable, a small piece of outside insulation was removed exposing many other individually wrapped wires inside. At every 6 inch (.2 m) interval, a unique individually insulated smaller wire within the geophone cable was cut. The end with the exposed wires was placed in the monitor wells. The end of the geophone cable with the exposed wires was fed through a sealable well cap designed to allow continuous monitoring of the water level within the well without loss of air. Next, the other end of the cable was connected to the roll-along switch; each individual inner wire correlated to one position on the roll-along switch. When the water level was above a cut wire, the roll-along switch would see a short circuit at that position. Conversely, when the water dropped below a cut wire and was no longer present to short the circuit, the roll-along switch would register an open circuit at that position. In addition to a hole made for the geophone cables, the monitor well caps were also made with pressure-relief valves built into them. Gauges were screwed into fittings on the valves to measure air pressure simultaneously with water-level measurements.

Air Injection Experiments

The first air injection and containment experiment was conducted northwest of the other ongoing groundwater experiment on the Robinson tract (site 1) and was located in Newman terrace deposits (Figure 4). The experimental setup consisted of one injection well (well 1-1) and one observation well 12 feet (3.7 m) away (well 1-2) (Figure 9). The injection well was rotary drilled to the final depth of 56 feet (17 m), with the final 26 feet (8 m) screened. Clay grades downward into sand at approximately 30 feet (9 m); hence the screened portion of the well was placed in sand. The observation well was also drilled, but only to a depth of 35 feet (10.7 m), with the last 5 feet (1.5 m) being screened. Wells 1-1 and 1-2 were the only wells that had sections made of plastic.

Air was injected by a compressor rated at 165 cfm (4.7 cmm). After six minutes, the water level in the monitor well began to drop. The rate of the water level drop in the monitor well was fast and steady for the first 20 minutes (Figure 10). For the remainder of the experiment, the water remained nearly constant. The air injection experiment continued for 2 hours and 50 minutes.

Several weeks later, a second experiment was performed using a second observation well, well 1-3, in addition to the first. This well was also placed at a distance of 12 feet (3. 7 m) from the injection well, but was azimuthally 90° away from the first observation well (Figure 9). It was drilled to a depth of 30 feet (9 m), and then driven another 13.5 feet (4.1 m). The first 8 feet (2.4 m) of this well was screened. For the second experiment, a slightly larger (185 cfm (5.2 cmm)) air compressor was used.

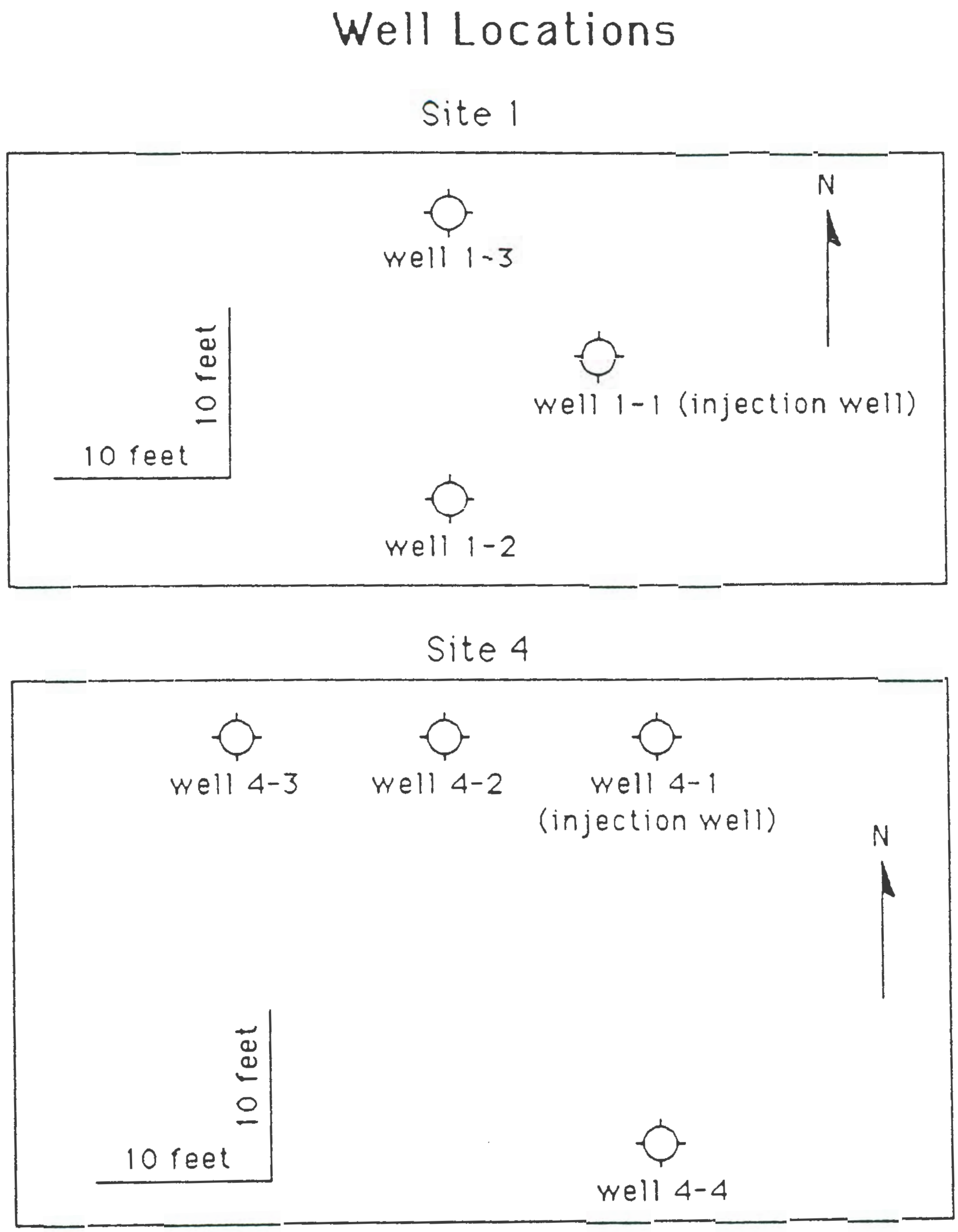

Figure 9. Well locations at site 1 and site 4.

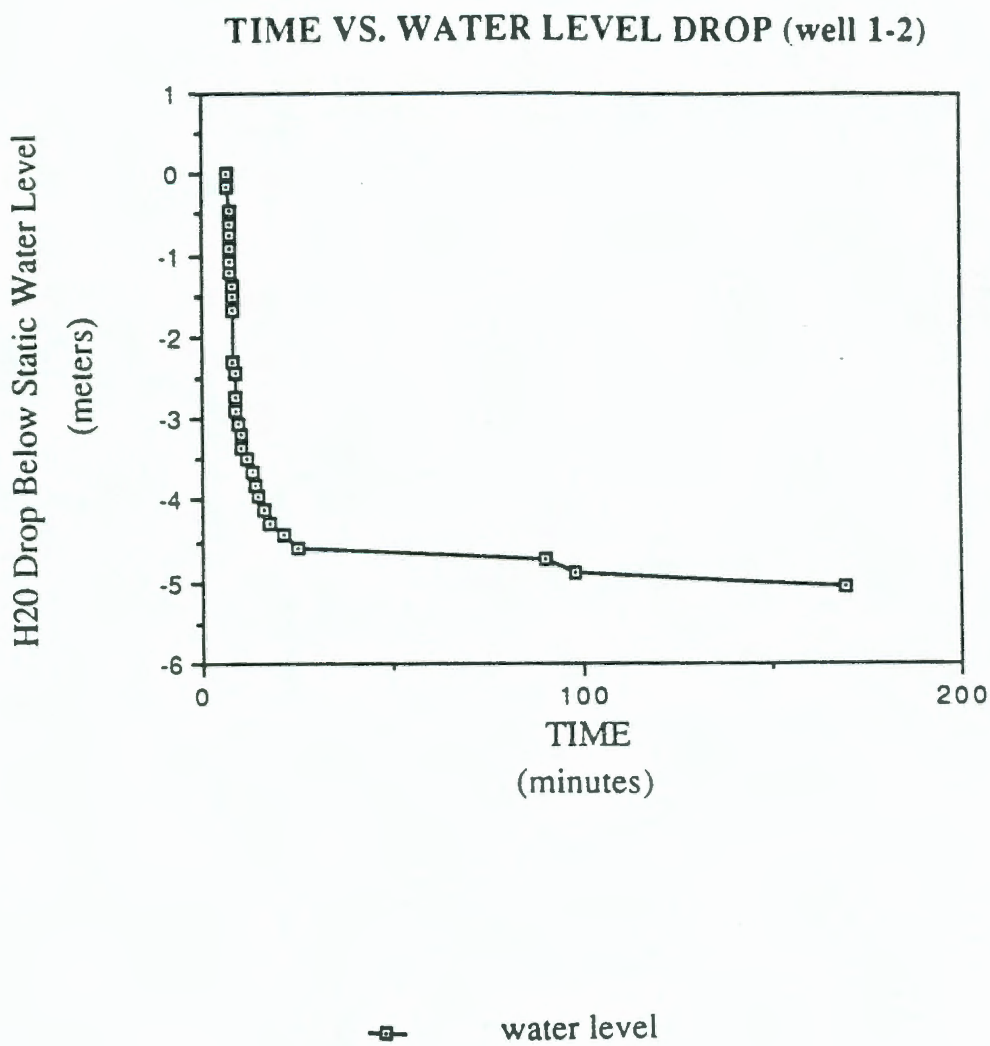

Figure 10. This drawdown curve, derived from observation well 1-2 data, was the same for the first two air injection experiments at site 1.

A marked difference in response of the two observation wells was recorded. Well 1-2 showed a drawdown similar to the first experiment, but well 1-3 (Figure 11) dropped at a higher rate that was beyond the capability of the measuring technique. Thus air must have been moving through the aquifer preferentially. Monitoring of the observation wells continued after air injection had ceased. For 1 hour 30 minutes, water level measurements were taken from both observation wells. During that time, the water level began to rise in both wells. However, neither well reached equilibrium before the end of the experiment. This suggests that the air pocket persisted for at least 90 minutes, which was long enough to allow seismic reflection measurements to be made after the compressor was shut down.

A third air injection experiment was performed a few days later. Air was injected into well 1-2. An almost immediate drop in the water table in well 1-3 was could not be recorded with the equipment available. This immediate water level drop was similar to that seen in the second experiment.

Two seismic surveys did not yield any identifiable reflection information from any depth at site 1. A new site (4), was chosen north and west of the previous experimental location (Figure 4). Initially, three wells were placed 12 feet (3.7 m) apart in a linear east-west direction (Figure 9). Each well was drilled to a depth of 30 feet (9 m) and then force-driven 11 feet (3.3 m) further. Well 4-1, farthest to the east, was chosen as the injection site, and wells 4-2 and 4-3 were sited 12 feet (3.7 m) and 24 feet (7.3 m) away respectively, were used to monitor the air injection. A well

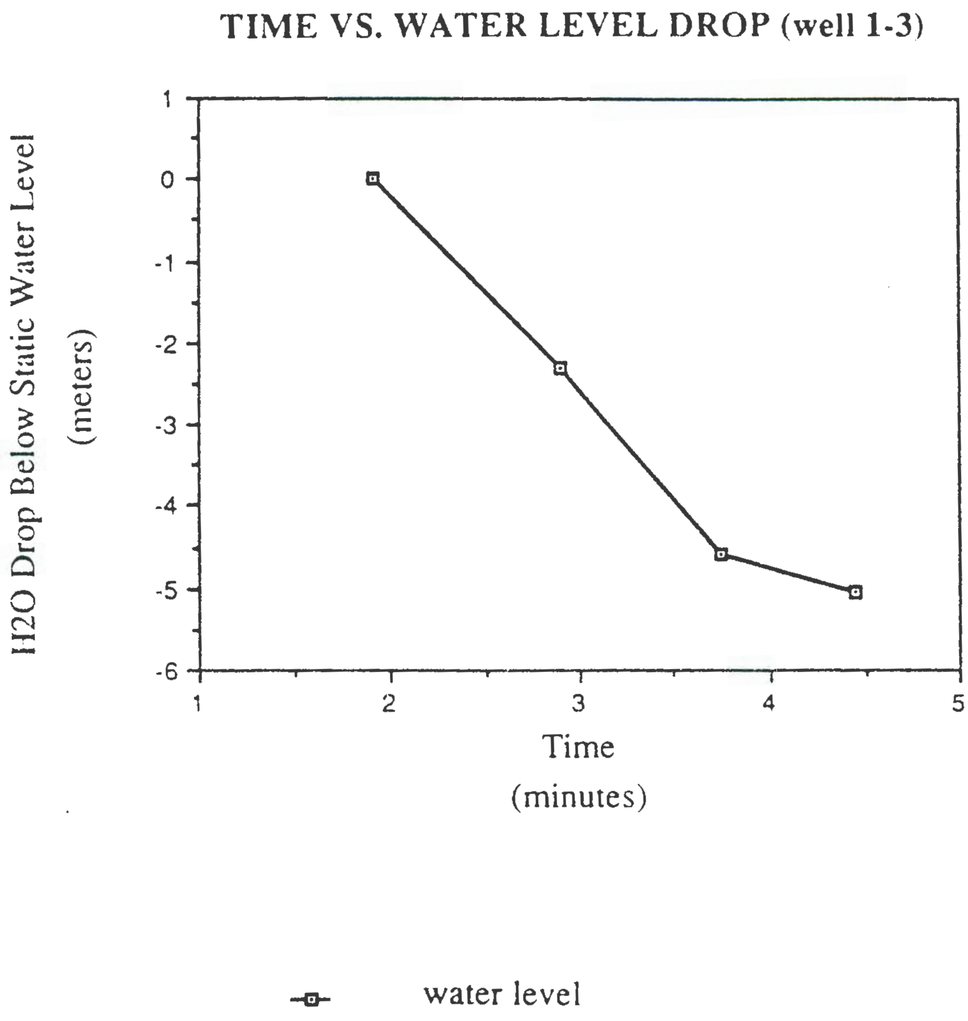

Figure 11. This drawdown curve was derived from observation well 1-3 data taken during the second air injection experiment site 1.

on the end was used to inject air to monitor the lateral extent of the air movement over a greater distance than that obtained from the middle well.

Air was injected in conjunction with seismic experiments at site 4 on May 26 and July 23, 1989. Air was injected using a 9 cfm (.25 cmm) gas-powered air compressor. A lower output compressor was used for these experiments to lesson the risk of damage to the aquifer and to increase the chance of expanding a uniform air pocket. Static water level in both monitor wells was measured at a depth between 23 feet (7.0 m) and 23.5 feet (7.2) before injection of air. After 12 minutes of air injection in well 4-1, the water level began to drop in well 4-2. The water level dropped at an approximate rate of 6 inches (.2 m) per 30 seconds in well 4-2. The first drop in water level seen in well 4-3 occurred 35 minutes after injection began. The water level dropped at a rate of approximately 6 inches (.2 m) per 3 minutes, almost five times slower between 6 inch drops than the drop in well 4-2. After one hour and twenty minutes of air injection, the water level in both monitor wells had stabilized at a level between 36.5 feet (11.1 m) and 37.0 feet(11.3 m). Nearly 10 psi of pressure was present on both wells after stabilization of the water level. Air injection for the first and second air injection experiments lasted 18 hour and 16 hours respectively. The final water level in the two monitor wells remained constant until air injection ceased.

A fourth well (4-4), was driven 24 feet (7.3 m) from the injection well and 90° azimuthally from well 4-3 (Figure 9) before a third and final seismic experiment on October 18, 1989. The purpose of well 4-4 was to test whether air was radiating uniformly from the injection well. This observation well was completed with the same specifications as the other three. The two geophone cables used to monitor water levels were placed in wells 4-3 and 4-4 for direct comparison of air expansion at 24 feet (7.3 m) ground distance from the injection well.

During the third air injection experiment at site 4, both water level and pressure measurements were taken. Air injection, using the 9 cfm (.25 cmm) air compressor, began at 4:20 PM on October 19, 1989. In well 4-3, a drawdown in water level similar to that observed in the other two air experiments at site 4 was recorded. The water level in this well had dropped to a level between 36 feet (11.0 m) and 36.5 feet (11.1 m) after 80 minutes of air injection. During the first hour of air injection, well 4-3 also showed a pressure increase of 9.5 psi. On the other hand, well 4-4 showed no measurable drop in the water level or increase in well pressure during the first 80 minutes of air injection.

Water level and pressure measurements were taken at random intervals during the remainder of the third air injection experiment. Table 3 shows the water level and pressure histories of wells 4-3 and 4-4 over three days of air injection. It is important to note that the water level in well 4-4 was still dropping 18 hours after air injection had begun and did not reach its final level for 40 hours. Another important event was the rise in water level and drop in pressure seen in both wells on the third day of air injection. Sometime in the late evening of October 20 or early in the morning of October 21, the air compressor ceased operation. This

Water Level History

Date	Time	Water level well 4-3	Water level well 4-4	Pressure(psi) well 4-3	Pressure(psi) well 4-4
10/18/89	4:20 PM	21.5-22.0' (6.6-6.7 m)	above 20' (6.1 m)	2.5	0.0
	4:29 PM	21.0-21.5' (6.4-6.6 m)	" "	2.5	0.0
	4:50 PM	23.0-23.5' (7.0-7.2 m)	" "	3.8	0.0
	4:53 PM	24.0-24.5' (7.3-7.5 m)	" "	4.7	0.0
	4:54 PM	24.5-25.0' (7.5-7.6 m)	" "	4.9	0.0
	4:55 PM	25.0-25.5' (7.6-7.8 m)	" "	5.0	0.0
	4:58 PM	26.0-26.5' (7.9-8.1 m)	" "	5.3	0.0
	4:59 PM	26.5-27.0' (8.1-8.2 m)	" "	5.5	0.0
	5:00 PM	27.0-27.5' (8.2-8.4 m)	" "	5.8	0.0
	5:01 PM	27.5-28.0' (8.4-8.5 m)	" "	6.0	0.0
	5:02 PM	28.0-28.5' (8.5-8.7 m)	" no change "	6.3	0.0
	5:02 PM	28.5-29.0' (8.7-8.8 m)	" "	6.5	0.0
	5:03 PM	29.0-29.5' (8.8-9.0 m)	" "	6.7	0.0
	5:04 PM	29.5-30.0' (9.0-9.1 m)	" "	6.8	0.0
	5:05 PM	30.0-30.5' (9.1-9.3 m)	" "	no readings	
	5:06 PM	30.5-31.0' (9.3-9.4 m)	" "	7.3	0.0
	5:16 PM	30.5-31.0' (9.3-9.4 m)	" "	9.0	0.0
	5:22 PM	35.5-36.0' (10.8-11.0 m)	" "	9.5	0.0
	5:25 PM	35.5-36.0' (10.8-11.0 m)	" "	no readings	
	5:42 PM	36.0-36.5' (11.0-11.1 m)	" "	no readings	
10/19/89	11:00 AM	36.5-37.0' (11.1-11.3 m)	29.0-29.5' (8.8-9.0 m)	no readings	
	3:45 PM	36.5-37.0' (11.1-11.3 m)	31.5-32.0' (9.6-9.8 m)	no readings	
	5:18 PM	" "	32.5-33.0' (9.9-10.1 m)	no readings	
10/20/89	10:30 AM	" no change "	35.5-36.0' (10.8-11.0 m)	10.0	10.0
	5:45 PM	" "	35.5-36.0' (10.8-11.0 m)	10.0	10.0
10/21/89	5:05 PM	35.5-36.0' (10.8-11.0 m)	35.5-36.0' (10.8-11.0 m)	9.0	9.0

Table 3

stoppage is believed to be the reason for the drop in air pressure and in water level on October 21.

Air pressure was monitored after the air injection experiment had been completed. A pressure of 8 psi was recorded on both monitor wells on October 24, three days after air injection ceased. Well caps were removed on October 24 to allow the water level to return to a level from which water samples could be taken. When the caps were removed, air rushed from the wells for quite some time in a manner similar to previous experiments in which the pressure was released immediately after the experiment has been completed. This proves that air containment, at least around the wells at site 4, can be sustained for at least 3 days.

Inorganic Chemical Analysis

Before and after the second and third air injection experiments at site 4, water samples were taken from three locations on the Robinson tract. The water samples were taken from wells 1-2 and 4-2 (Figure 9), and a spring located northeast of site 4 (Figure 4). Water samples were taken before and after air injection to study the effect of injected air on the formation water chemistry. Before sampling, water was bailed from the wells to ensure that formation water was being collected. Approximately 5 gallons (19 l) of water were bailed before sampling for the second air injection experiment at site 4. Approximately 8 gallons (30 l) of water were bailed before sampling for the third experiment at site 4.

The results of the chemical analysis before and after the second and third air injection experiments at site 4 are shown in Table 4. The major

INORGANIC CHEMICAL ANALYSIS

Log #	sp cond (umho)	pH	Ca (ppm)	Mg (ppm)	Na (ppm)	K (ppm)	Sr (ppm)	CL (ppm)	SiO_2 (ppm)	SO_4 (ppm)	HCO_3 (ppm)	NO_3 (ppm)	Fe (ppb)	Mn (ppb)	Location	Date
890486	560	7.2	106	3.5	10	0.9	0.2	3.8	19	25	339	3.0	<29	<7	old inj. site	7/18
890487	353	7.0	47	7.3	12	1.4	0.3	3.5	22	29	189	1.1	9100	2500	site #3	7/18
890488	443	7.6	82	3.3	8.3	0.6	0.2	3.1	25	16	264	8.4	49	55	spring	7/18
890534	570	7.3	109	3.6	11	1.2	0.2	5.8	21	24	337	3.2	46	10	old inj. site	7/31
890535	345	7.0	45	7.3	13	1.5	0.3	5.3	23	31	174	1.1	1700	3900	site #3	7/31
890536	448	7.6	84	3.5	8.4	0.6	0.2	4.4	26	16	260	9.1	130	110	spring	7/31
890841	550	7.4	104	3.3	10	0.7	0.2	3.5	20	22	328	2.2	240	52	old inj. site	10/16
890842	328	7.3	41	6.8	12	0.9	0.3	3.8	28	31	166	0.7	900	2800	site #3	10/16
890843	465	7.6	85	3.4	8.4	0.5	0.2	3.1	26	16	275	7.2	78	110	spring	10/16
890863	542	7.4	103	3.2	10	0.5	0.2	3.5	20	22	328	2.1	230	24	old inj. site	10/25
890864	300	7.4	38	6.0	12	0.9	0.2	4.2	28	31	143	1.1	110	1800	site #3	10/25
890865	466	7.6	85	3.3	8.3	0.5	0.2	2.6	25	16	276	7.4	110	42	spring	10/25

Table 4

finding in this experiment is the change in iron content after air injection in well 4-3. During both air injection experiments, the iron content dropped by more than 80% from their levels before air injection. The decrease in iron content is the result of oxygen causing iron to precipitate from solution. The drop in iron content from 9100 ppb to 900 ppb between the samples taken before air injection in the second and third air experiments at site 4 is thought to be due to the added bailing of well 4-2 before the third air experiment. The iron content near well 4-2 may have been artificially high because the entire length of the well, including the screen, was made of steel. The screen in well 1-2 was made of plastic. In addition to added bailing, the decrease in iron content may also be due to continued precipitation of iron from the second air experiment. In any case, the injection of air apparently changes the oxidation environment enough to substantially change the iron content in the water.

Conclusions from Air Injection Testing and Chemical Analysis

The final air injection experiment at site 4, like the initial air injection experiments, produced evidence that the air travels preferentially within the sand layer below the capping clay layer of the Newman terrace deposits. It appears that wells 4-1, 4-2, and 4-3 are positioned along a line of preferential air flow, at least relative to the direction connecting wells 4-1 and 4-4.

The water level and air pressure measurements taken at site 4 were made for two specific reasons: to ensure that air was traveling from the air injection well to the monitor wells and to estimate the relative amount of air traveling to the monitor wells. In every air injection experiment, air was observed at each monitor well. However, the rate at which air reached each monitor well and forced down the water level differed greatly.

Neither the spring nor the initial air injection site was affected by air injection at site 4. Even though the preliminary air injection site did not show any signs that air from well 3-1 reached this location, the possibility of an area several hundred feet across being affected by air is still good. Because the spring was located above the elevation and stratigraphic location of the alluvial deposits, it is probably not connected to the alluvial aquifer. In addition, inorganic chemical analysis does not reveal how the organic environment is affected by air injection. The air could be promoting biological changes in the normally anaerobic environments.

SEISMIC GOAL AND TEST SUMMARY

Seismic Goals

To test the validity of the seismic model, experiments at a site with recordable reflection information and suitable air containment were necessary. The Newman terrace deposits on the Robinson tract fulfill air injection and containment criteria. However, several other seismic properties are desirable in an air injection location:

1. High-frequency broad-bandwidth reflection information.
2. More than one reflection.
3. Reflections at near-vertical incidence.

Increasing the high-frequency content and broadening the bandwidth of reflection information increases resolution of target zones (Widess, 1973). This is important when analyzing detailed seismic events.

Reflection events at the clay/sand interface, below which the air would be pumped, and below the clay/sand interface indicated that this area was an ideal location for this study. A reflection at the clay/sand interface would allow a check for spectral changes as a result of injected air. Reflection events below the clay/sand interface could be checked for changes in arrival time and spectral changes resulting from the presence of air.

Finally, reflection information gathered near the critical angle can cause amplitude and phase distortion of the resulting data (Pullen and Hunter, 1985). A comparison in wavelet character between seismic data collected before and after air injection at near-critical angle would leave many questions, such as how much change was due strictly to the air and how much to the angle of incidence, unanswered.

Seismic Test Summary

Once successful injection and containment of air and proper acquisition equipment had been attained, planning was begun for a combined air injection and seismic experiment. The remainder of the study was completed in 1989. During the last two weeks of March, three additional sites on the Robinson tract were seismically investigated as possible locations for combined experiments. Site 4 showed prominent shallow reflections, and three wells were drilled there for later experiments (Figure 4).

Over the next four months, two air injection and seismic experiments and several supporting seismic test experiments were conducted at site 4. Extensive seismic testing was conducted before each air injection experiment. The experiments were designed to test combinations of acquisition equipment and recording parameters that would give the greatest chance for detection of air using seismic reflection techniques.

The first air injection experiment was conducted at site 4 in May. A single CDP line and set of walkaways were run before and after air was injected into the ground. The quality of the seismic data from the first air injection experiment was extremely poor and produced no evidence that injected air had been detected.

A second air injection experiment was planned with knowledge gained from the first air injection experiment and the seismic testing. For this experiment three separate CDP lines were collected. Each line was designed for a separate target in hopes that one line would produce evidence of injected air. Although the quality of seismic data improved considerably over the first air injection experiment, none of the lines provided conclusive evidence that air had been detected.

Conclusions made from the first two air injection experiments were used to formulate a third and final air injection experiment. The quality of seismic data in the final air injection experiment improved again. Although a difference that might be linked to air was found between pre-air and post-air data sets, the change was small. A calculation of the experimental error was made to determine whether the small changes were significant. A final seismic test was conducted at site 4 to acquire the data necessary for the error calculation.

AIR EXPERIMENTS I AND II

The following section is an account of the seismic testing and the first two combined air-injection seismic experiments along with the conclusions made from these experiments.

Seismic Testing I

On March 22, seismic test site 1 was chosen to test for reflection information (Figure 4). For this test, the 30.06 rifle was used as a source with two 100 Hz geophones grouped in series as receivers. Field observation of the recorded data showed both the possibility of a shallow intra-alluvial reflection and a deeper reflection from the alluvial-bedrock interface or deeper. More detailed study in the laboratory showed that the first arrival was the 1100 ft/s (335 m/s) air-coupled wave and what that was believed to be the shallow reflection event was actually a refracted event (Figure 12). The first refractor was calculated to be at a depth of 1.5 feet (.46 m) and began at a critical distance of .75 feet (.22 m). The deeper event (~60 ms) is still believed to be a reflection. Spectral analysis indicates that the dominant frequency of this event is nearly 400 Hz (Figure 13).

Site 3 was chosen in the far western portion of the Robinson tract (Figure 4). On March 27, a walkaway noise spread was collected parallel to a fence running east-west along the property boarder. The acquisition parameters used for this test were similar to those run on the March 22 experiment. No usable reflection information was found during this

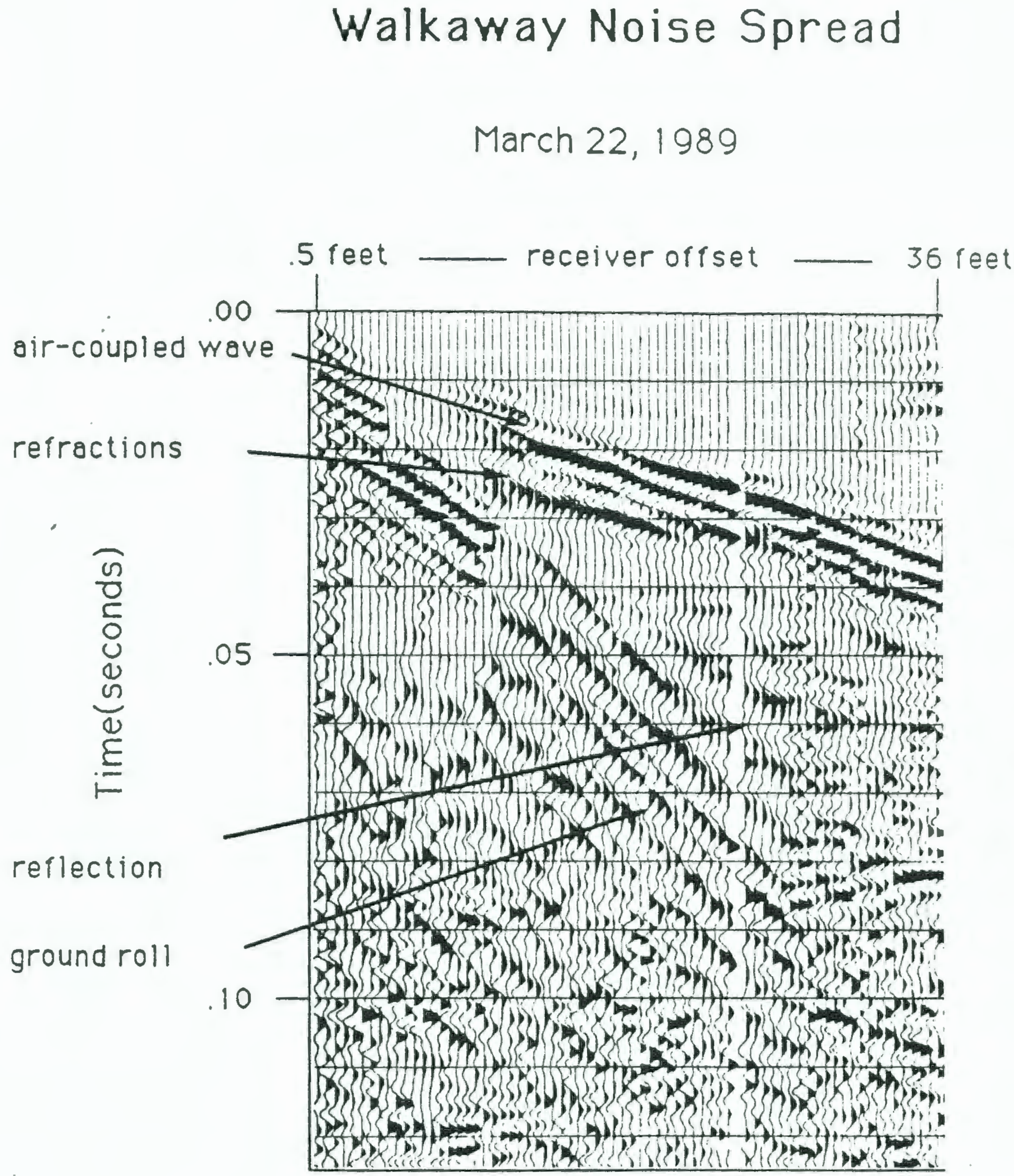

Figure 12. This walkaway was collected using 340 Hz low-cut filters. The space in the walkaway is due to a bad trace.

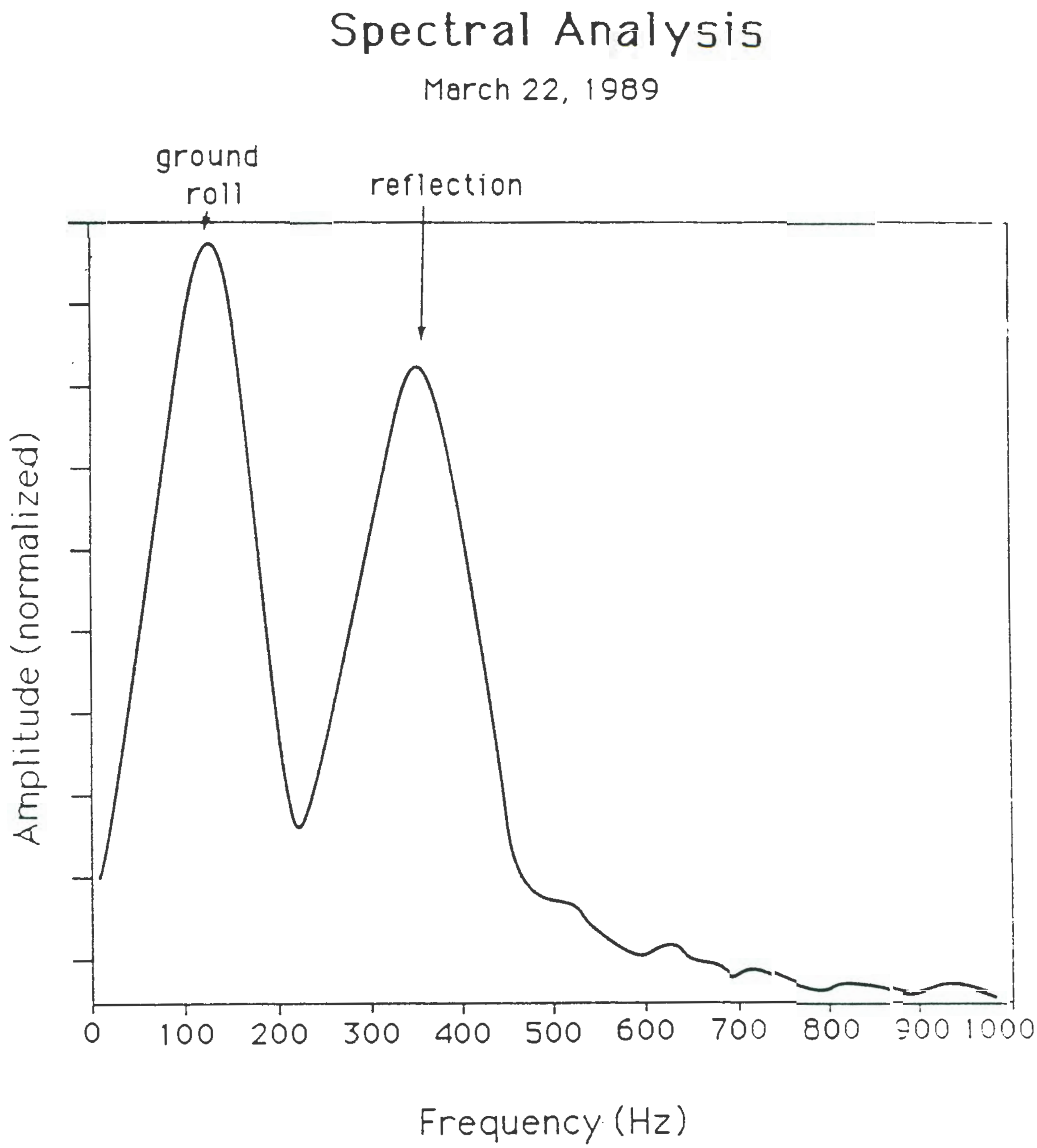

Figure 13. Spectral analysis of the reflection found at site #1.

experiment because of intense interference from the air-coupled wave (Figure 14).

On March 29, a fourth experimental site, site 4 was chosen just south and east of the third experiment (Figure 4). Like site 3, the walkaway noise test was also run in an east-west direction. Most of the acquisition parameters were the same as those used to collect the data at sites 2 and 3. However, before planting the geophones for this experiment, a truck was run back-and-forth along the line to pack the ground. Compacted near-surface soil produces a better ground coupling with the geophones and reduces the attenuation of seismic energy in the extreme near-surface. Testing at this site produced several reflection events (Figure 15), between 50 ms and 70 ms and another near 90 ms. The dominant frequency of the recorded reflection information from this site was nearly 300 Hz (Figure 16).

In addition to using the downhole 30.06 rifle as source at this site, a surface 30.06 rifle source with a silencer was used to try to reduce the effects of the air-coupled wave. Several test shots using the surface source and silencer were found to increase air-coupled wave amplitude and degrade reflection quality of the data (Figure 17). In addition, it was noticed that the refracted arrival was lower in frequency and nearly 10 ms later on the surface 30.06 rifle field records.

Site 4 was chosen as the location for the air injection experiments because of the high quality of reflection information collected there. During May, three 41-feet (12.5-m) deep wells were drilled twelve feet apart along the seismic test line at site 4. The wells were placed along the

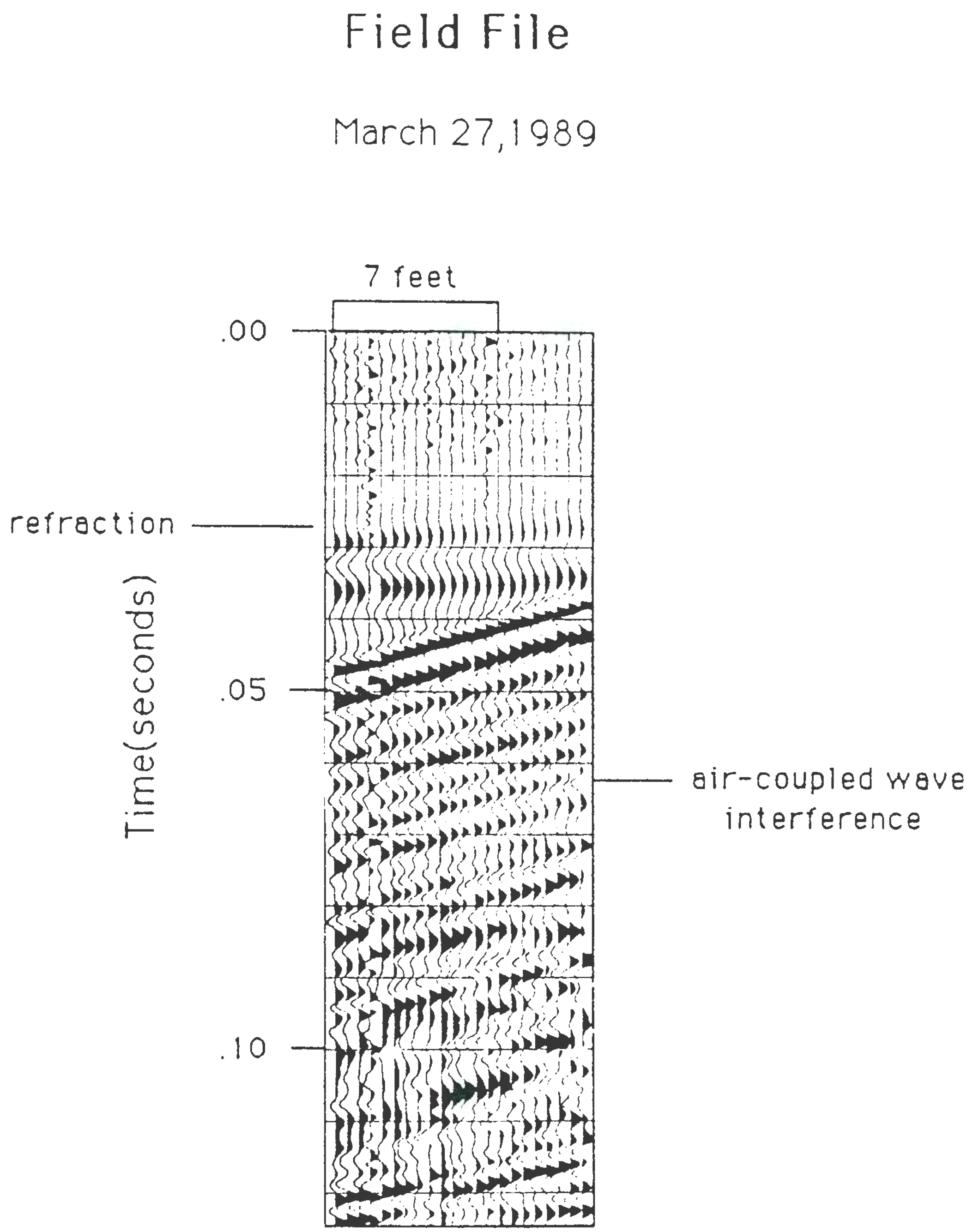

Figure 14. This field file was collected using 220 Hz low-cut filters. The air-coupled wave interference is thought to be due to seismic energy reverberating off nearby trees.

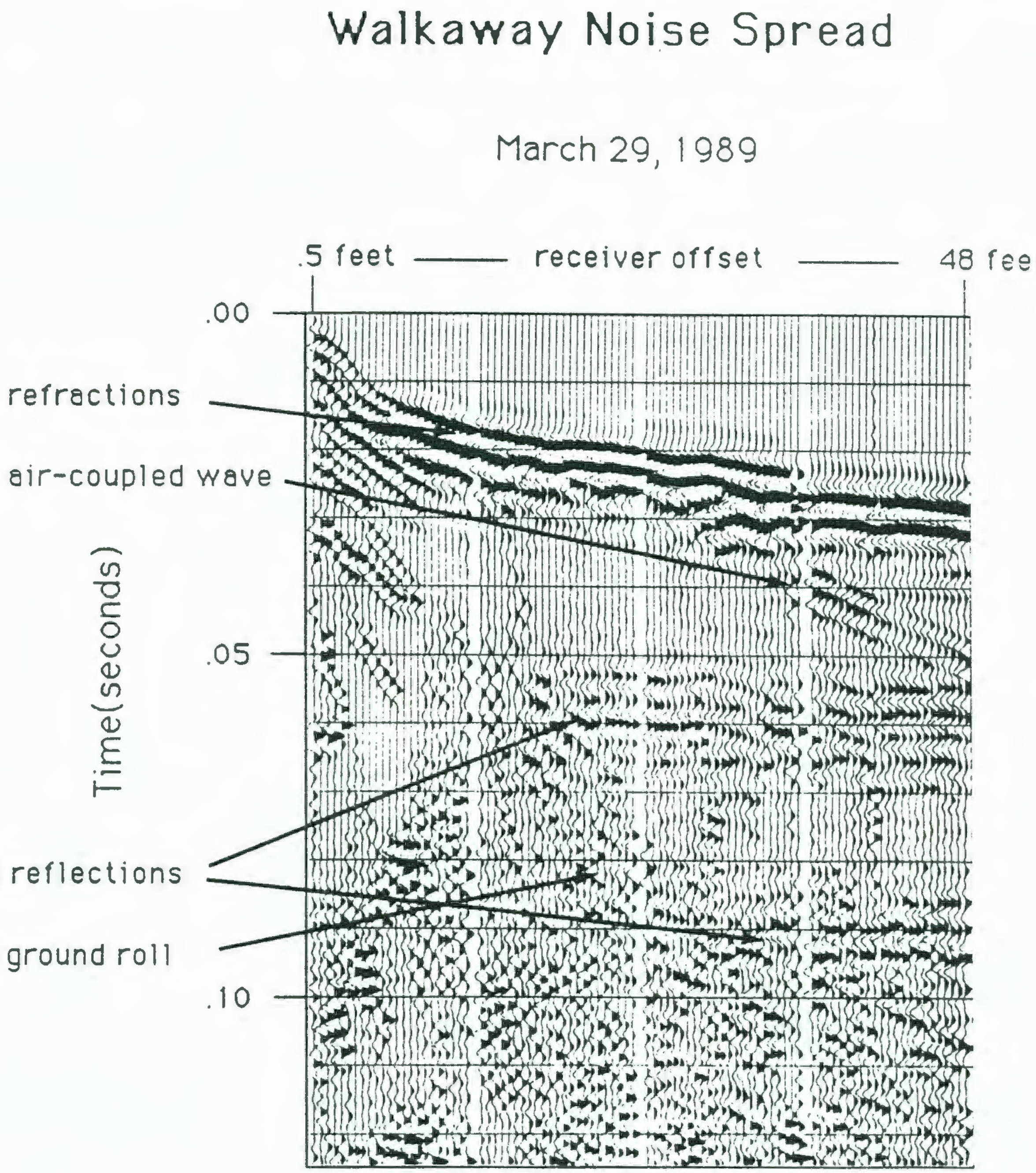

Figure 15. This walkaway was collected using 340 Hz low-cut filters. Once again the spaces in the walkaway are due to bad traces.

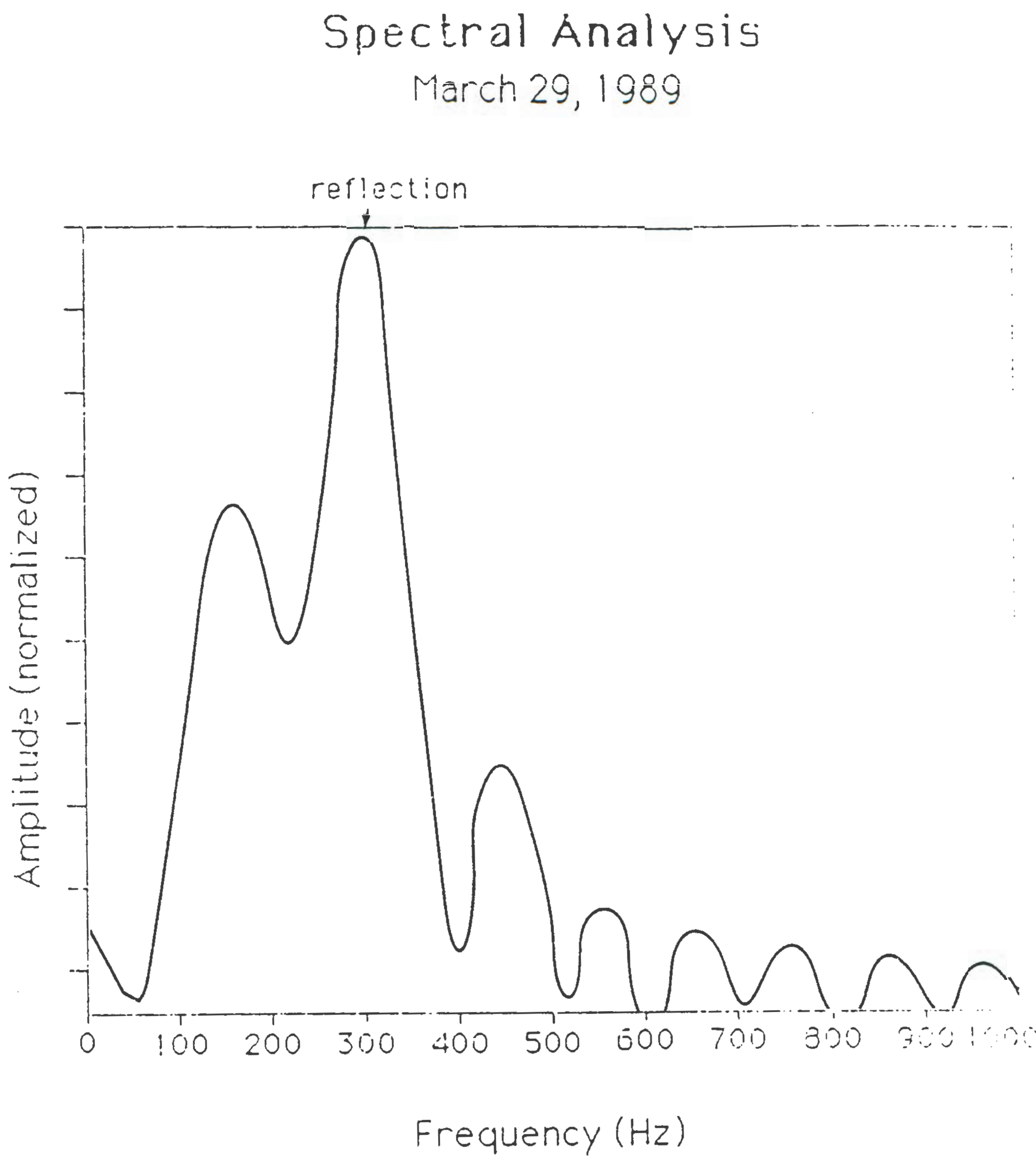

Figure 16. Spectral analysis of the reflected events at site #3.

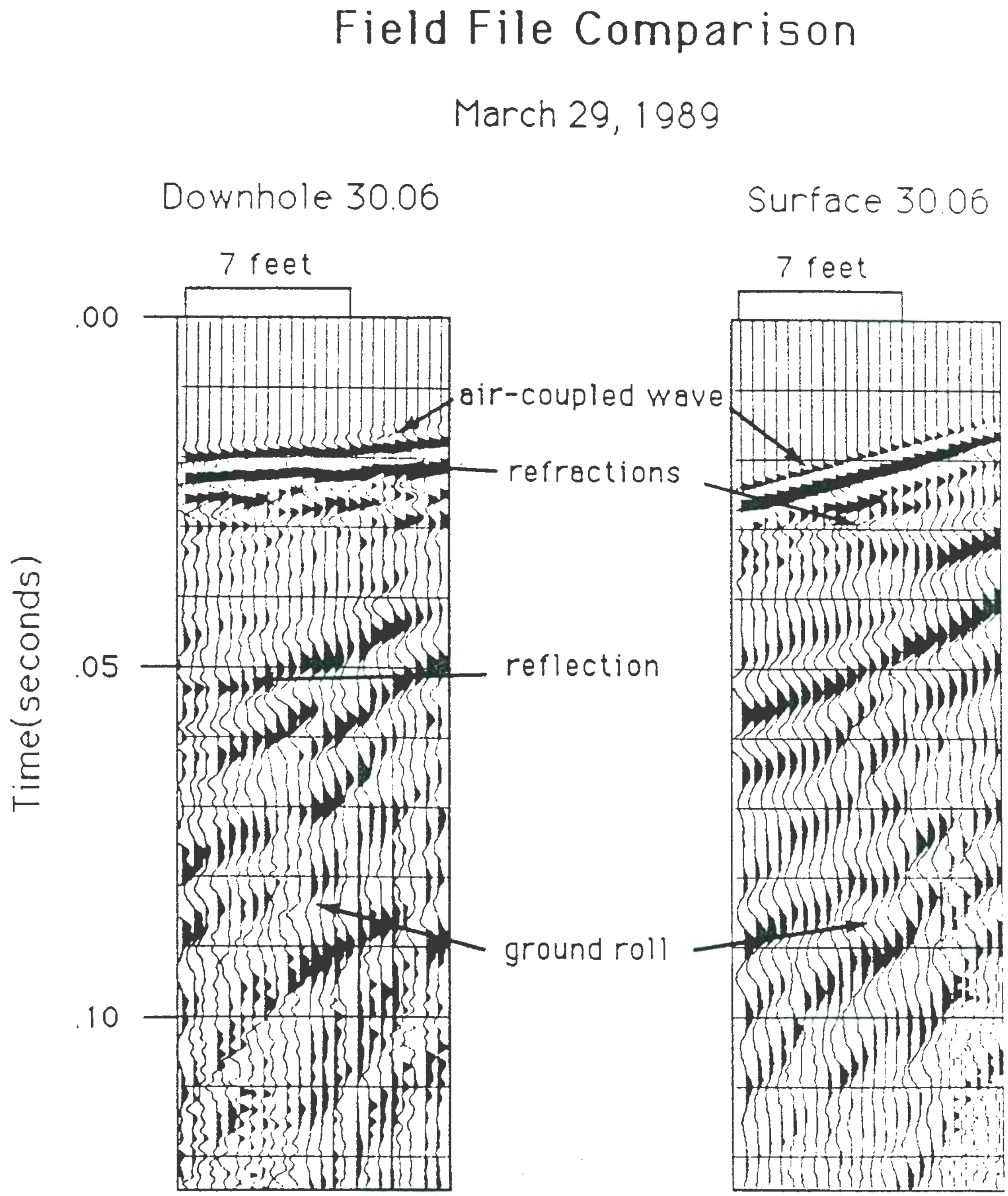

Figure 17. Notice that a reflected event can be seen on the downhole 30.06 field file which is not seen on the field file produced by the surface source. These field files were collected using 340 Hz low-cut filters.

same line from which the walkaway-noise spreads were acquired on March 29. One of the three wells was used for injection, and the other two were for monitoring.

On May 23, a walkaway noise test using similar acquisition parameters to the test on March 29 was run at site 4. The line was placed within 1 feet (.3 m) of the injection and monitor wells to simulate the March 29 walkaway as nearly as possible. The receivers, however, were not placed in tire tracks because of the proximity of the line to the wells. The reflection information from this test was of much poorer quality than the March 29 data (Figure 18). Disturbed ground near the wells, interference from diffractions off the wells, and changes in the coupling of geophones were all possible reasons for the reduction in data quality.

On May 24, another suite of tests was conducted to determine better seismic acquisition parameters for the air experiment. Once again, two 100 Hz geophones were placed in 6 inches (.2 m) group intervals; and the downhole 30.06 rifle was used as the source. The walkaway noise test was run approximately 10 feet (3 m) south of the wells with geophones planted in tire tracks and parallel to the previous seismic test lines. This experiment produced reflection information similar to the data recorded on March 29 (Figure 19). Once again the dominant frequency of the reflection data was nearly 300 Hz (Figure 20).

Additional testing was run on May 24 to further enhance recordable reflection energy. The first additional experiment involved stacking several records together. Summing records, like using multiple geophones, can increase the amplitude of the reflection energy relative to

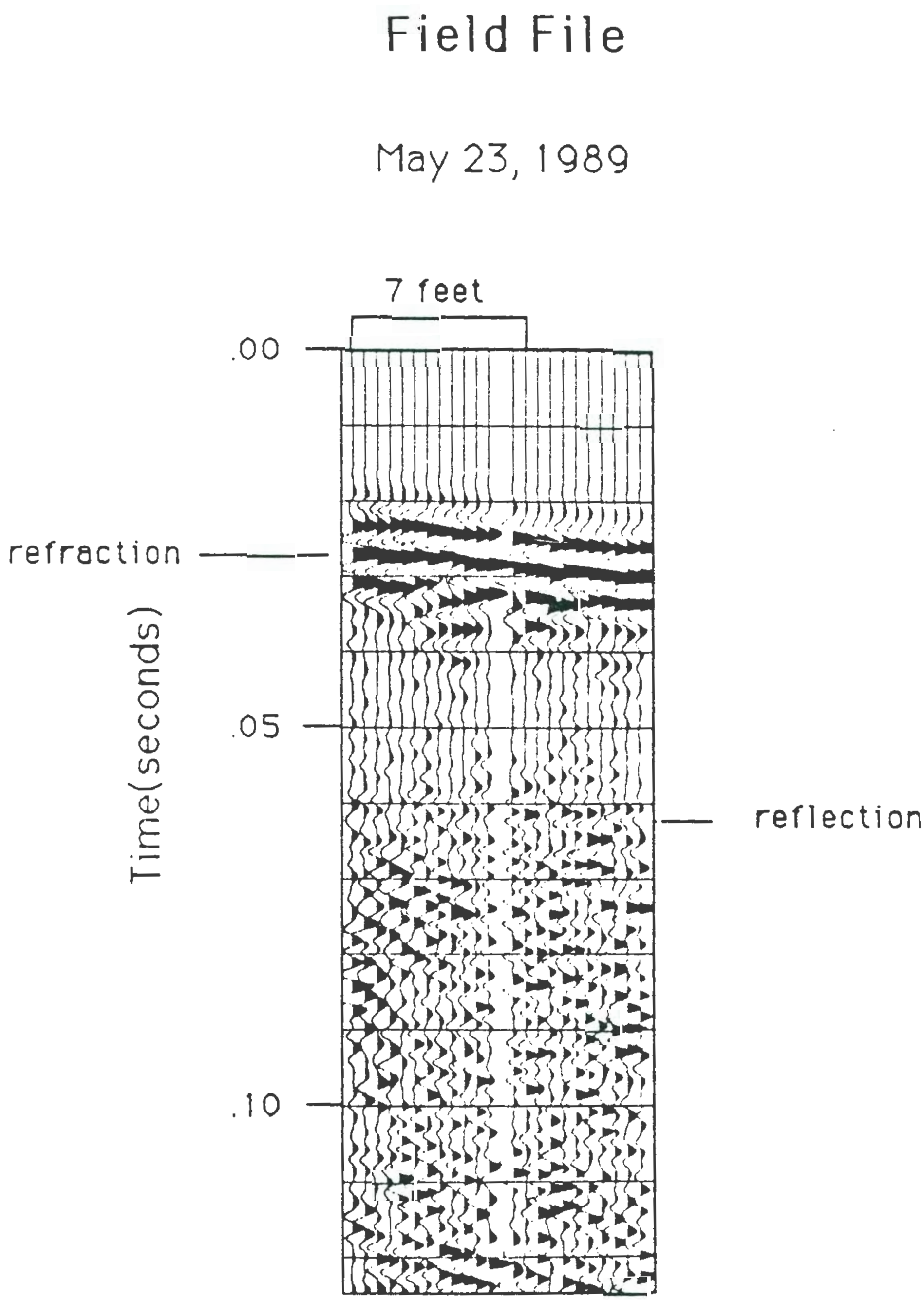

Figure 18. Notice the lack of seismic events other than the refracted arrival and a weak reflection event. The field file was collected using 340 Hz low-cut filters.

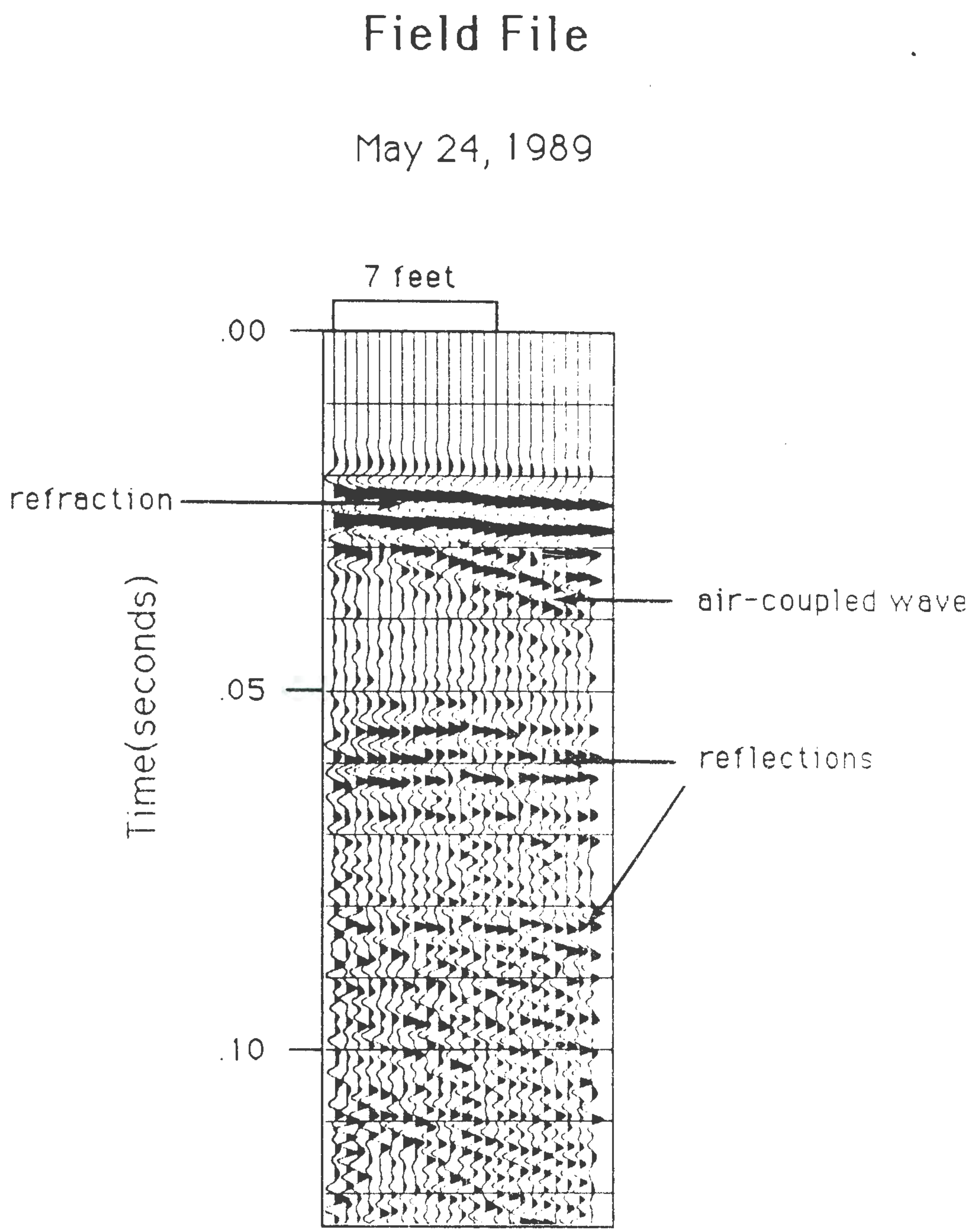

Figure 19. The field file was collected using 340 Hz low-cut filters.

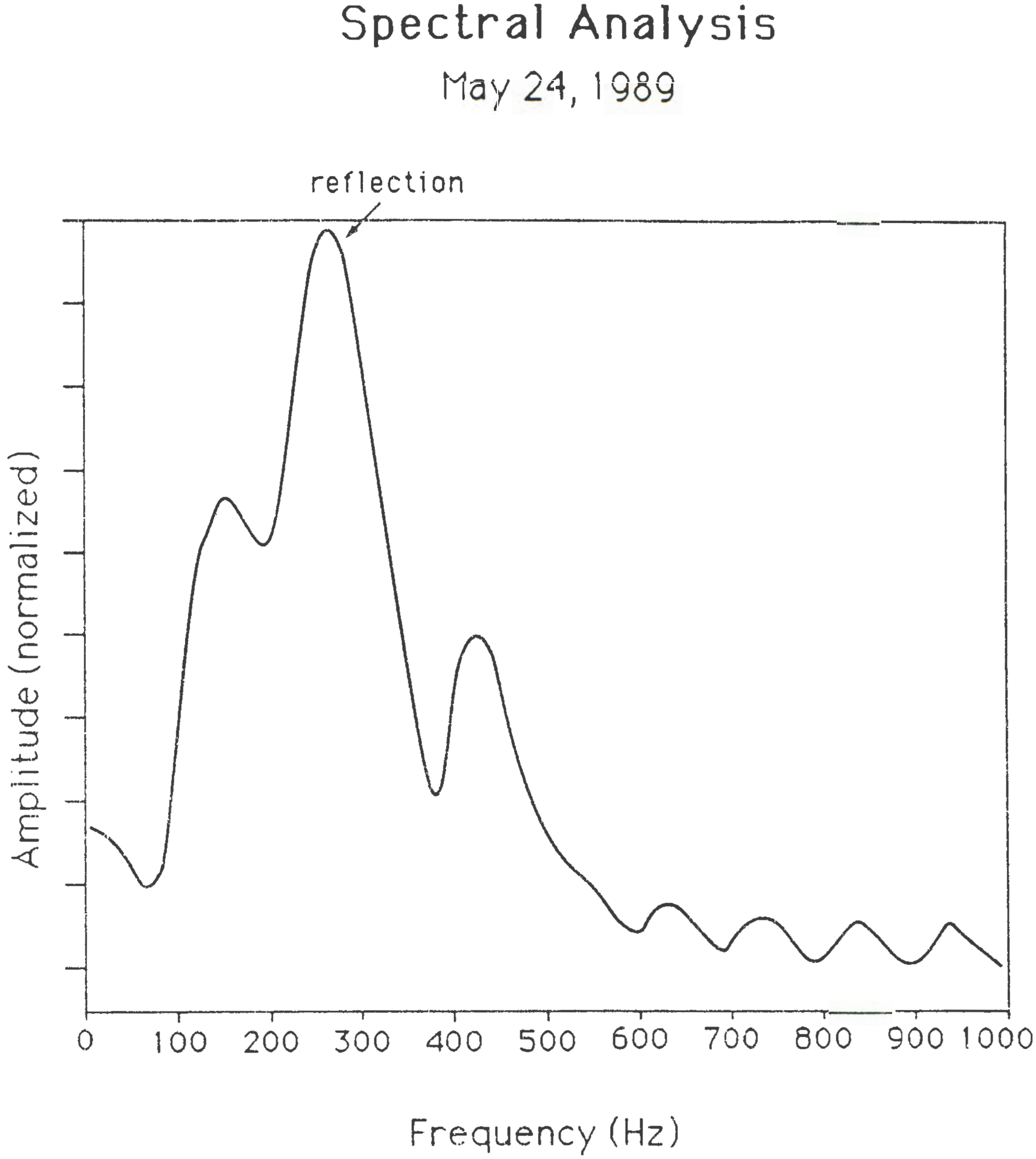

Figure 20. Spectral analysis of the reflected events at site #3.

random noise. The resulting record does not show significantly higher quality data than the record from a single shot (Figure 21). The second additional experiment measured the effects of shot hole depth and reused shot holes when compared with unused shallow shot holes. Reflection events recorded when the source was fired in holes 3 feet (.91 m) deep are more easily seen than those from the shots fired in shallow unused holes 6 inches (.15 m) deep. The best data came from source holes of >3 feet (.91 m) where multiple 30.06 rifle shots had already been fired (Figure 22). On both of the deeper shots, the effect of ground roll was greatly reduced. The sources were fired both in the tire track and out. There was no visible affect on the resulting data.

Air Experiment I

Upon successful acquisition of reflection data on May 24, the first air injection experiment was conducted at site 4. Air injection experiment I was completed in three parts: acquisition of a shallow seismic reflection CDP line and walkaway noise spread, injection of air, and acquisition of another shallow reflection CDP line and walkaway noise spread immediately after injection of air.

Using the results from the May 24 tests, acquisition parameters were assigned for the seismic portion of Air Injection Experiment I (Table 5). A 20 feet (6 m) source to first receiver offset was chosen from the walkaway noise spreads to maximize the amount of reflected energy collected during a single shot (Figure 23). The station interval was lengthened from 6 inches (.15 m) to 1 feet (.3 m) for the air injection experiment to increase

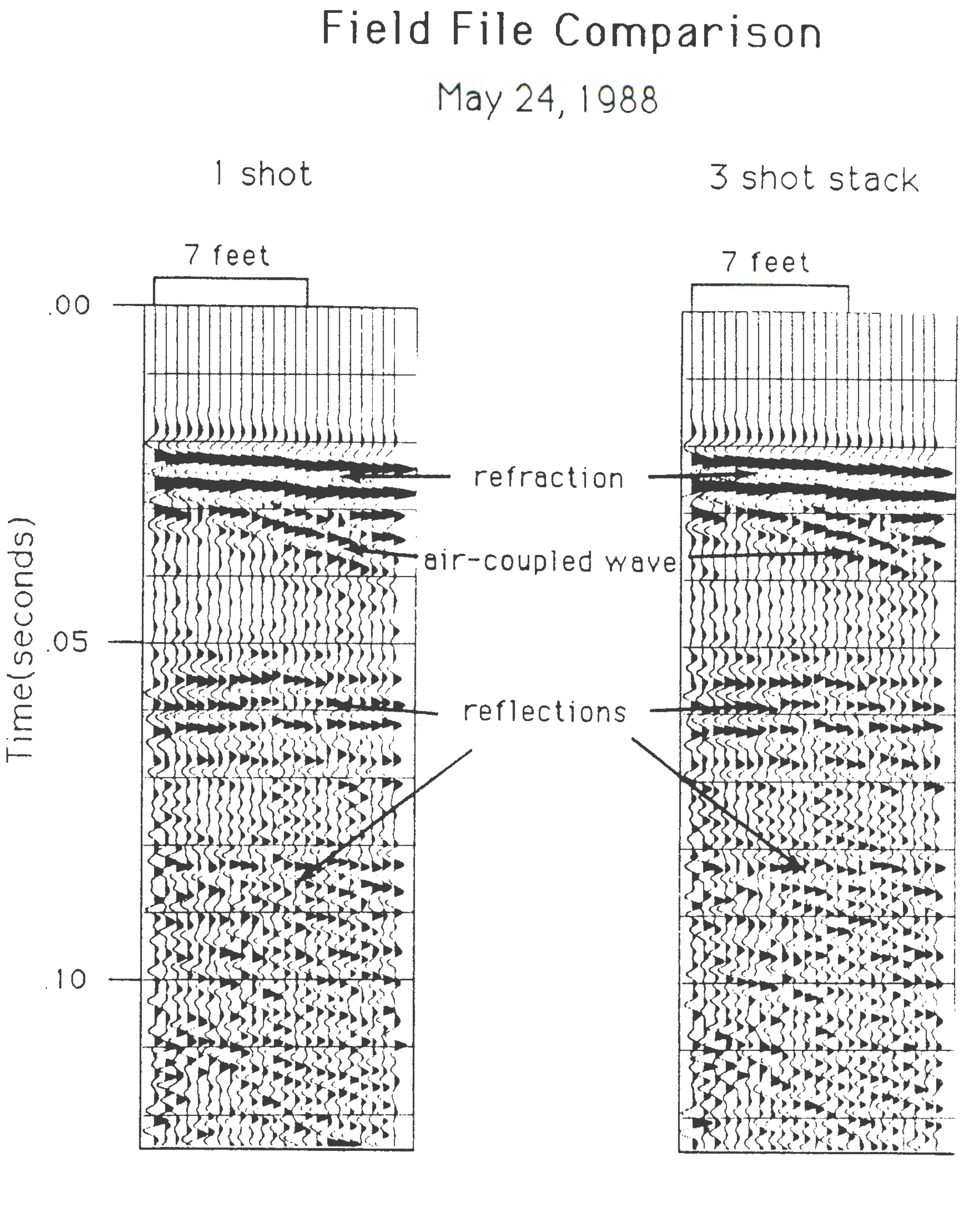

Figure 21. Both were recorded using 340 Hz low-cut filters.

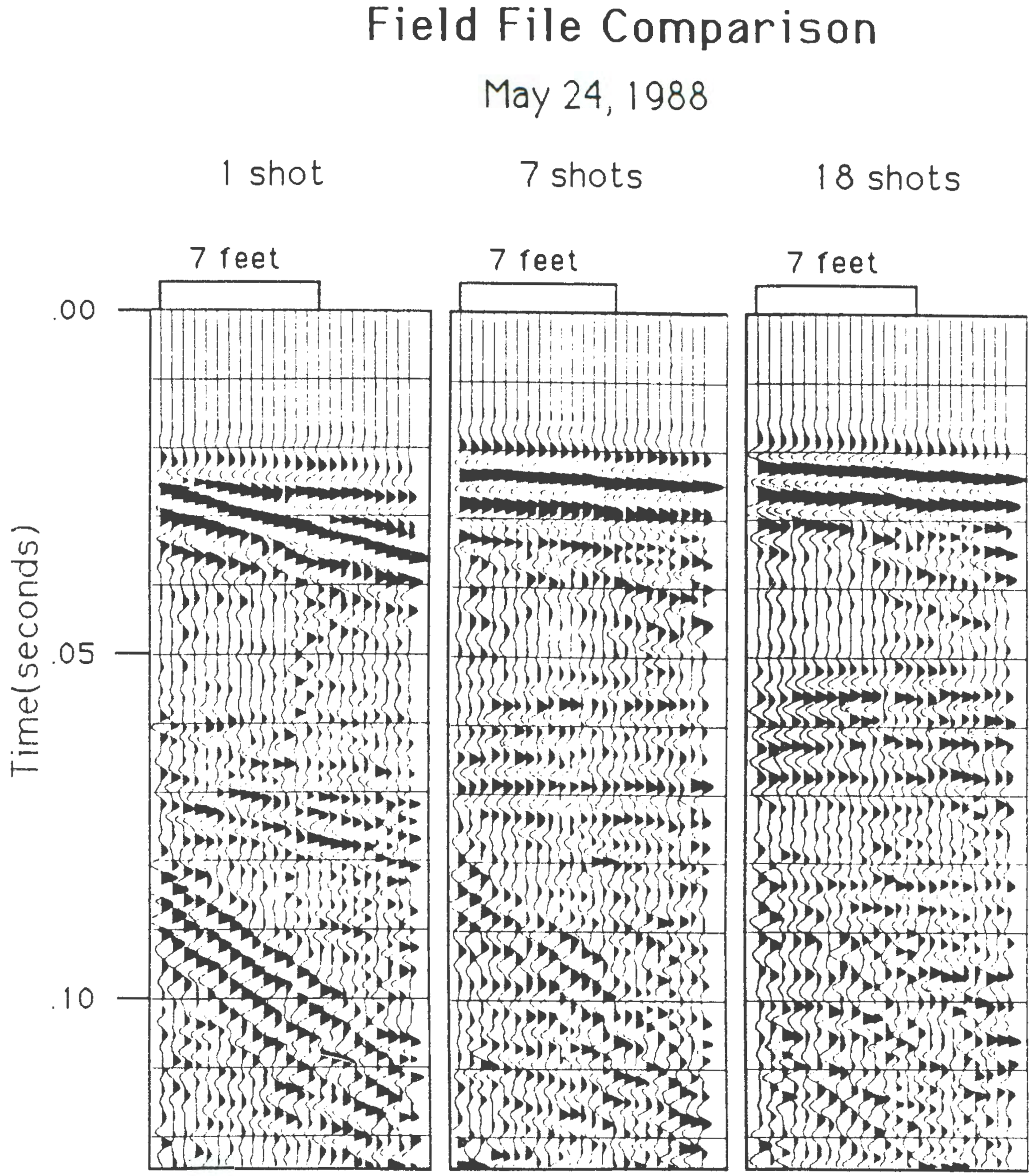

Figure 22. Notice the decrease in arrival time, decrease in ground roll, decrease in air-coupled wave, and increase in reflection strength as more shots are fired in the same hole. All of the shots were collected using 240 Hz low-cut filters.

Recording Parameters

SEISMOGRAPH (DHR 2400):	PARAMETERS
LOW-CUT FILTERS (24 dB/octave rolloff)	220 Hz
HIGH-CUT FILTERS (24 dB/octave rolloff)	none
ANTIALIAS HIGH-CUT FILTER (60 dB point)	3000 Hz
NUMBER OF SAMPLES	500
SAMPLE INTERVAL	1/4 ms
RECORD LENGTH	125 ms

SOURCE:	PARAMETERS
TYPE	downhole 30.06
SPACING	1' (.30 m)

RECEIVERS:	PARAMETERS
TYPE (natural frequency)	100 Hz Marks Products
GROUP SPACING	1' (.30 m)
ARRAYS (connected in series)	2 geophones, .75' (.23 m)
RECORDING GEOMETRY	end-on geometry
SOURCE-NEAR-RECEIVER DISTANCE	20' (6.1 m)
SOURCE-FAR-RECEIVER DISTANCE	43' (13.1 m)

WEATHER/SOIL CONDITIONS	PARAMETERS
WIND SPEED	calm
WIND DIRECTION	not recorded
NEAR-SURFACE MATERIAL	soil
NEAR-SURFACE MOISTURE	damp dew
TEMPERATURE	65° F (18° C)

Table 5

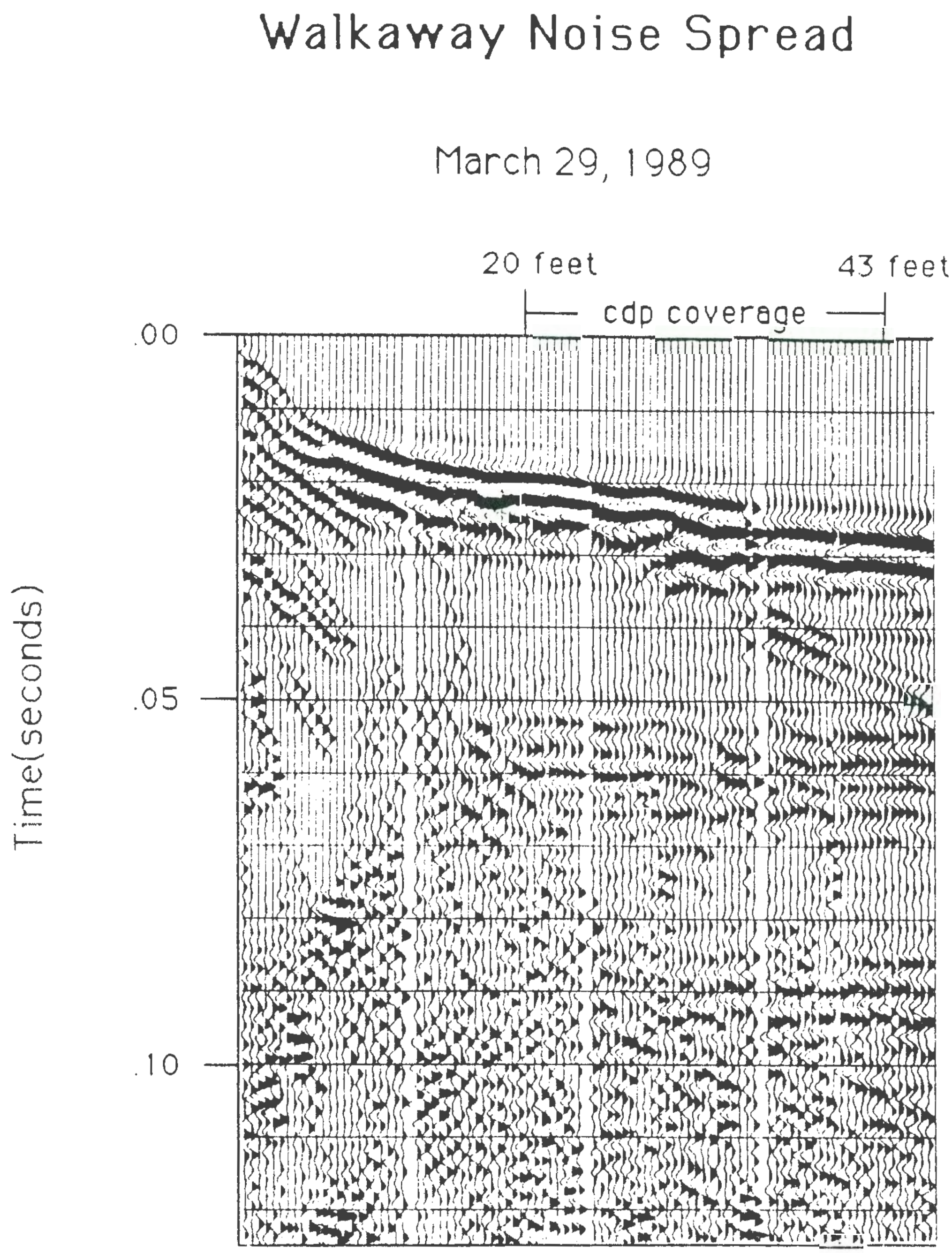

Figure 23. The walkaway noise spread from March 29, 1989 displays the entire CDP coverage. Notice that the coverage window is outside the effects on the ground roll on the 60 ms reflector and is large enough to record a portion of the event at 90 ms.

subsurface coverage and the source-to-far receiver offset for improved velocity calculations while maintaining an acceptable level of reflector coherency. Two shot holes were drilled at each source location; one for the seismic experiment before air injection and another for after. Geophones were planted on tire tracks in previously undisturbed ground 3 feet (.9 m) north of the air injection wells. Figure 24 shows the location of the resulting CDP coverage.

Because deeper holes had been shown to decrease interference from ground roll and air-coupled wave, 3.75 feet (1.14 m) deep shot holes were drilled for the downhole 30.06 rifle source. This hole depth was the maximum depth that the auger bit could drill. An additional attempt was made to decrease ground roll effects by placing each 100 Hz set of two geophones .75 feet (.23 m) apart in an inline array. Properly designed geophone arrays reduce the amplitude of undesirable seismic energy by spacing the geophones within a group so that the frequencies corresponding to undesirable apparent seismic wavelengths will add destructively.

On the morning of May 26, a 72-feet (22-m) walkaway noise spread and a 58 shot point CDP line were acquired at site 4. All pre-air injection seismic data was collected before 9:30 A.M. that day.

At 3:00 PM on May 26, air injection began at site 4. Air was injected in well 4-1, and wells 4-2 and 4-3 were used for monitoring.

At 7:30 A.M., on May 27, sixteen hours and thirty minutes after air injection had begun, the air compressor was shut off and seismic acquisition began. Another CDP line was collected using the same

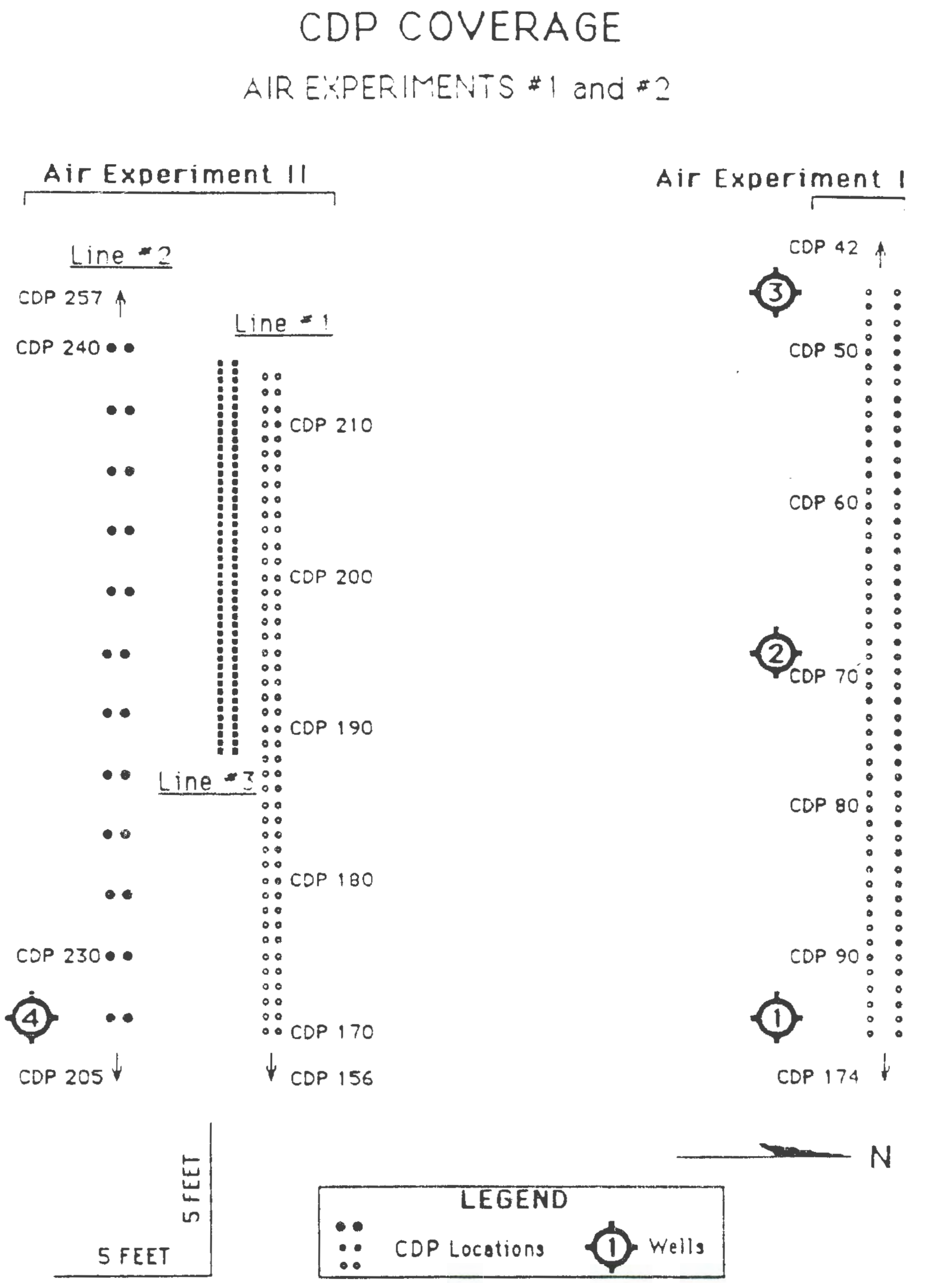

Figure 24. CDP coverage and well locations for Air Experiment I and II at site #3.

acquisition parameters as the previous day. A walkaway noise spread was again collected, although the gain settings were not the same as those used during the pre-air injection walkaway noise spread experiment. Acquisition of all seismic data was completed by 9:00 A.M. that morning.

The reflection data collected on May 26 and May 27 during the air injection experiment had a much lower signal-to-noise ratio than the test data collected on May 24. More than three-quarters of the 58 CDP shots had no visible reflection energy present in either data set. In fact, not one pre-air field file and its corresponding post-air field file could be found with reflections to compare. The air-coupled wave was so prominent throughout the entire record that amplitude versus frequency analysis of the data was of no value.

Frequency filtering, using a narrow band-pass filter, was applied to the CDP data to attempt to bring out hidden reflected energy by decreasing the amplitude of unwanted seismic energy while permitting desirable reflection energy to pass unaffected. Unfortunately, even frequency filtered records with the most reflection energy were of poorer quality than the test data taken on May 24 (Figure 25).

CDP processing was next attempted on the data taken before the injection of air on May 26 in hopes that a reflection could be uncovered during the stacking process. Table 6 shows the processing flow used to create a final stacked section. An event occurring at near 70 ms on field file 59 was selected as the target reflection. Unfortunately, stacking did not produce a coherent reflection event on a CDP section (Figure 26). There appears to be some interference in this section as a result of the air-coupled

CDP Field Record

May 26, 1989

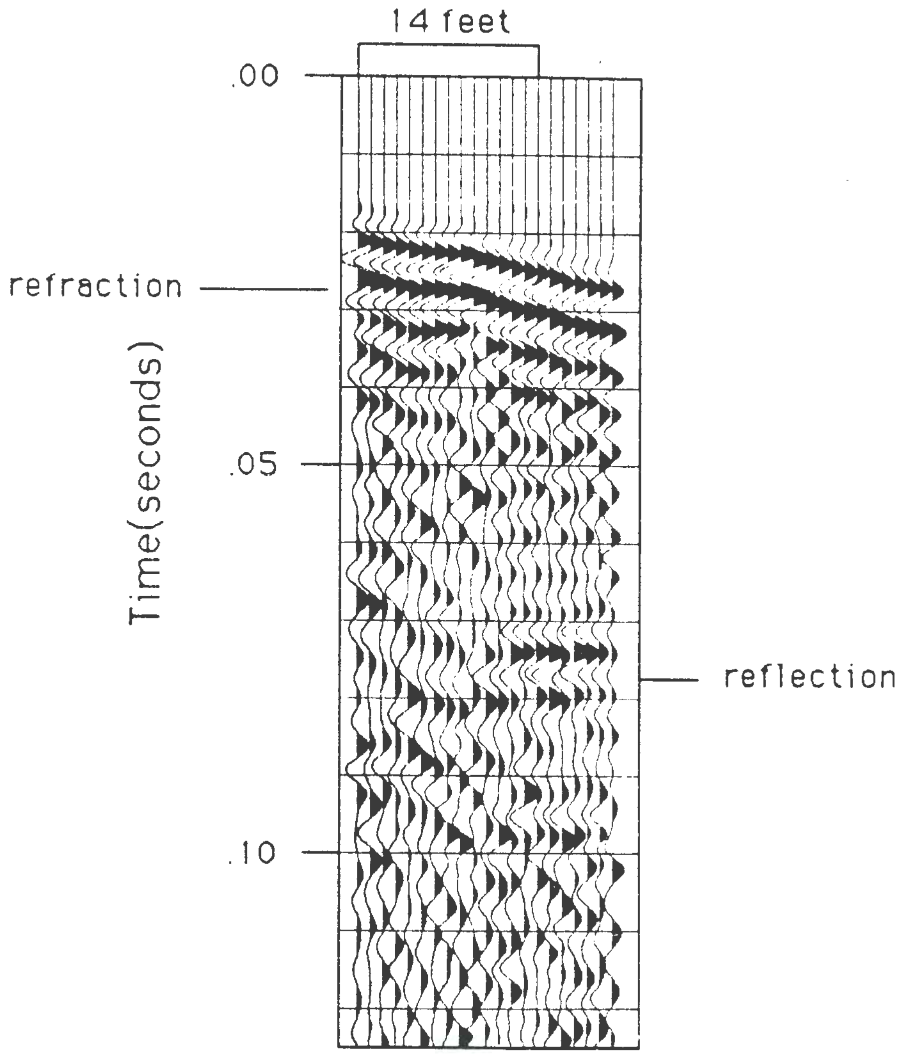

Figure 25. This field file was the best field file taken during the May 26-27 air experiment. The reflected event seen between 70 ms and 80 ms was focused on during CDP processing.

Processing Flow

Processing Step	Description
1. Bad trace editing	Seismic traces of poor quality or dead during acquisition were removed.
2. CDP sort	Seismic traces were sorted into gathers containing the same midpoints (common-depth points).
3. NMO correction	Shift applied to the CDP gathers to correct for the time differential due to different source to receiver offsets.
4. Automatic statics	Surface-consistent time shifts applied to CDP traces to correct for near-surface velocity anomalies at a shot or receiver. The same auts table was used for both before- and after-air data sets.
5. Frequency filter	A process used to reduce the amplitude of unwanted seismic energy while leaving the desired seismic energy alone.
6. Stack	A linear addition of samples from same CDP location into one trace to enhance the data.
7. AGC scaling	A step which boosts the amplitude of events occurring later in the seismic record.

Table 6

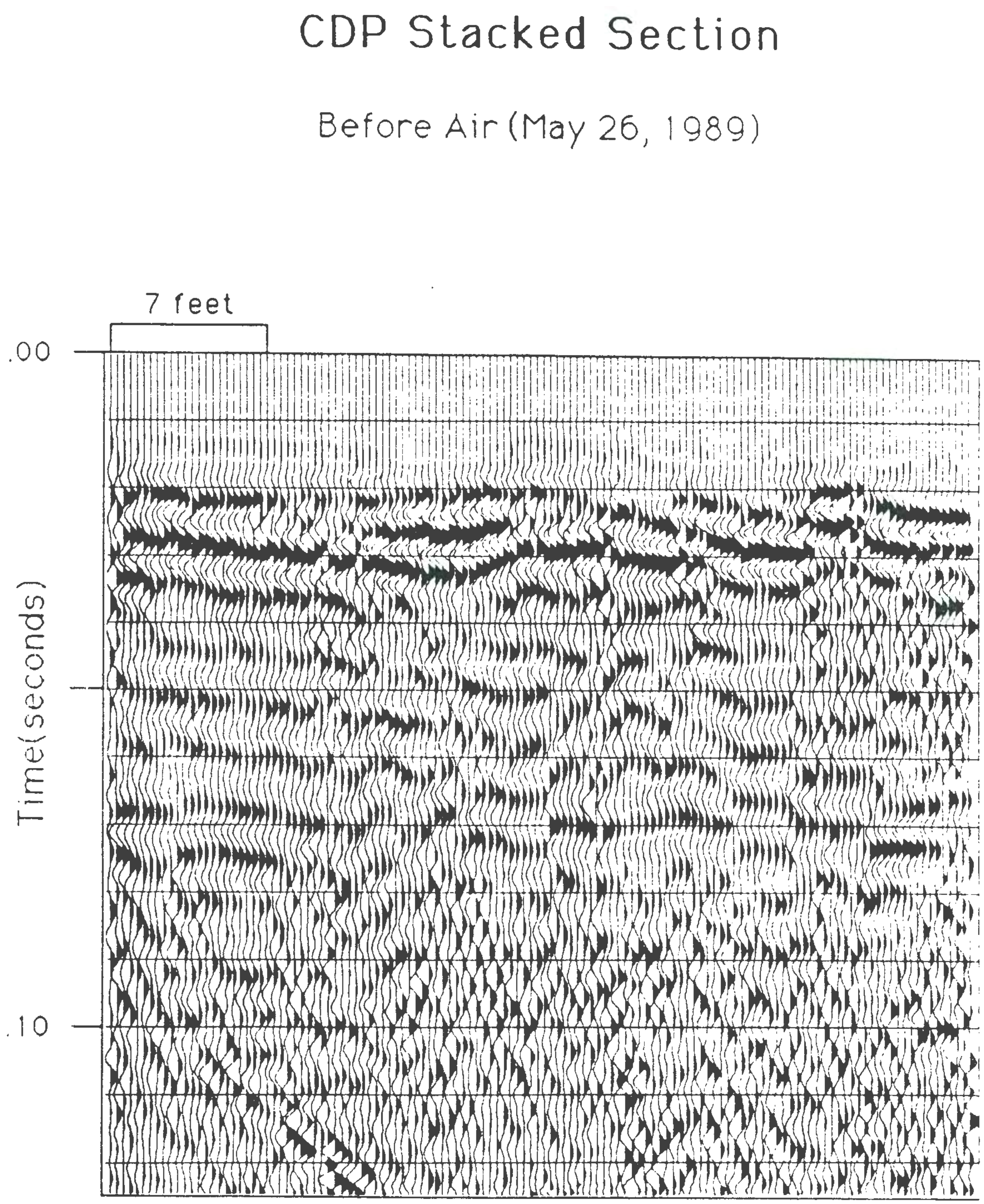

Figure 26. CDP seismic section collected prior to the injection of air.

wave reverberating off the air injection wells. All the wells drilled during this study had a 3 foot (.9 m) section of pipe protruding from the ground. Wells could be better designed in the future to reduce the effects of air-coupled wave interference by eliminating the protrusion above ground level.

The post-air injection line was processed using the same parameters as the CDP line shot before air injection. By using the same processing parameters, the number of differences between the two data sets were once again reduced. A somewhat coherent event can be seen on this seismic section between 60 ms and 70 ms (Figure 27). There appears to be less interference from the air injection wells on this section.

Comparison of the pre-air and post-air seismic sections did not produce conclusive results. Because of a general lack of visible information in 90% of the records from either line, it is impossible to know whether the events appearing on the seismic sections are real or processing artifacts. Regardless, the events in the pre-air seismic section are too incoherent to be compared with confidence to the post-air section.

The walkaway noise spreads taken before and after air injection were also analyzed. Even after frequency filtering it is difficult to pick out two similar reflection events on both sets of walkaway data (Figure 28). Because identical gain settings were not used before and after air injection, amplitude analysis of the noise spreads was not attempted.

Apparent velocity calculations were made, however, from the refracted arrivals found on the walkaways. Three refracting events were analyzed on both noise spreads. Assuming a flat refracting surface, the velocity of

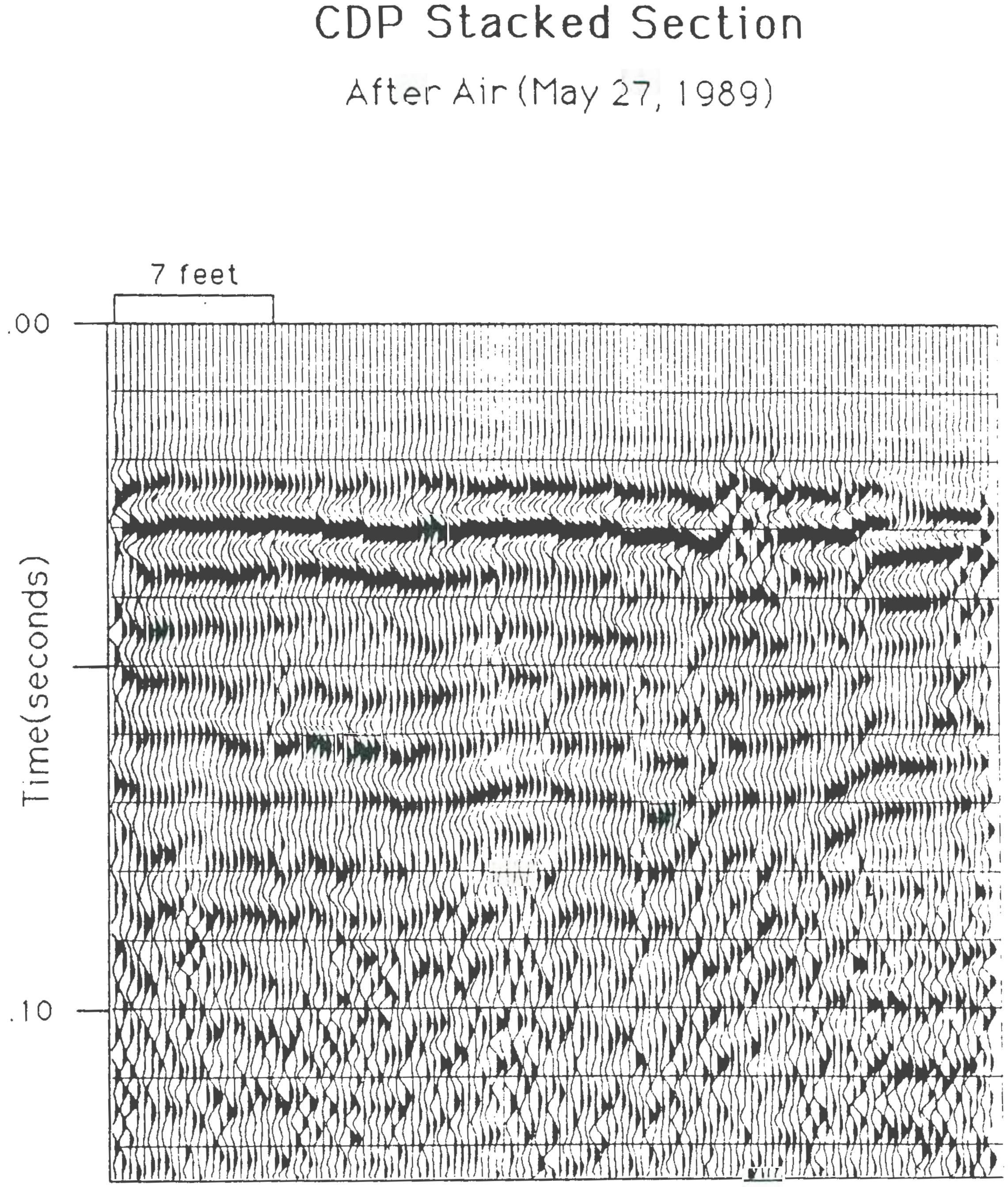

Figure 27. CDP seismic section collected after the injection of air.

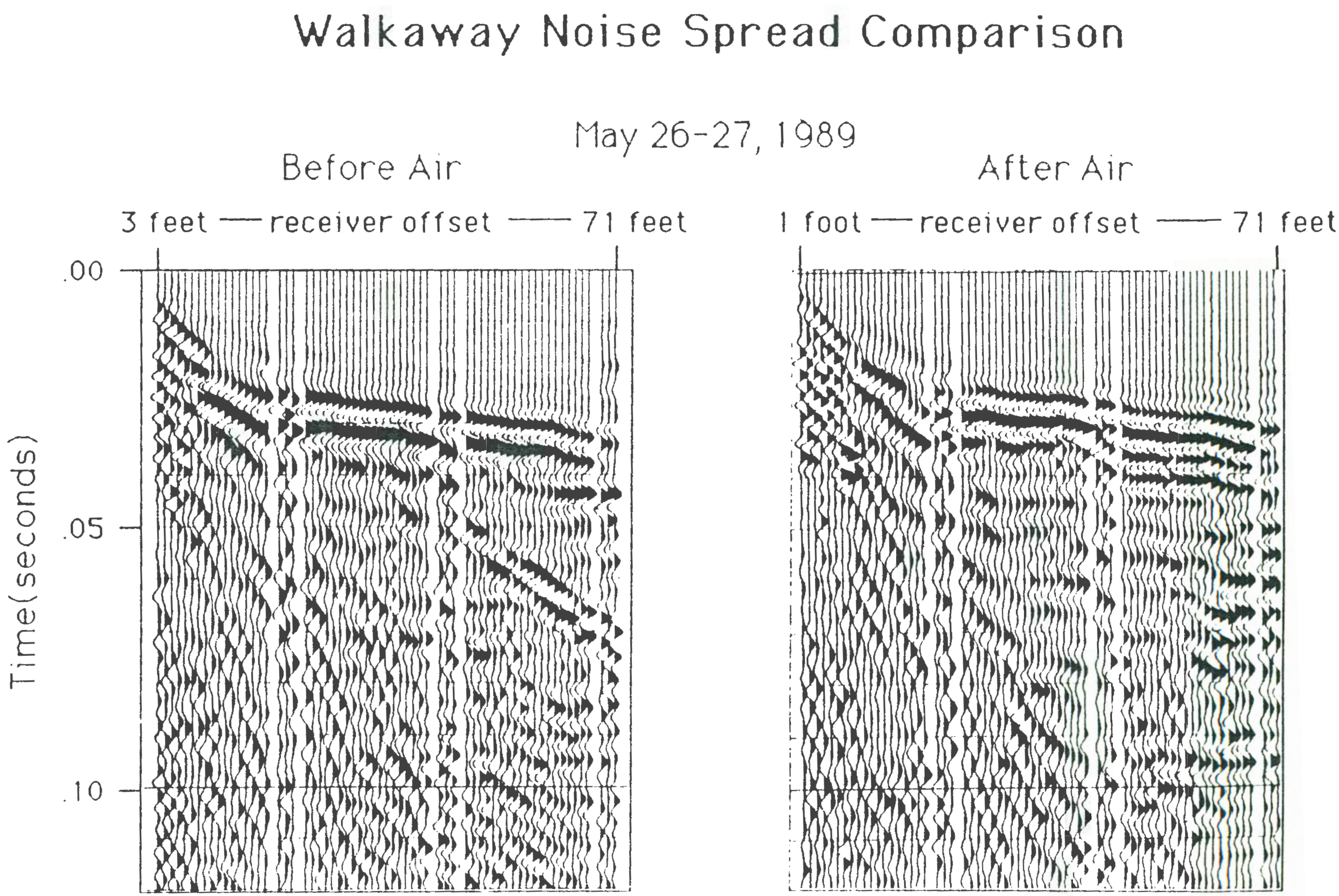

Figure 28. Both sets of data were collected using the same filters, but different gains.

layer one is nearly 600 ft/s (180 m/s), the velocity of layer two is approximately 1400 ft/s (430 m/s), and the velocity of the third layer is approximately 5800 ft/s (1770 m/s). These velocities remained constant for both experiments. The depth to the first refracting interface was calculated to be 3 feet (.9 m) and the second refracting interface to be 4.5 feet (1.4 m).

A decrease in arrival time and an increase in dominant frequency was noticed in the refracted events of the post-air walkaway when compared to the pre-air walkaway (Figure 28). This phenomenon was not due to the presence of air in the subsurface but the pre-air walkaways, being shot in a new hole. The energy released in the new hole had to pass through more of the low-velocity, highly-attenuative extreme near-surface than the source energy released in the used hole.

Seismic Testing II

Because the data from the first air injection seismic experiment were not sufficient in quality to draw definitive conclusions about detection of air using shallow seismic reflection techniques at site 4, more seismic testing was undertaken to design a better air injection experiment. The single goal of the ensuing tests was to design and test an acquisition procedure that would consistently produce high signal-to-noise reflection data.

On June 6 another walkaway noise spread was run at site 4. The seismic line used in the first air injection experiment was also used for this test. Once again the 30.06 rifle was used as the seismic source. The first experiments measured the reduction in air-coupled wave using some equipment designed for that purpose. Three pieces of flexible closed-cell foam rubber insulation were placed around the barrel of the 30.06 for the first experiment. Their function was to create a better couple with the ground and also absorb part of the air-coupled wave energy. Figure 29 shows that the addition of three pieces of foam to the 30.06 rifle was more detrimental than helpful in reduction of air-coupled wave. One and two pieces of foam were also added to the 30.06 rifle in separate tests, yielding similar results. In fact, the best reduction in air-coupled wave seemed to occur when the source plate for the rifle was placed perfectly flat against the ground.

In another attempt to decrease the effect of the air-coupled wave, a large metal bulletin board was placed between the source and the receivers. The idea behind this experiment was that an air-coupled wave traveling in the direction of the receivers would be disrupted by the bulletin board and thus reduced in amplitude. Once again, this technique appeared to have little or no effect on the recorded air-coupled wave (Figure 30).

Another experiment measured the effect of filling the holes with water before firing the source. In some instances water in shot holes has been found to increase the amount of seismic energy which is transmitted into the subsurface (Miller et al., 1989). A drop in seismic energy would account for the inconsistency in record quality seen in previous seismic tests. However, even with water in the shot holes, no change was seen in the recorded reflection signal (Figure 31).

Because none of the tests on June 6 significantly improved the quality of data at site 4, another set of experiments was planned on June 28.

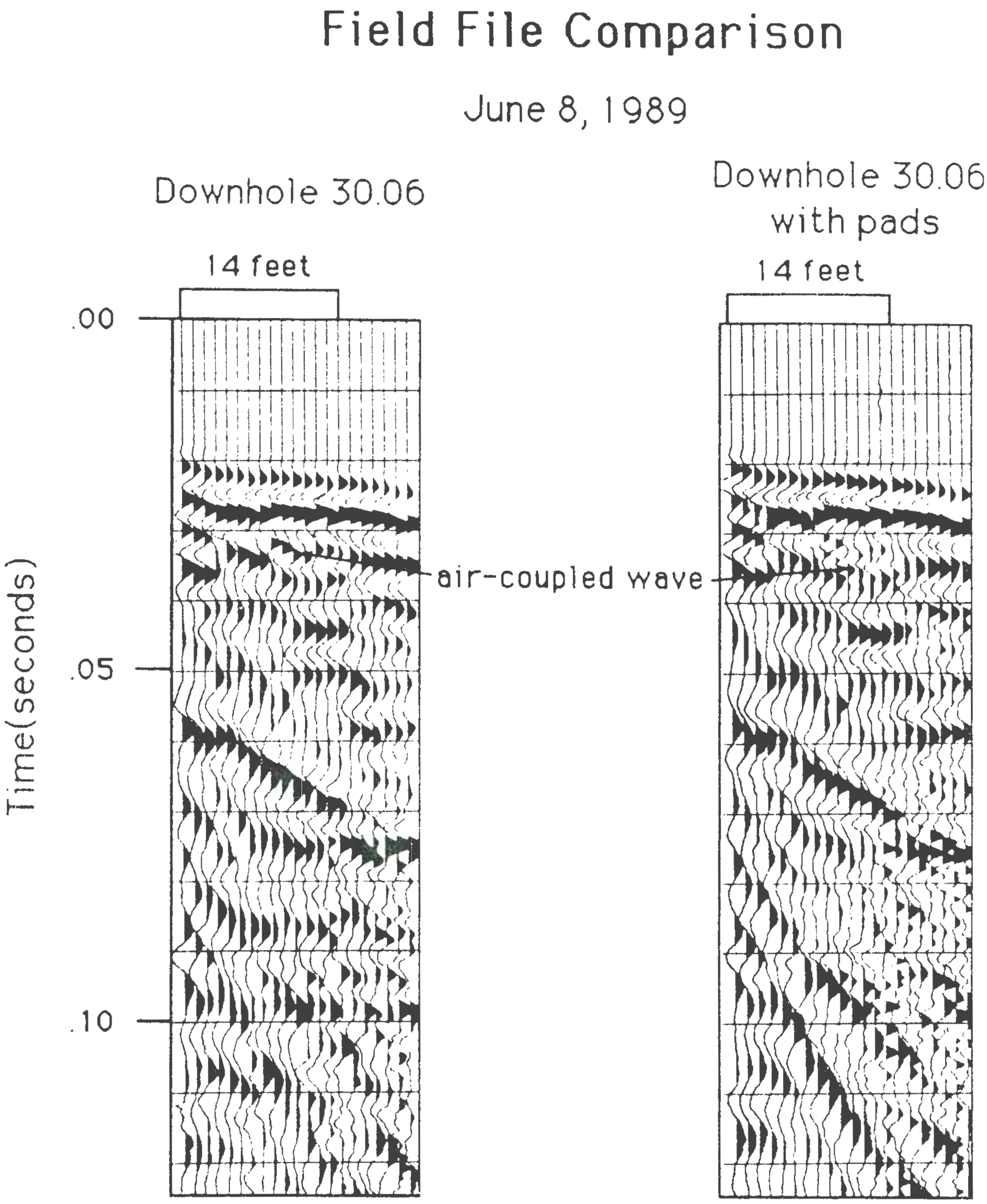

Figure 29. These field files were shot with similar gain, filter, and offset parameters. Notice the increased interference from air-coupled wave on the shot taken with the pads on the 30.06.

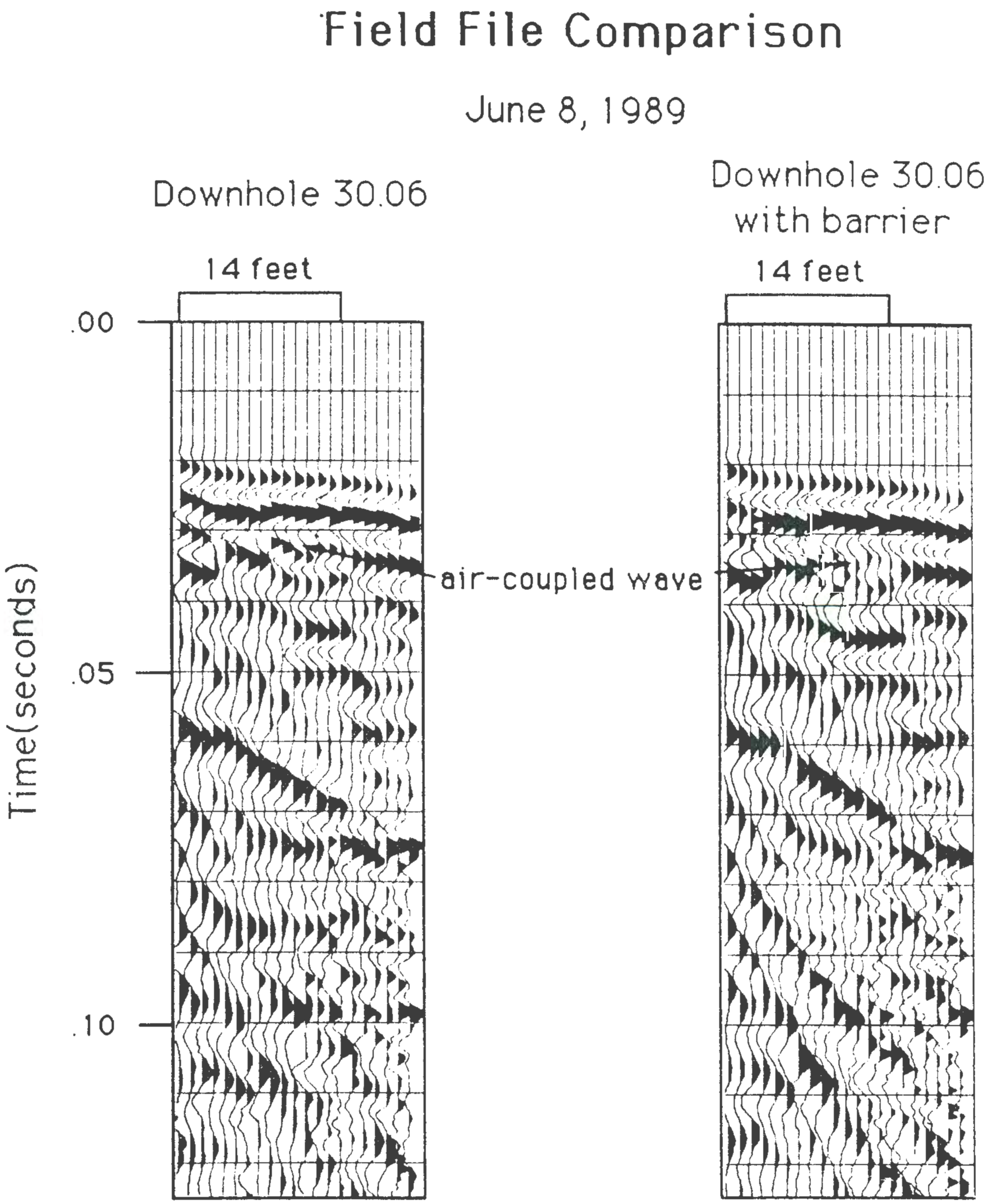

Figure 30. These field files were shot with similar gain, filter, and offset parameters. There seems to very little difference in air-coupled wave interference.

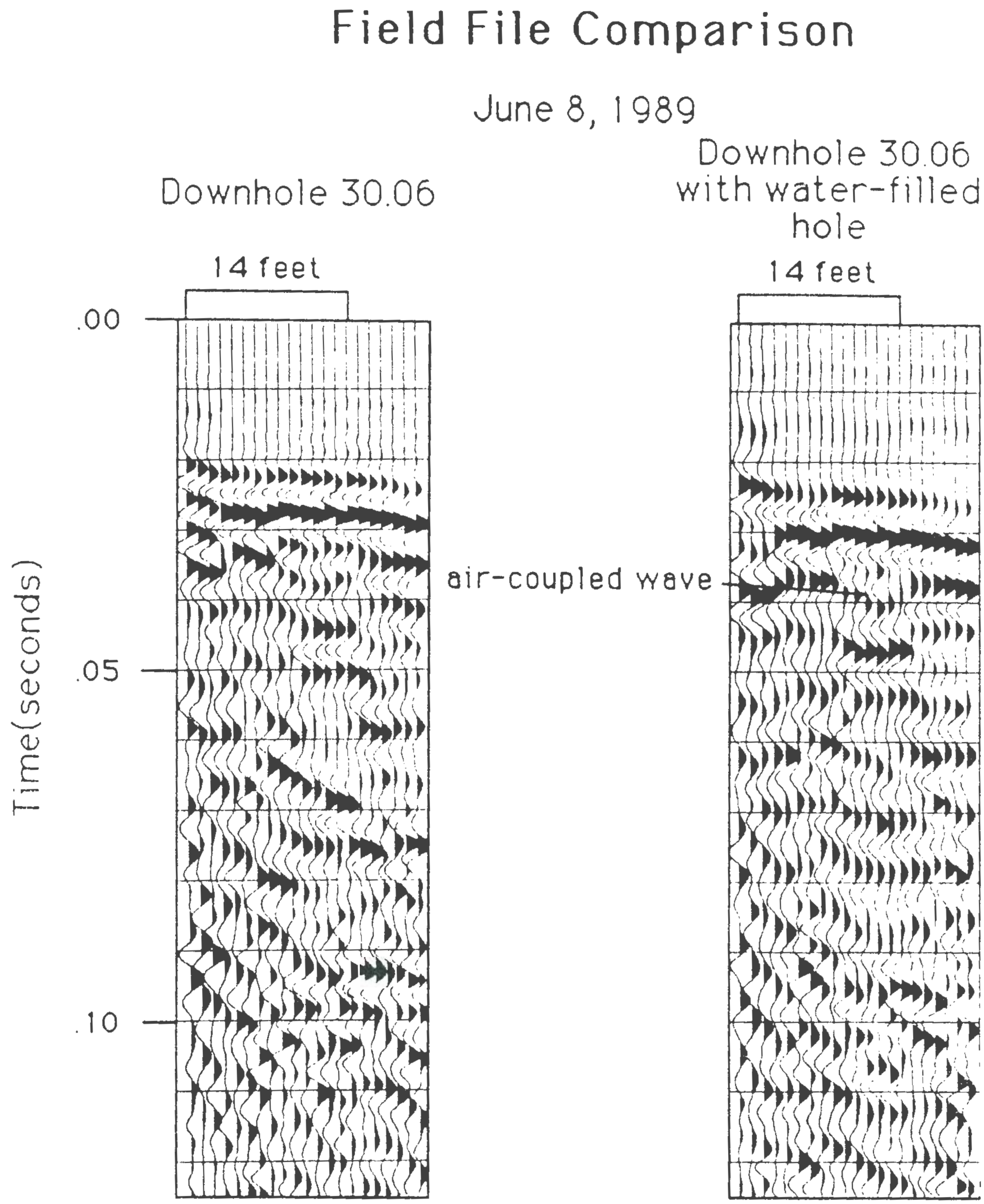

Figure 31. These field files were shot with similar gain, filter, and offset parameters. There does not appear to be a significant increase in seismic energy.

Because high signal-to-noise data had been taken from the south side of the wells, the seismic test line was moved back to that side. On June 28 another set of experiments was run using the same acquisition parameters as on May 24. The data collected during this experiment were similar in quality to the data collected during the June 6 test.

A final set of seismic experiments was designed for July 5. The 50 caliber downhole source was used to increase the amount of seismic energy transmitted into the ground. The downhole 50 caliber source produced higher quality reflection events at greater offsets than the 30.06 source (Figure 32).

The final experiment called for a trench eight inches (.2 m) wide to be dug for the 100 Hz geophone groups. The geophones were planted in the trench and then covered with dirt. The first twelve of the twenty-four channels recorded signals from buried geophones, whereas the final twelve channels recorded signals from surface geophones immediately adjacent to the buried geophones. A frequency-filtered record from this test reveals that the reflected events recorded by the surface geophones are more visible than those recorded by the buried geophones (Figure 33). However, amplitude versus frequency analysis showed that the peak amplitude of the buried geophones was actually 9 dB greater than that of the surface geophones. Most of the increase in amplitude seen with the buried phones is due to the refracted arrival. Ground roll also increased in amplitude on the buried geophone traces. The amplitudes of the reflection events from the buried and surface geophones are almost identical, although there appears to be more interference from the

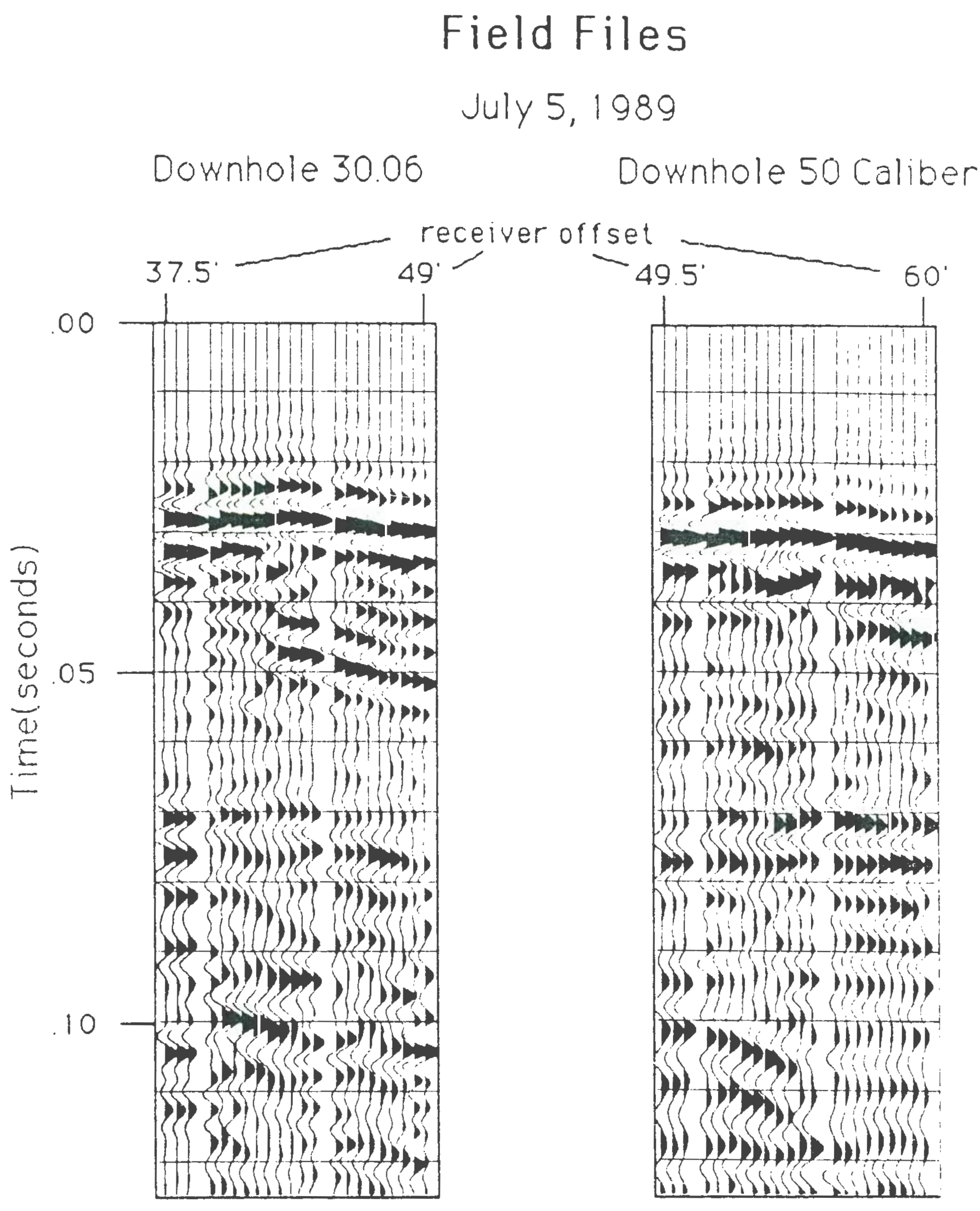

Figure 32. These field files were collected using 220 Hz low-cut filters.

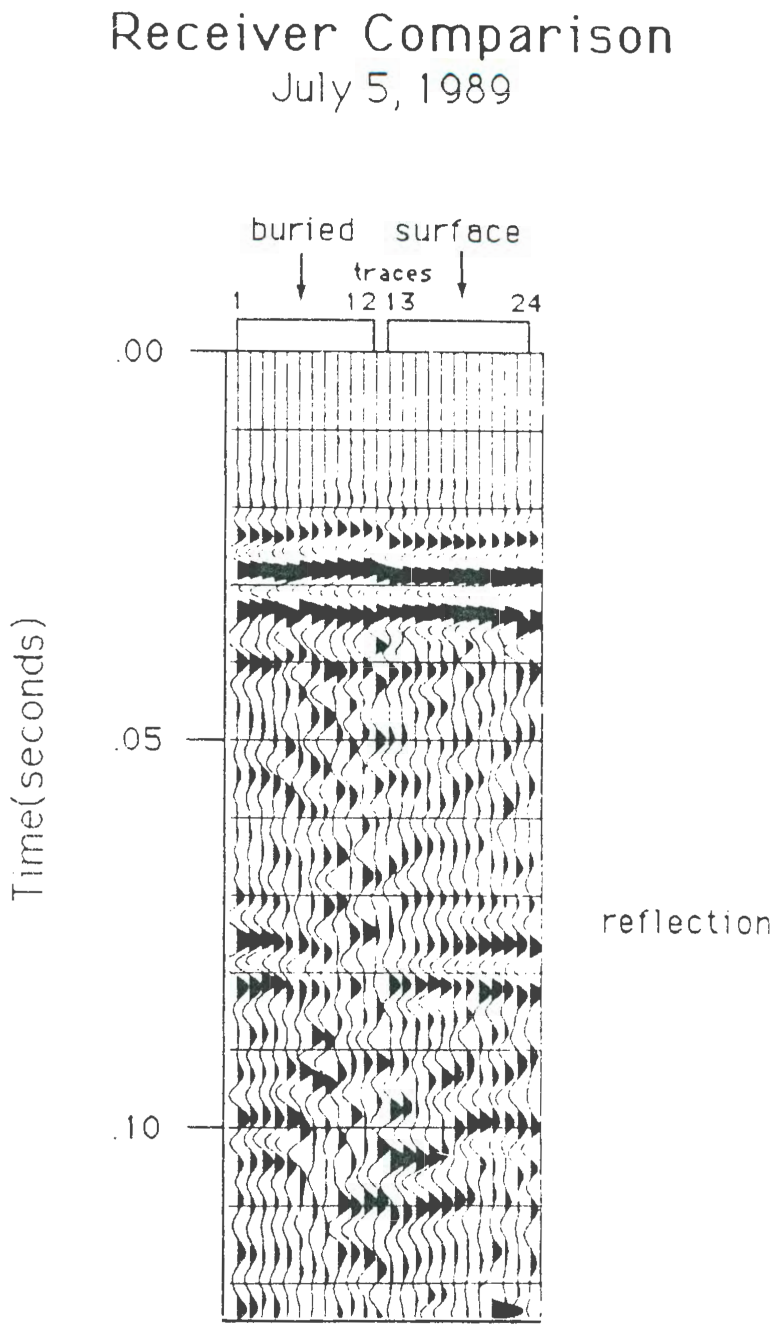

Figure 33. Traces 1 and 24 are both 37.5 feet from the source, while traces 12 and 13 are 43 feet from the source. Notice that a few inches in receiver depth makes a 1ms travel time difference in the first arrivals.

refracted wave or air-coupled wave energy in the same time window for the buried geophones. It was concluded that buried geophones would not help the data quality at this site.

Air Experiment II

Because the 50 caliber rifle had produced sufficient energy to attain repeatable results, a second air experiment was planned for site 4. Three specific CDP seismic lines were planned for air experiment II. Two experiments were designed using the 50 caliber source to find a reflection from below the injected air. A third experiment was designed using the 30.06 to image the sand/clay contact or possibly the air itself. Table 7 shows the acquisition parameters used to collect lines 1,2,and 3. Figure 24 shows the location of each line in relation to the air injection wells and the resulting CDP coverage.

Line 1 was designed to target an event at 60 ms. A 60 feet (18 m) source-to-near receiver offset was used to record most the target event outside the effects of the air-coupled wave (Figure 34). Because the dominant frequency of the event being recorded at site 4 had dropped by almost 100 Hz, three 40 Hz geophones connected in series were used as receivers for this experiment. Besides adding an additional voltage source at each receiver location, the use of 40 Hz geophones lessened the risk of energy being reduced by the low-cut filter effect of the geophone.

The goal of line 2 was to record reflection events below 100 ms. A 104 feet (31.7 m) source-to-near receiver offset was used to image an event

Recording Parameters

SEISMOGRAPH (DHR 2400):	PARAMETERS		
	Line #1	**Line #2**	**Line #3**
LOW-CUT FILTERS	240 Hz	240 Hz	340 Hz
HIGH-CUT FILTERS	-----------1000 Hz---------		
ANTIALIAS HIGH-CUT FILTER	-----------3000 Hz --------		
NUMBER OF SAMPLES	500	1000	500
SAMPLE INTERVAL	-----------1/4 ms----------		
RECORD LENGTH	125 ms	250ms	125ms

SOURCE:	PARAMETERS		
	Line #1	**Line #2**	**Line #3**
TYPE	dh 50 cal	dh 50 cal	dh 30.06
SPACING	1' (.30 m)	4' (1.2 m)	6" (.15 m)

RECEIVERS:	PARAMETERS		
	Line #1	**Line #2**	**Line #3**
TYPE (natural frequency)	40 Hz	40 Hz	100 Hz
GROUP SPACING	1' (.30 m)	4' (1.2 m)	6" (.15 m)
ARRAYS (connected in series)	3 phone gp	3 phone gp	2 phone gp
RECORDING GEOMETRY	--------end-on geometry---------		
SOURCE-NEAR-RECEIVER OFFSET	64'(19.5m)	104'(31.7m)	4.5'(1.4m)
SOURCE-FAR-RECEIVER OFFSET	87'(26.5m)	196'(59.7m)	16'(4.9m)

WEATHER/SOIL CONDITIONS	PARAMETERS
WIND SPEED	calm
WIND DIRECTION	not recorded
NEAR-SURFACE MATERIAL	soil
NEAR-SURFACE MOISTURE	dry
TEMPERATURE	65° F (18.° C)

Table 7

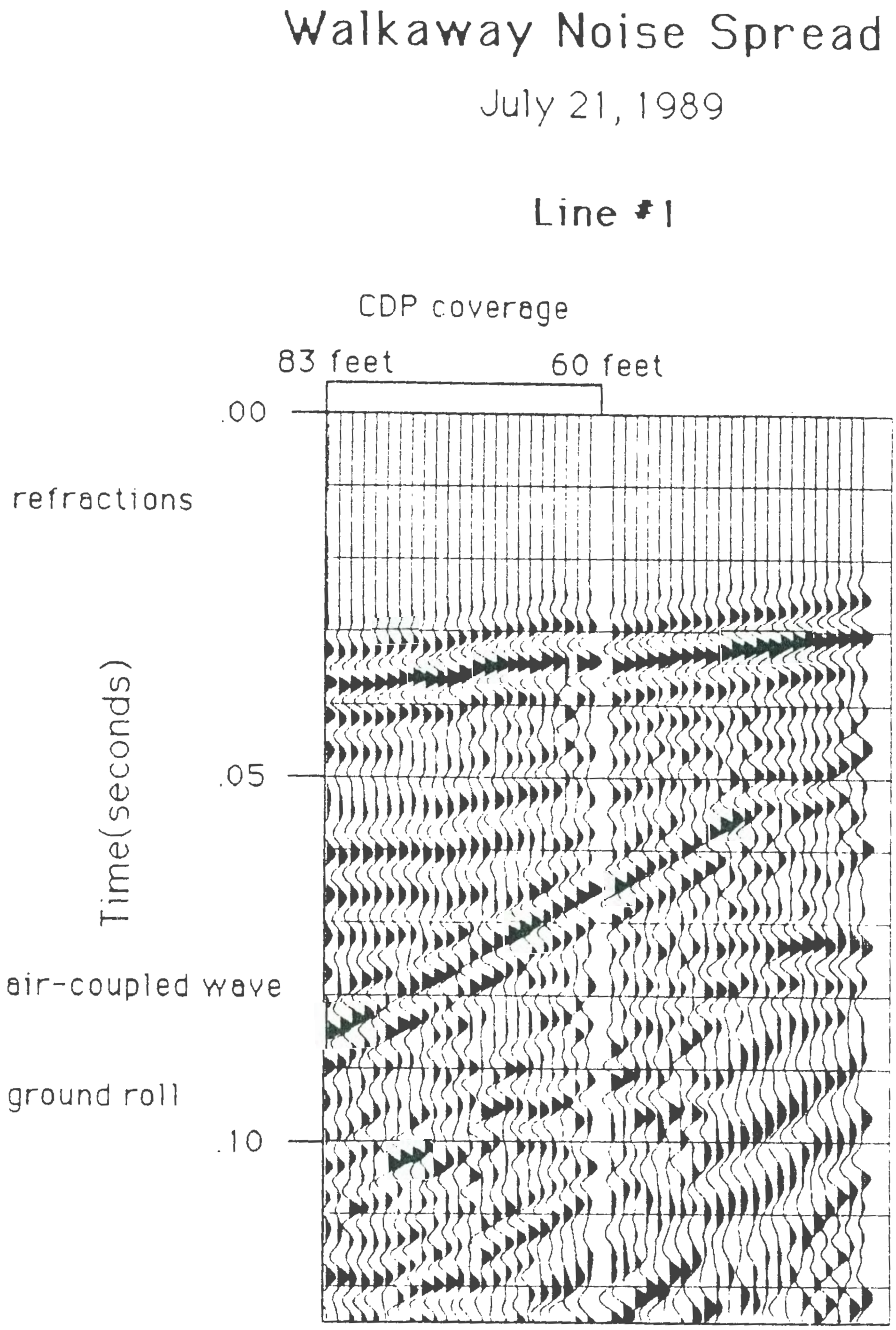

Figure 34. The coherent event at 55 ms is refracted energy.

at 105 ms (Figure 35). Line 2 also used three 40 Hz geophones connected in series as receivers.

Line 3, designed to image the clay/sand interface, used 100 Hz geophones as receivers. The 100 Hz geophones were used to increase the possibility of retrieving higher frequency information by adding the low-cut filtering effect of these geophones. In addition, 340 Hz low-cut filters rather than 240 Hz low-cut filters were used during data collection on line 3. These higher low-cut filters were also used to help retrieve high-frequency information similar to the May 24 and prior data. A 4 feet 6 inches (1.37 m) source-near-receiver offset was used to image an event that was believed during testing to be the clay/sand interface interface (Figure 36).

On July 21, data for all three CDP lines were acquired. Acquisition of the CDP data was completed by 10:30 A.M. At 2:00 P.M. on the same day, air injection began at site 4. Once again, air was injected into well 4-1 using a 9 cfm (.25 cmm) gas-powered air compressor; wells 4-2 and 4-3 were used for monitoring. The water level was once again measured at between 23 feet (7.0 m) and 23 feet 6 inches (7.2 m) before air injection. The water level had similar drawdown characteristics to the first air injection experiment at site 4 and fell to 37 feet (11.3 m) after only one hour and twenty minutes of pumping.

At 6:00 A.M on July 22, 18 hours after air injection had begun, air injection ceased at site 4. Seismic lines 1,2, and 3 were collected using the same parameters as the previous day. In addition to CDP data, an uphole survey was run in well 4-1. The goal of an uphole survey is to measure

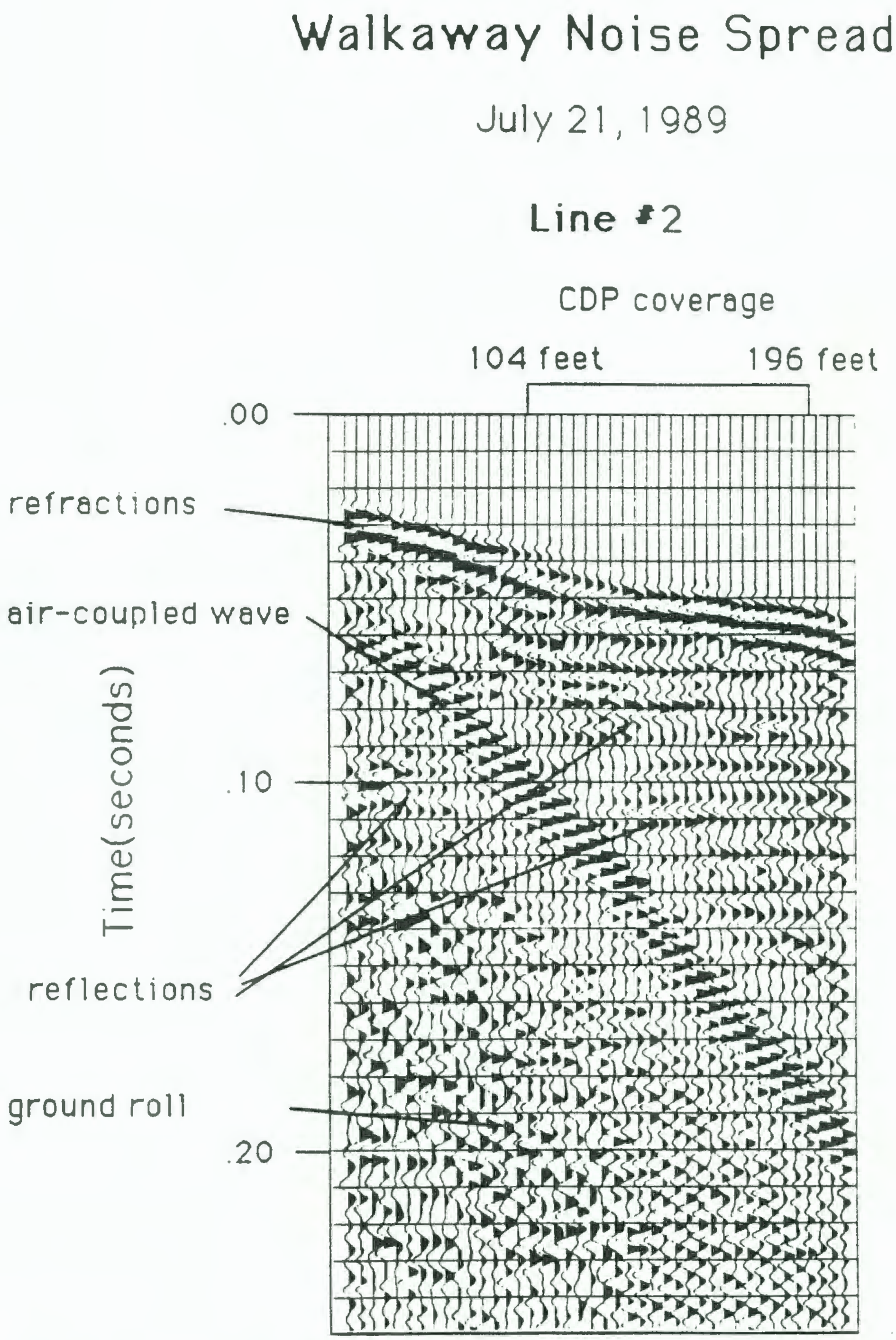

Figure 35. Notice that the 105 ms reflector is outside the effects of the air-coupled wave and ground roll.

Field File

July 21, 1989

Line #3

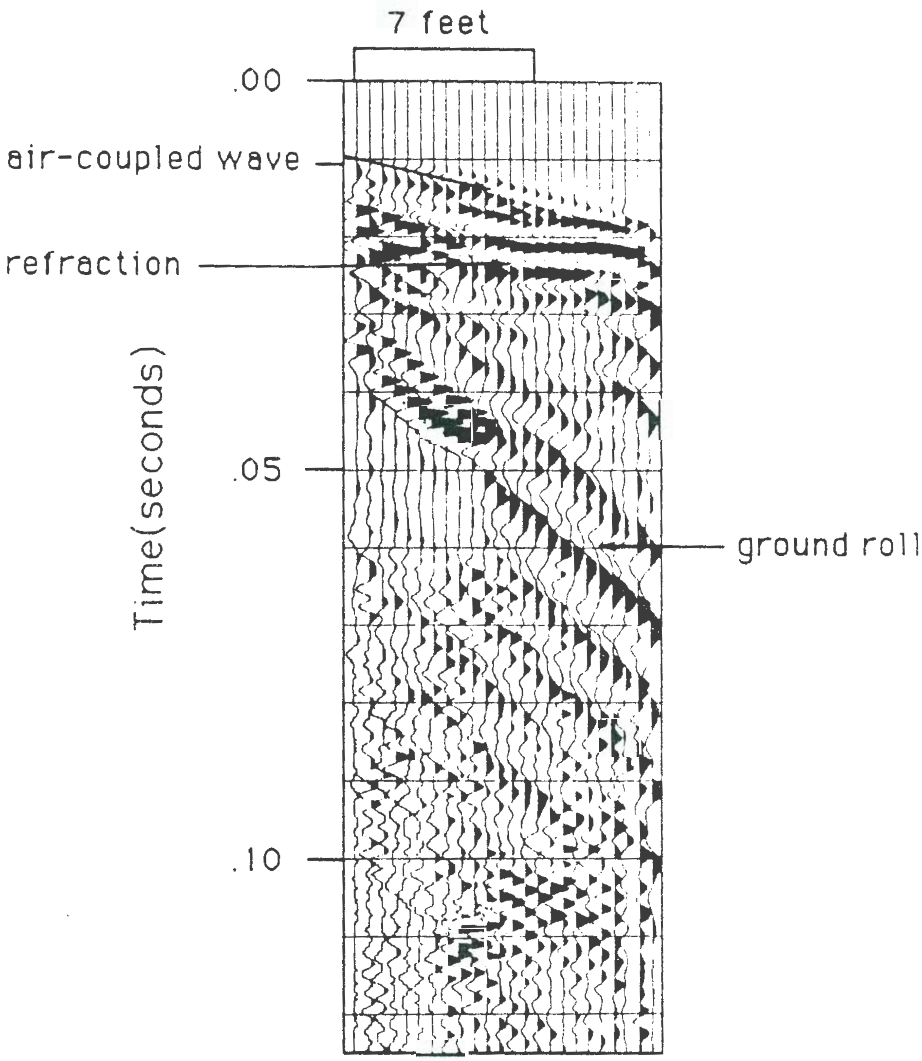

Figure 36. This field file has the same source-to-receiver offset as those acquired in line 3. Notice that the refraction appears to be a reflected event in similar manner to the data collected at site 1.

the average velocity of the subsurface between the source and the receivers. The source was placed downhole, and the receivers were planted on the surface. All seismic testing was completed by 9:30 A.M.

Only two measurements were taken during the uphole survey. The first shot was taken at a depth of 36 feet 8 inches (11.2 m) below the surface. This measurement was made where air had been injected below the sand/clay contact. The average velocity calculated from the uphole survey for this depth was 1880 ft/s (570 m/s). A second shot was taken 23 feet 8 inches (7.2 m) below the surface. This shot was taken above the clay/sand contact in an environment free of injected air. The average velocity from the second shot of the uphole survey was calculated to be 2090 ft/sec (637 m/s). The calculations show a velocity inversion, or reduction in velocity, between 23 feet 8 inches (7.2 m) and 36 feet 8 inches (11.2 m). In fact, an interval velocity of 1620 ft/s (490 m/s) is calculated for the 13 feet (4.0 m) interval between the two shots. This is consistent with another more detailed uphole survey from nearby Kansas River alluvium that shows several velocity inversions (Figure 37).

Line 1 was analyzed first. Common-offset sections were made from the CDP data collected before and after air injection of seismic data. Common offset sections are plots of seismic data taken from the same source-to-receiver offset. These sections were not processed in any manner, other than scaling, in order to detect minor changes that may have occurred in the post-air injection data. Figure 38 shows a typical before and after-air injection common-offset section. Unfortunately, no consistent change could be seen in the event between 45 ms and 55 ms or in any of the other

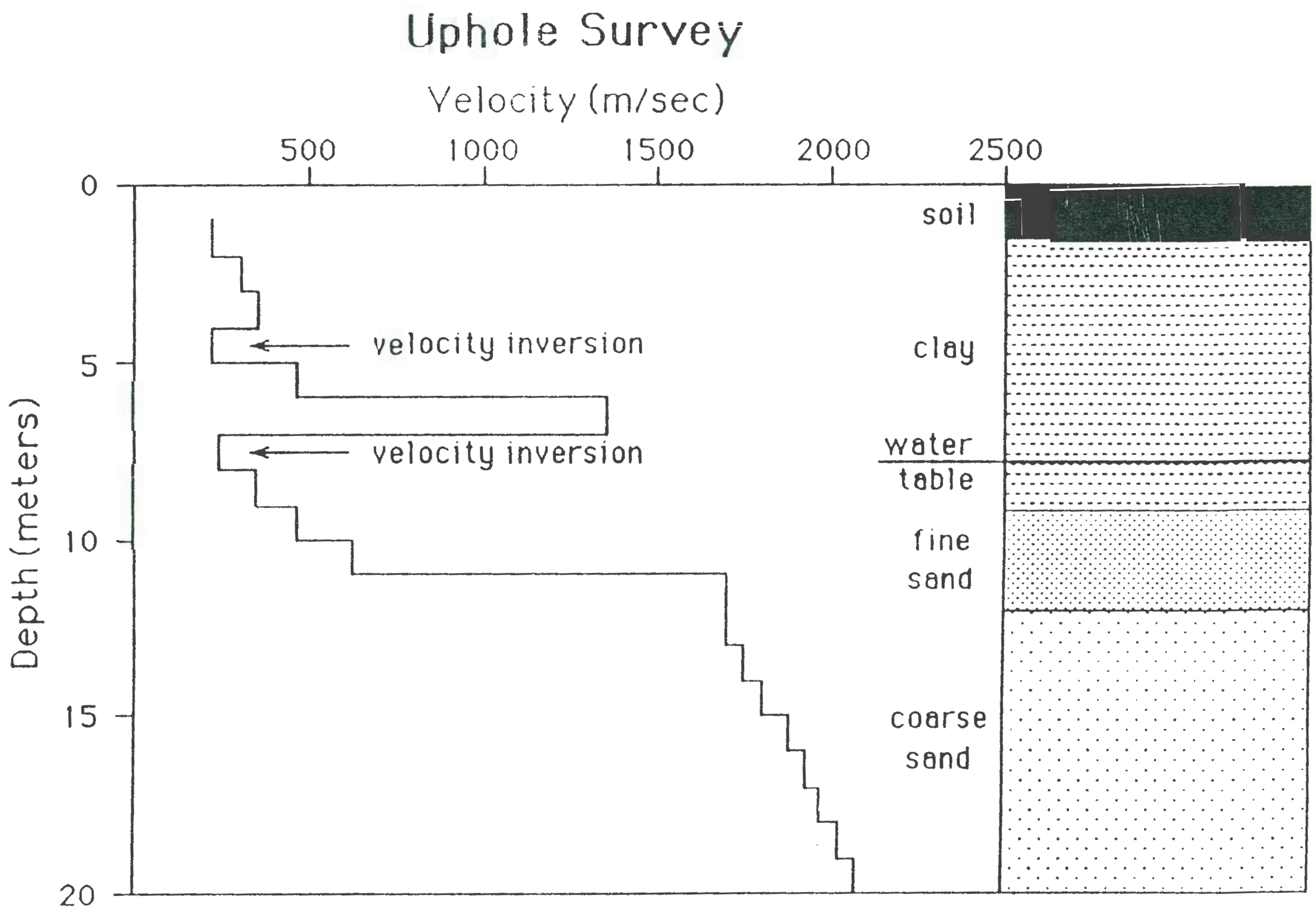

Figure 37. Notice the two velocity inversions which occur in the first 8 meters (26 feet).

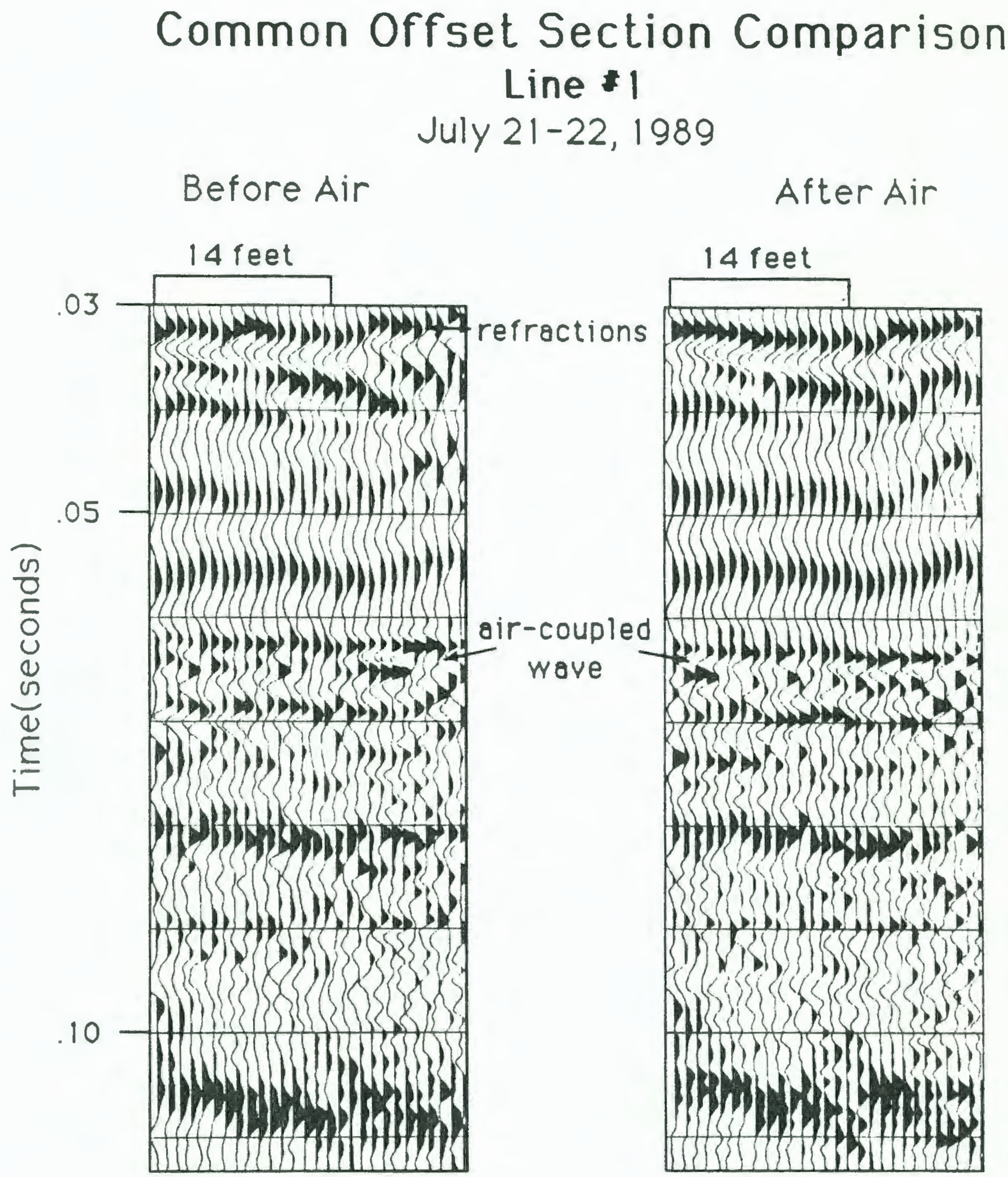

Figure 38. These common offset seismic sections have had no processing other than AGC scaling applied. The first 30 ms of record had no recorded energy. All traces were collected at a 62 foot offset.

coherent seismic energy on line 1 data. It was later determined that the targeted events were actually refracted events.

Line 2 was sorted into common-offset plots. Like line 1, the common-offset sections were not processed in any manner other than scaling. Although there were some minor differences in the arrival time of some seismic events between the two data sets, the differences were neither temporally or spatially consistent. Special attention was paid to the reflected event at 105 ms. This event was especially consistent on the two sets of data (Figure 39).

Line 2 was next processed into a CDP stacked section. The flow used to process the line 2 data taken before the injection of air is shown in Table 8. An event at 105 ms was the main target of the CDP processing (Figure 40). A velocity of 7500 ft/s (2290 m/s) was used to stack the data. Using this velocity, the depth of the reflection horizon would be approximately 400 feet (122 m). Because a straight line raypath is assumed when determining stacking velocties, the reflection depth may be less than that calculated using the stacking velocity. The post-air CDP data was processed into a finished stacked section using the same parameters as the pre-air data.

A comparison between the two stacked sections from line 2 produced some variation in the event at 105 ms (Figure 40). The reflection appears to remain flatter and more coherent on the first data set. Because both of these data sets were completed using the same processing flow, the slight undulations seen in the data may be due to static corrections. The best static corrections made to the data set before air injection may not be the proper static corrections for the post-air section. A separate post-air section

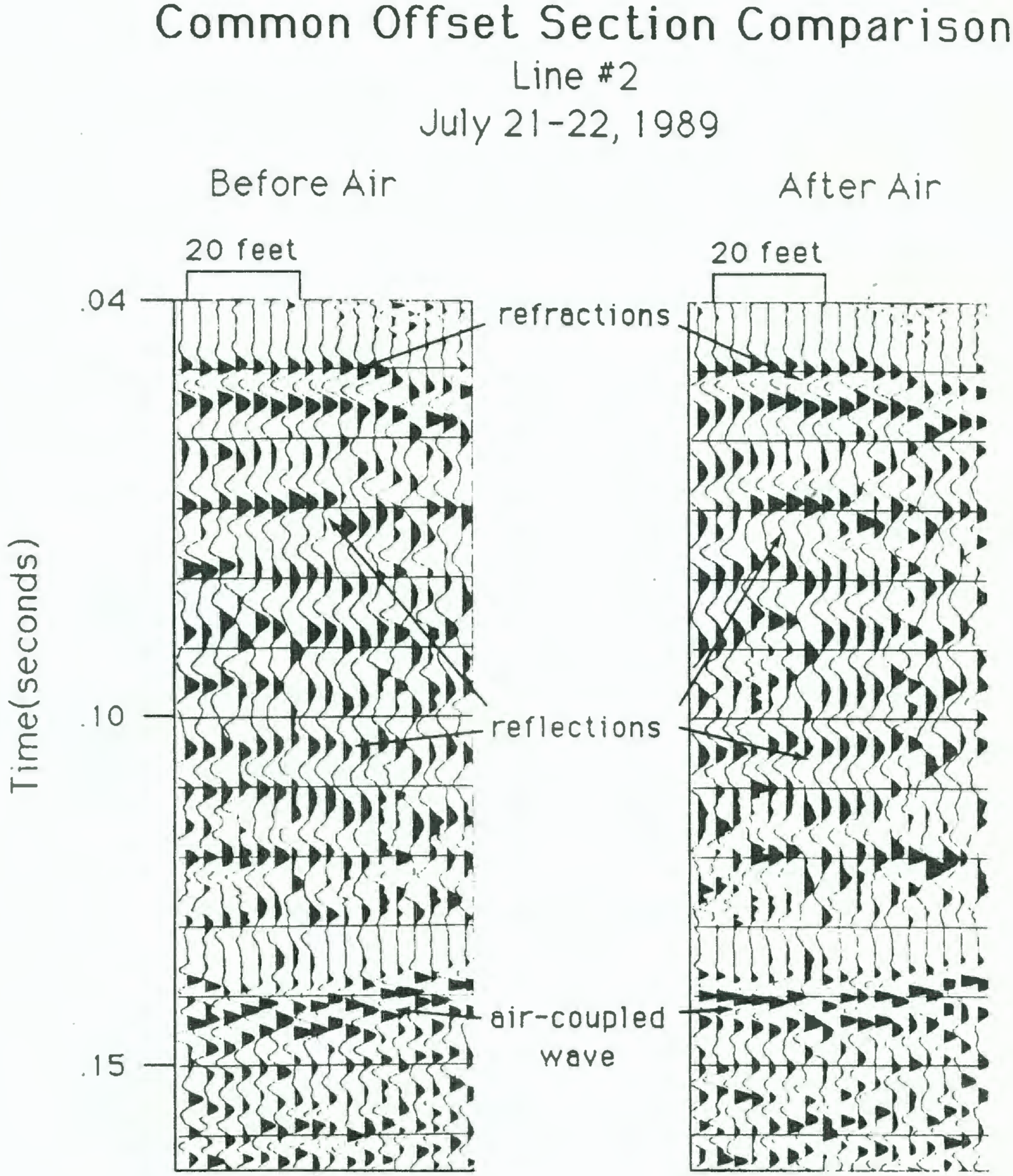

Figure 39. These common offset seismic sections have had no processing other than AGC scaling applied. The first 40 ms of record had no recorded energy. All traces were collected at a 156 foot offset.

Processing Flow

Processing Step	Description
1. Bad trace editing	Seismic traces of poor quality or dead during acquisition were removed.
2. AGC scaling	A step which boosts the amplitude of events occurring later in the seismic record.
3. First arrival mute	Mute of seismic energy above the first reflected event.
4. Air-coupled wave mute	Mute of main air-coupled wave event.
5. CDP sort	Seismic traces were sorted into gathers containing the same midpoints (common-depth points).
6. NMO correction	Shift applied to the CDP gathers to correct for the time differential due to different source to receiver offsets.
7. Automatic statics	Surface-consistent time shifts applied to CDP traces to correct for near-surface velocity anomalies at a shot or receiver. The same auts table was used for both before-air and after-air data sets.
8. Frequency filter	A process used to reduce the amplitude of unwanted seismic energy while leaving the desired seismic energy alone.
9. Stack	A linear addition of samples from same CDP location into one trace to enhance the data.

Table 8

CDP Seismic Section Comparison

Line #2

July 21-22, 1989

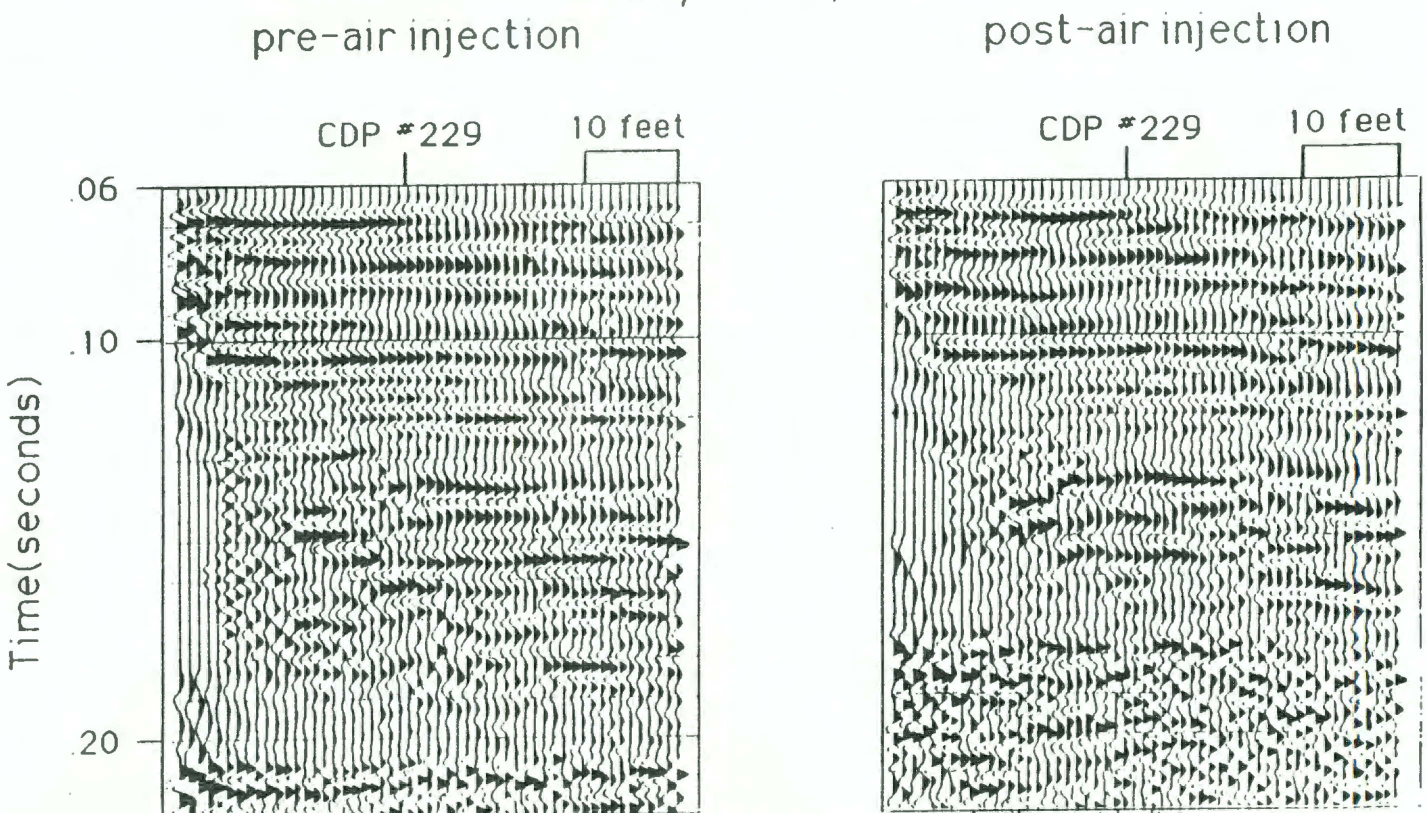

Figure 40. CDP #229 was the nearest common depth point to the injection well. Both sets of data were processed using the best automatic static corrections for the pre-air injection data set.

was processed using best-case static corrections. The results show that the reflected event at 105 ms on the post-air section resembles the event on the pre-air section better. By comparing the best-case data sets, a difference of at most 1 ms exists in the two-way travel time. This change does not appear to be consistent with the location of the injection well (Figure 41).

Many different seismic events can be seen in the first 30 ms of the data taken for line 3. A set of narrow bandwidth frequency filters was used on these data to decide whether reflection energy was present. Figure 42 shows several plots that distinguish the events on these records as being air-coupled wave, ground roll, and refraction energy from this pre-air plot. Similar results were found for after-air injection data. Because a reflection could not be found on the field data, even after frequency filtering, CDP processing was not attempted on line 3.

Results

None of the seismic experiments conducted after the injection of air in the first two experiments produced evidence to support the model used as a basis for this study. Some small changes were seen within the data sets but none was consistent or could be definitely tied to the influence of the air. Although CDP techniques have classically been used to increase the signal-to-noise ratio and to aid geoscientists in interpreting seismic data, they may have added more ambiguity than clarity to these data. Even when tightly constrained, processing steps such as deconvolution and static correction alter the position of the data in time.

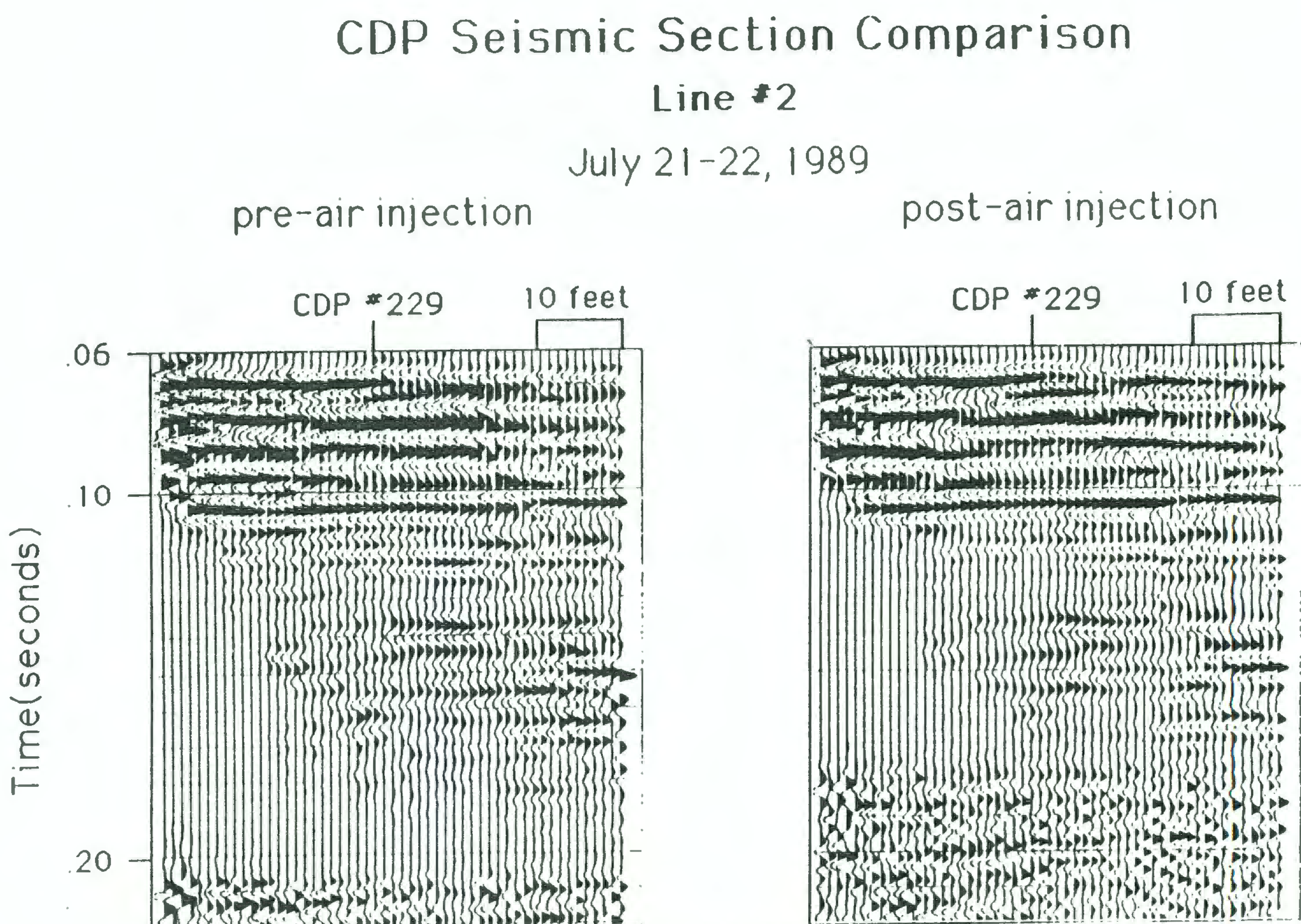

Figure 41. CDP #229 was the nearest common depth point to the injection well. Each set of data was processed using the best automatic static corrections for that data set.

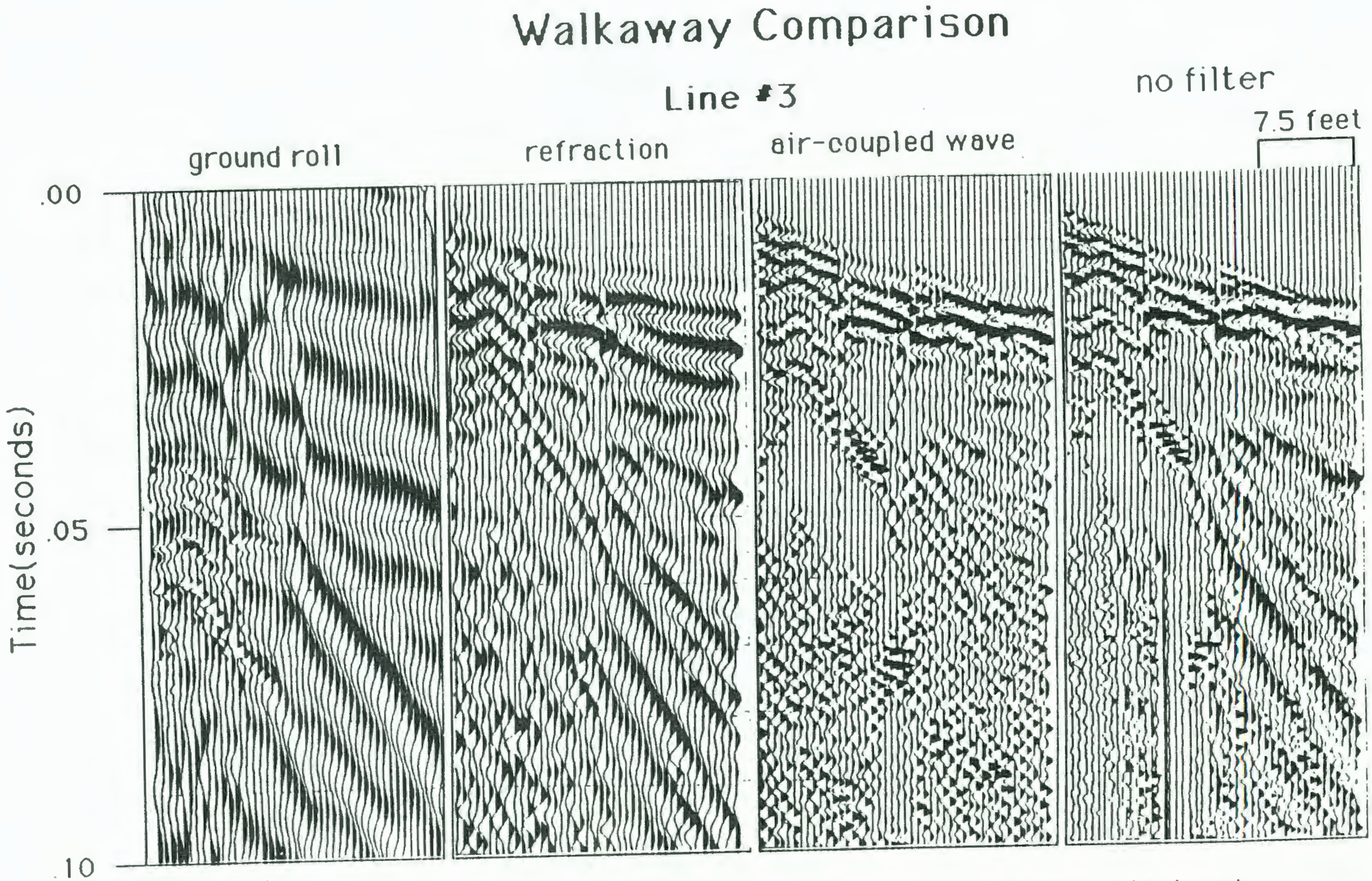

Figure 42. Three bandpass filters which increase in frequency from left to right show the seismic energy components of the composite walkaway (far right).

There are several possible reasons why the expected results were not seen during the air injection experiments at the Robinson tract, for example, seismic resolution limits, insufficient air injection, and inhomogeneity of sand in the injected interval.

Dominant reflection frequencies from seismic data taken during air injection testing range from 100 Hz to 200 Hz. These frequency values and the velocity values collected during the uphole survey can be used to interpret lateral and temporal resolution at the depth of the injected air.

Lateral resolution refers to how close two reflecting points can be situated horizontally and yet be recognized as two separate points (Yilmaz, 1987). Lateral resolution is usually quantified by the calculation of the first Fresnel zone. The Fresnel zone is the portion of a reflector from which reflected energy can reach a detector within one-half wavelength of the first reflected energy (Sheriff, 1984). The first Fresnel zone is circular for a horizontal reflector. The formula used to calculate the radius R of the first Fresnel zone is

$$R = \sqrt{\left[(\lambda * z)/2 + \left(\lambda^2/16\right)\right]}$$

where

λ (wavelength) = v/f = 9.4 feet (2.9 m),

z (depth to reflector) = 30 feet (9.1 m),

f (frequency) = 200 Hz,

v (velocity) = 1880 ft/s (573 m/s).

By using the best case values taken from the test data, a circle of R = 12 feet (3.7 m) would be sampled to create one reflection point from a depth of 30 feet (9.1 m). It is obvious from this calculation that every CDP experiment conducted at site 4 oversampled the first Fresnel zone. In other words, the reflection points were too close together to be resolved as separate points. This is an important factor to consider during lateral mapping of an air pocket's dimensions. However, even oversampled data taken after air injection should show the effects of air on the subsurface when compared to pre-air data if any difference had occurred. A more important point than oversampling of the subsurface is that the Fresnel zone may have been too large to allow us to see the injected air. The change in seismic properties resulting from the presence of air are directly proportional to the amount of air located within the Fresnel zone at that reflector point. If a small enough portion of the Fresnel zone contains air, then the resulting effects of the air on reflected energy might be undetectable. Because the lateral extent of the injected air pocket is unknown, the fraction of the Fresnel zone filled with air is unknown.

Vertical resolution also depends on the frequency and velocity of the seismic energy. One-quarter of the wavelength is on average the thinnest bed that can be resolved (Widess, 1973). Using the same values of velocity and frequency, the smallest bed that could be resolved would be approximately 2.5 feet (.76 m) thick. This calculation is for resolution of both the top and bottom of a reflector.

It is possible to image only the top or the bottom of a reflector without meeting the one-quarter wavelength requirement. The only requirements for detecting such an event are that the seismic energy put into the ground be strong enough to reach the reflector and that the reflector have a great enough acoustic impedance contrast so that the energy from the reflection makes it back to the surface with sufficient strength to be recorded.

The change in acoustic impedance after air injection does not appear to be strong enough to create a new recordable reflection event after air injection. Using the average velocity of 1880 ft/s (570 m/s) from the uphole survey, a reflection from the clay/sand interface should appear at 32 ms on a field record. However, other coherent noise, such as ground roll, air coupled waves, and refracted energy, was present in the area predicted for the near-surface reflected event as seen on line 3. Another possibility is that no distinct contact between air-filled sand and clay existed. The air may decrease in quantity near the clay/sand interface because of differential permeability or some other factor.

It is also possible that air was not injected long enough at site 4 on the Robinson tract. A 9 cfm (.35 cmm) compressor pumping for 18 hours would inject a minimum of 9720 cubic feet (275 cubic m) of air. The output of the compressor is rated at 9 cfm at 90 psi. Thus, a larger but not proportional air output would be expected at 10 psi, the pressure seen in the monitor wells. Assuming 25% porosity and 100% replacement of water with air, the air would fill a cylinder with a radius of 50 feet (15.2 m) and a height of 5 feet (1.52 m). Although, this is probably a sufficient amount of air, it may not have been left in place long enough to affect the seismic data. Birkelo et al. (1987) saw a drop in the top of the saturated zone using seismic reflection techniques after eight days of pumping.

However, after water was pumped for eight days, the top of the saturated zone and the water level were not at the same depth because the saturated zone dropped at a slower rate than the water table. Thus it is possible that the level of saturation in the pore spaces at site 4 was still too high to measure a difference. If the air was present for a longer period, the saturated zone may have had a greater chance to recede or dry out.

Another possibility is that the sand and gravel layer transmits the injected air preferentially. By assuming 25% porosity, 100% replacement of water with air, and a uniformly expanding cylinder, and by using 12 minutes as the first arrival of air in well 2, 12 feet (3.6 m) away from the injection well, a vertical extent of 1 feet (.30 m) is calculated for the air. Even if the normal output of the compressor is tripled, the vertical volume of air would be only 3 feet (.91 m). If these assumptions are correct, the vertical extent of the air pocket may be too small to have a delaying effect on the seismic wavelet. The amount of delay caused by the air assuming vertical incidence of the seismic raypath can be calculated using the formula

$$T = 2*[(h/v(a) - h/v(na)],$$

where

$T =$ 2-way time delay,

$v(na) =$ interval velocity without air,

$v(a) =$ interval velocity with air,

$h =$ vertical thickness of air pocket.

Assuming an initial interval velocity of 2000 ft/s (607 m/s) and a post-air velocity of 1000 ft/s (305 m/s) the delay would be only 1.0 ms for a 1 feet (.30 m) high air pocket or 3.0 ms for a 3 feet (.91 m) high air pocket. A 1000 ft/s (305 m/s) change in interval velocity would be a 50% reduction from the pre-air assumption. It is also possible that only one of the reflection raypaths is passing through the air, cutting the delay time in half.

The final possibility is that the basis for the model used to create this experiment is incorrect. In other words, the air does not substantially change the seismic characteristics of the subsurface. It is possible that the air percolates through the subsurface in multiphase flow and not as a pocket. The laboratory results, which show that only a small volume of gas is necessary to make a large decrease in compressional wave velocity, may not hold true in this environment. If this is the case, the velocity contrast between a partially saturated and a fully saturated zone may be too small to affect the seismic record either directly, in the case of spectral characteristics or a new reflection, or indirectly, in the case for an arrival delay.

Conclusions from Air Experiments I and II

The seismic experiments conducted after the first two air injection experiments at site 4 on the Robinson tract were unsuccessful in detecting the presence of air in the subsurface. Although it was not possible to make a decision about the overall feasibility of the technique, it is possible to say that the technique was not feasible at the Robinson tract using the parameters prescribed in Air Injection Experiment I and II. However, these experiments did produce a better set of guidelines for future air injection experiments at the Robinson tract.

First, CDP shooting should be de-emphasized as a means of data acquisition. Source inconsistency and the averaging affects of CDP processing make detailed measurements of differences between similar pre-air and post-air data sets difficult.

A walkaway noise spread run over a large source to receiver offset should be the best way initially to detect air in the subsurface. A source location that is repeatedly used such that the next shot does not significantly affect the characteristics of the data should be used both before and after air injection seismic data collection. This should eliminate the problem with source inconsistency and decrease the affects of ground roll and air-coupled wave. In addition, the source should be located at a safe distance from any objects of significant diameter found above ground level and where the source plate can lie perfectly flat against the ground to reduce the affects of air-coupled wave.

Air injection should continue for several days to ensure that a sufficient amount of air is present in the subsurface. The added time could also help the air dry or displace water that was not initially moved. Thus a larger velocity change might be seen in the seismic data.

Finally, additional monitor wells should be added at site 4 on the Robinson tract to observe whether the air is indeed expanding uniformly. The seismic lines from air injection experiment II have the best quality seismic data but were run parallel to the monitor wells a sizable distance away (Figure 24). Thus at least one monitor well should be located far enough to the south of the injection well to ensure that the center of the CDP coverage from the seismic lines will fall between the injection well and the new monitor well.

AIR INJECTION EXPERIMENT III AND ERROR ANALYSIS

Seismic Testing III

Using the results from air injection experiments I and II, a final air experiment was planned for site 4 at the Robinson tract. A third monitor well, well 4-4, was drilled 24 feet (7.3 m) south of the injection well and azimuthally 90° away from wells 4-2 and 4-3 (Figure 24). Well 4-4 was drilled a greater distance away from well 4-1 than any of the CDP lines used during air injection experiment II. Two walkaway noise spreads were planned for this experiment, one walkaway noise spread was designed to record a time delay in reflection information and the other to record a time delay in refracted arrivals.

On October 17 several tests were run to determine the best pre-A/D filter and channel gain settings for the reflection tests. The walkaway test lines for this study were run parallel to wells 4-1 and 4-4 and perpendicular to all the other test and CDP lines at site 4. Figure 43 shows the layout of the reflection walkaway line. Special attention should be paid to the offsets where the first set of 24 geophones were used. Before recording any of the walkaway data, 18 shots were fired into each shot hole because repeated shots in a hole produce higher signal-to-noise reflection energy. Table 9 outlines the remainder of the acquisition parameters.

Two sets of complete walkaway reflection data were collected on October 17. One set was recorded using 220 Hz low-cut filters and the other using 340 Hz low-cut filters (Figure 44). Two separate sets of filters were used to ensure recordable reflection energy with the highest dominant

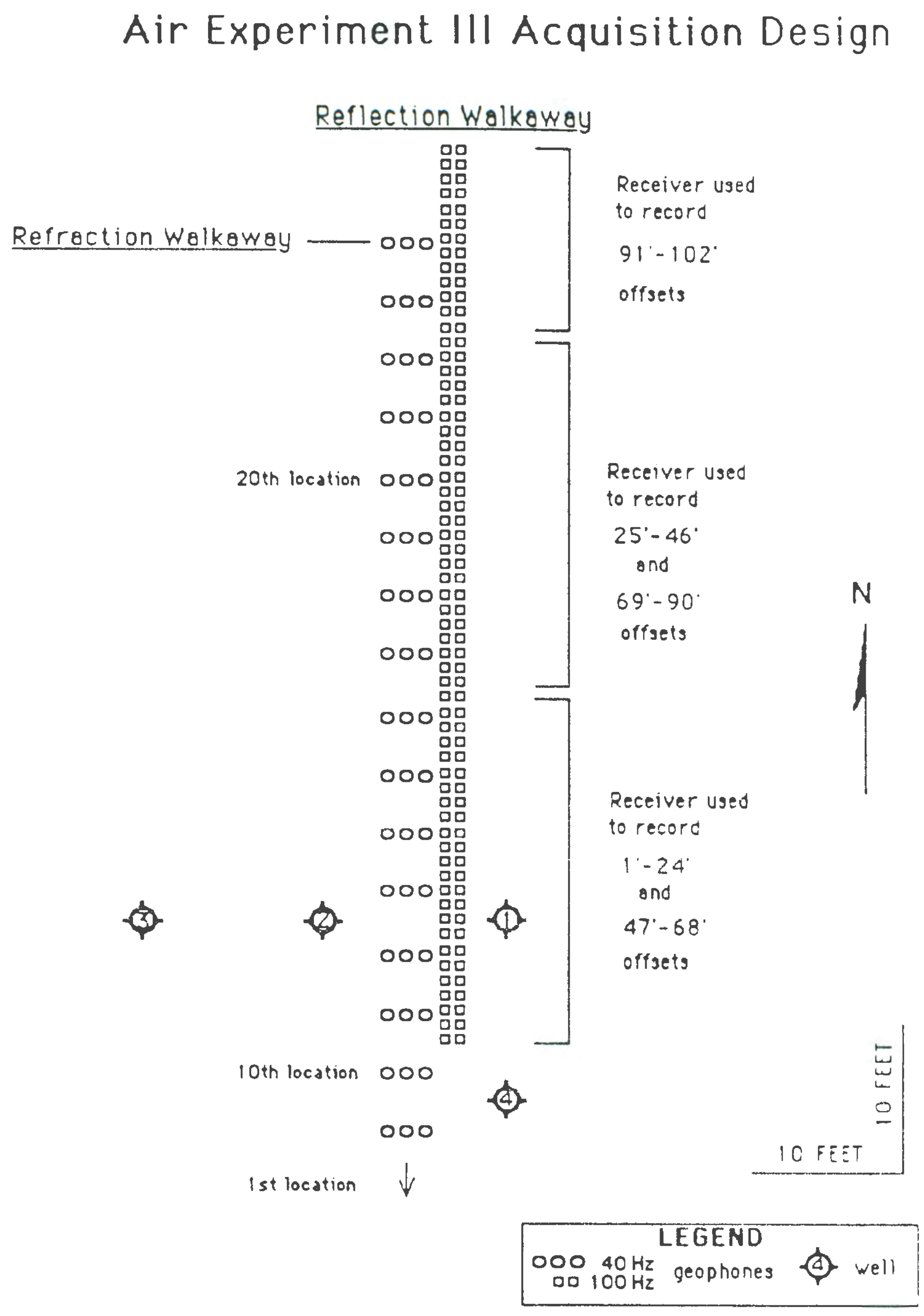

Figure 43. Receiver and well locations for Air Experiment III. Also shown are which receivers correspond to which offsets on the walkaway noise spreads.

Recording Parameters

SEISMOGRAPH (DHR 2400):	PARAMETERS
LOW-CUT FILTERS	220/340 Hz
HIGH-CUT FILTERS	none
ANTIALIAS HIGH-CUT FILTER	3000 Hz
NUMBER OF SAMPLES	500
SAMPLE INTERVAL	1/4 ms
RECORD LENGTH	125 ms
SOURCE:	**PARAMETERS**
TYPE	downhole 30.06
SPACING	walkaway
RECEIVERS:	**PARAMETERS**
TYPE (natural frequency)	100 Hz Marks Products
SPACING	1' (.30 m)
ARRAYS (connected in series)	2 geophones (grouped)
RECORDING GEOMETRY	walkaway
SOURCE-NEAR-RECEIVER DISTANCE	1' (.30 m)
SOURCE-FAR-RECEIVER DISTANCE	102' (31.1 m)
WEATHER/SOIL CONDITIONS	**PARAMETERS**
WIND SPEED	10-15 mph (4.5-6.7 m/s)
WIND DIRECTION	from NE
NEAR-SURFACE MATERIAL	soil
NEAR-SURFACE MOISTURE	moist
TEMPERATURE	45° F (7.° C)

Table 9

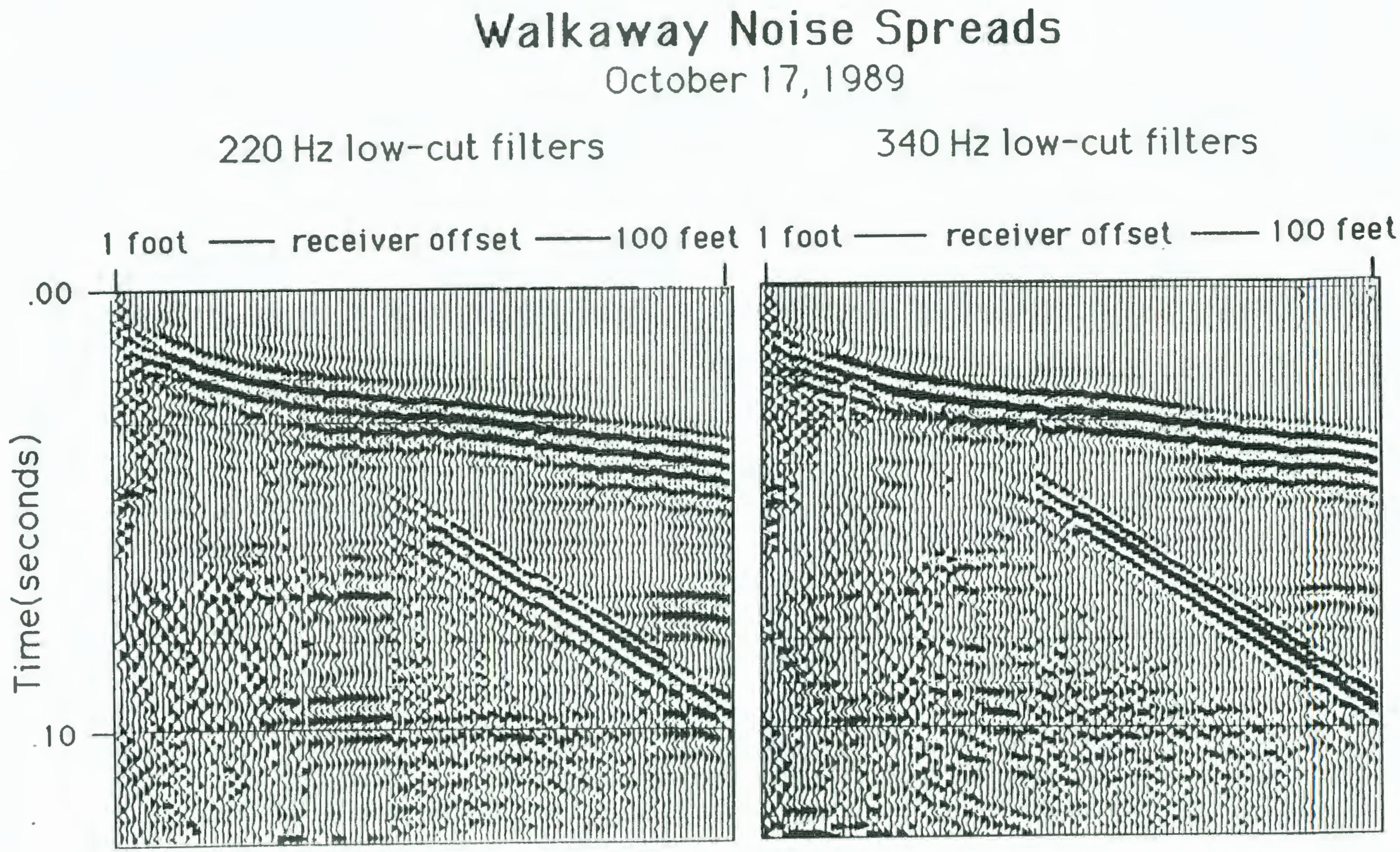

Figure 44. Walkaway noise spreads prior to air injection.

frequency. All offset and gain values were recorded to ensure duplicate experiments on successive days of air injection.

Also on October 17 a refraction data were collected parallel to the reflection walkaway (Figure 43; Table 10). The 50 caliber source was used to acquire refraction information from larger distances. Although refraction information is best recorded without low-cut filters, 40 Hz geophones and 220 Hz low-cut filters were used during acquisition so that reflection information could be used with the refraction information from this survey.

The refraction information from site 4 was taken with 10-feet (3.0-m) to over 300-feet (91-m) source-to-receiver offsets (Figure 45). The refracted arrivals do not appear to have clean breaks between them. The 5800 ft/s (1770 m/s) arrival appears to be the first break for most of the record until the 11,600 ft/s (3540 m/s) arrival that is assumed to be bedrock. No coherent reflection events could be extracted from the pre-air refraction data. There does appear to be a discontinuous reflection event between 100 ms and 110 ms.

On October 18 a 20 lb (9.1 Kg) sledge hammer and 3/4 inches (.02 m) steel plate were used as a seismic source in another walkaway noise test. A source comparison test in Chino, California, revealed that a 20 lb (9.1 Kg) sledge hammer produced higher quality reflection data than a downhole rifle source (Miller et al., 1989). The sledge hammer was tried as an alternative source, but all other acquisition parameter were identical to those used to acquire the reflection walkaways with the rifle source. The 3/4 inches (.02 m) steel plate was planted firmly in the ground before it

Recording Parameters

SEISMOGRAPH (DHR 2400):	PARAMETERS
LOW-CUT FILTERS	220 Hz
HIGH-CUT FILTERS	none
ANTIALIAS HIGH-CUT FILTER	3000 Hz
NUMBER OF SAMPLES	500
SAMPLE INTERVAL	1/4 ms
RECORD LENGTH	125 ms

SOURCE:	PARAMETERS
TYPE	downhole 50 cal
SPACING	walkaway

RECEIVERS:	PARAMETERS
TYPE (natural frequency)	40 Hz Marks Products
SPACING	4' (1.2 m)
ARRAYS (connected in series)	3 geophones (grouped)
RECORDING GEOMETRY	walkaway
SOURCE-NEAR-RECEIVER DISTANCE	10' (3.0 m)
SOURCE-FAR-RECEIVER DISTANCE	342' (104.2 m)

WEATHER/SOIL CONDITIONS	PARAMETERS
WIND SPEED	10-15 mph (4.5-6.7 m/s)
WIND DIRECTION	from NE
NEAR-SURFACE MATERIAL	soil
NEAR-SURFACE MOISTURE	moist
TEMPERATURE	45° F (7.° C)

Table 10

Walkaway Noise Spread

October 17, 1989

Refraction Test

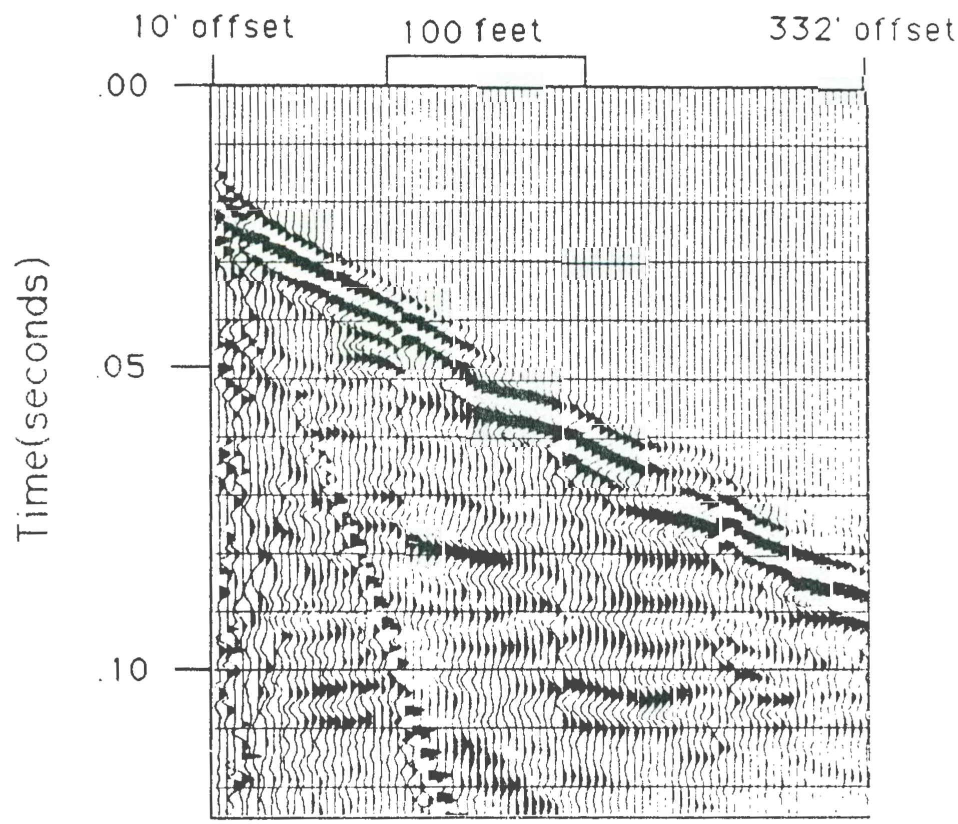

Figure 45. Notice the flattening of all first arrival information near 300' receiver offset.

was struck with the sledge hammer. The data quality using this source was much poorer than the data recorded using the rifle source (Figure 46). The highly attenuative near-surface is thought to be responsible for the poor data quality. Because the sledge hammer is a surface source, the extra distance traveled by the seismic energy in the near-surface reduces the effectiveness of the source. Because the data produced using the sledge hammer were inferior to data collected from the rifle source, the sledge hammer was not used further.

Air Experiment III

Air injection began at site 4 for the third time on October 19 at 4:20 PM. Once again a 9 cfm (.25 cmm) gas-powered air compressor was used to inject air into well 4-1. Wells 4-3 and 4-4 were monitored for water level and pressure measurements. Every 24 hours for 3 days, refraction and reflection walkaways were collected using the same parameters as the walkaways taken before air injection. During the first two days of air injection, seismic data were collected while the air compressor was operating. Before the third full day of air injection, the air compressor quit operating, and therefore the seismic data were collected without the air compressor in operation.

The reflection data collected from the three consecutive days of walkaway testing are shown in Figures 47 and 48. Figure 47 is a plot of the seismic data acquired using 220 Hz low-cut filters over a four day period; Figure 48 shows data acquired with 340 Hz low-cut filters. Once again, a time inconsistency was seen among first breaks from shot to shot and day

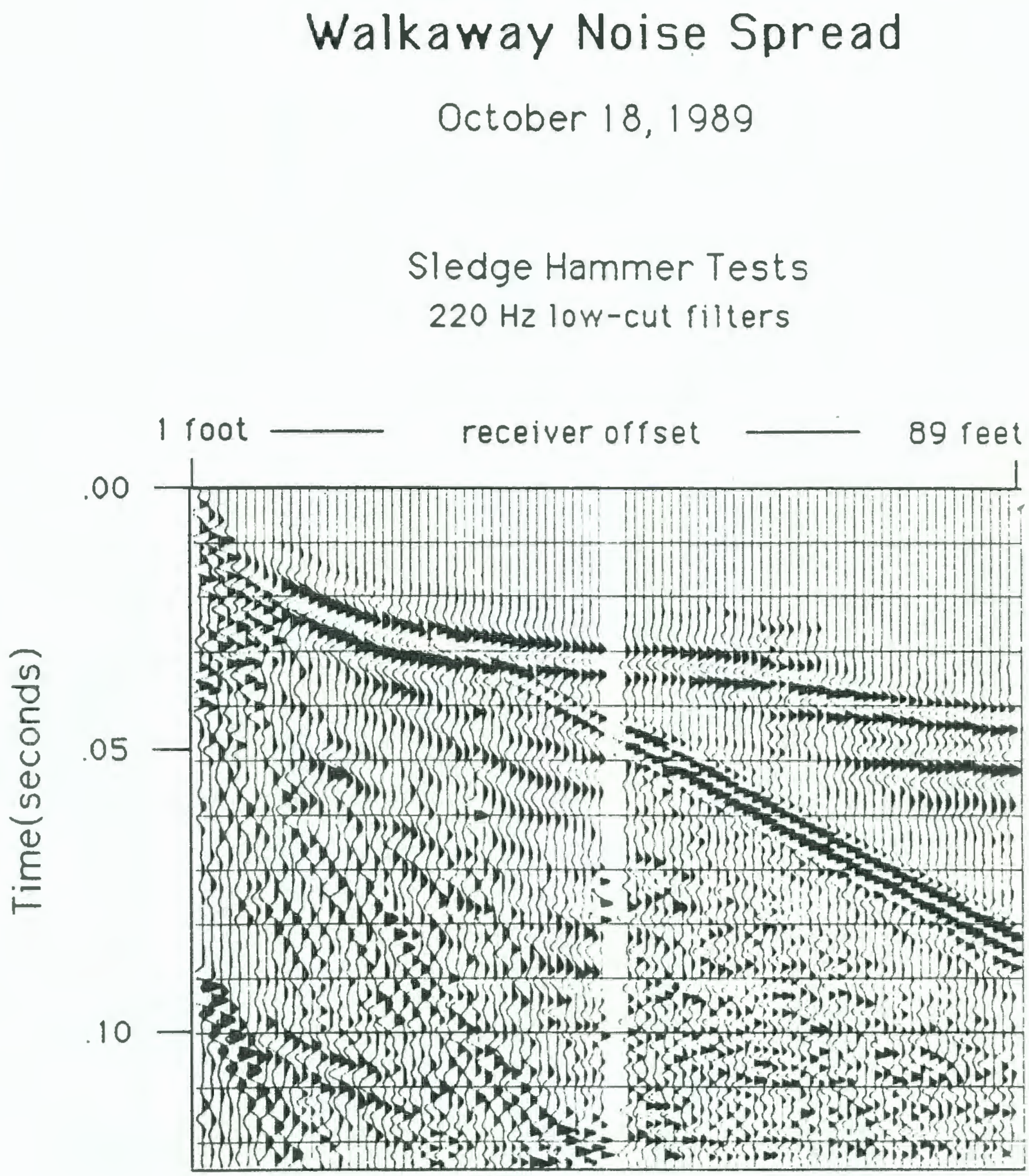

Figure 46. Notice the lack of reflection information below the air-coupled seen at 50 ms and 45 foot offset.

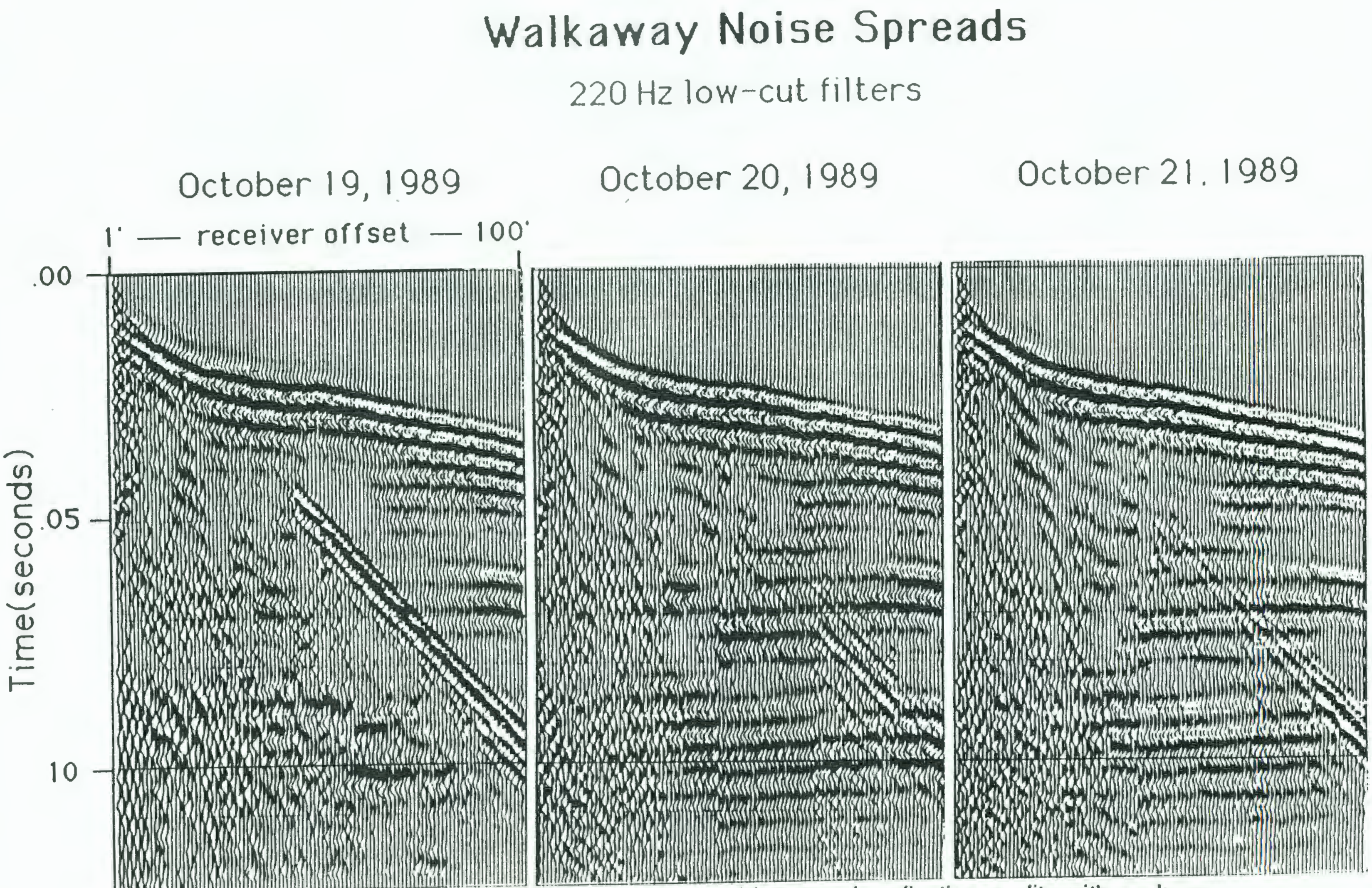

Figure 47. Notice the general increase in reflection quality with each day of air injection.

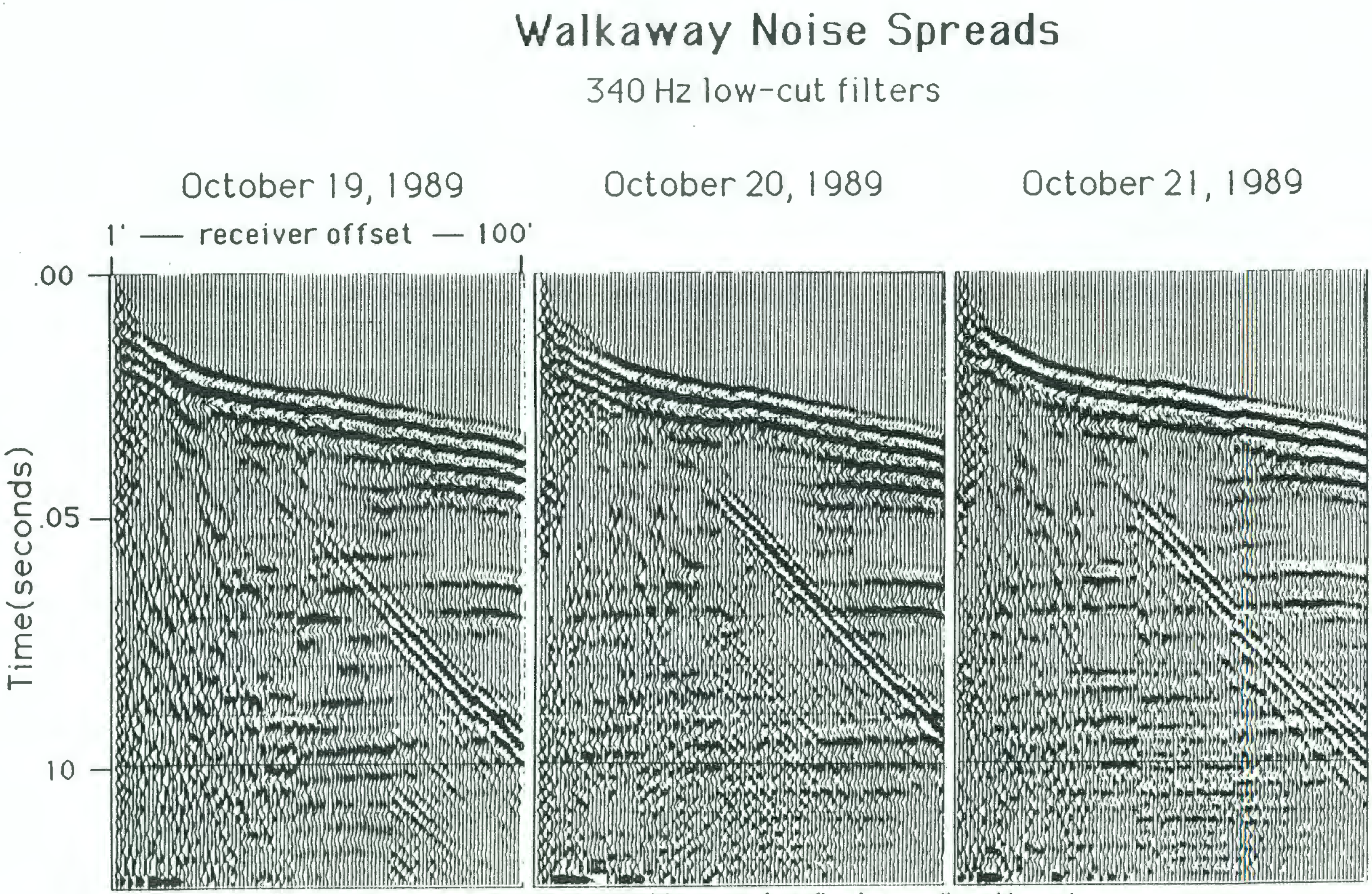

Figure 48. Notice the general increase in reflection quality with each day of air injection.

to day. Alignment of walkaways and comparisons between reflection data sets were made under the assumption that the first breaks corresponded to refraction data from above the influence of air. The most prevalent refraction across the walkaway was calculated to be 5800 ft/s (1770 m/s) from a depth of 4.5 feet (1.4 m) in air experiment I. The initial arrival time of a refraction could change between shots because of time break inconsistency or shot hole depth. However, the refraction velocity, or slope of the refraction on the walkaway, should not change if it is unaffected by air. A relative alignment of first breaks corresponding to refracted events was made so that absolute differences could be measured between reflected events.

As expected, the 220 Hz low-cut filters helped produce higher amplitude and more coherent reflection energy, whereas the 340 Hz low-cut filters produced reflection energy of higher dominant frequency. Except for the data collected one day after air injection, the overall data quality of the walkaways appears to increase with time for both data sets. However, there was still inconsistency in reflection quality from shot to shot. Random amounts of air-coupled wave amplitude were also a factor in the data quality.

In an attempt to increase the signal-to-noise ratio, F-K filtering was applied to the reflection data. An F-K filter removes linear seismic data of known velocity while maintaining other nonlinear events and linear seismic energy not found within the desired filter window (Yilmaz, 1987). Figures 49 and 50 show the affects of F-K filtering on the 220 Hz and 340 Hz

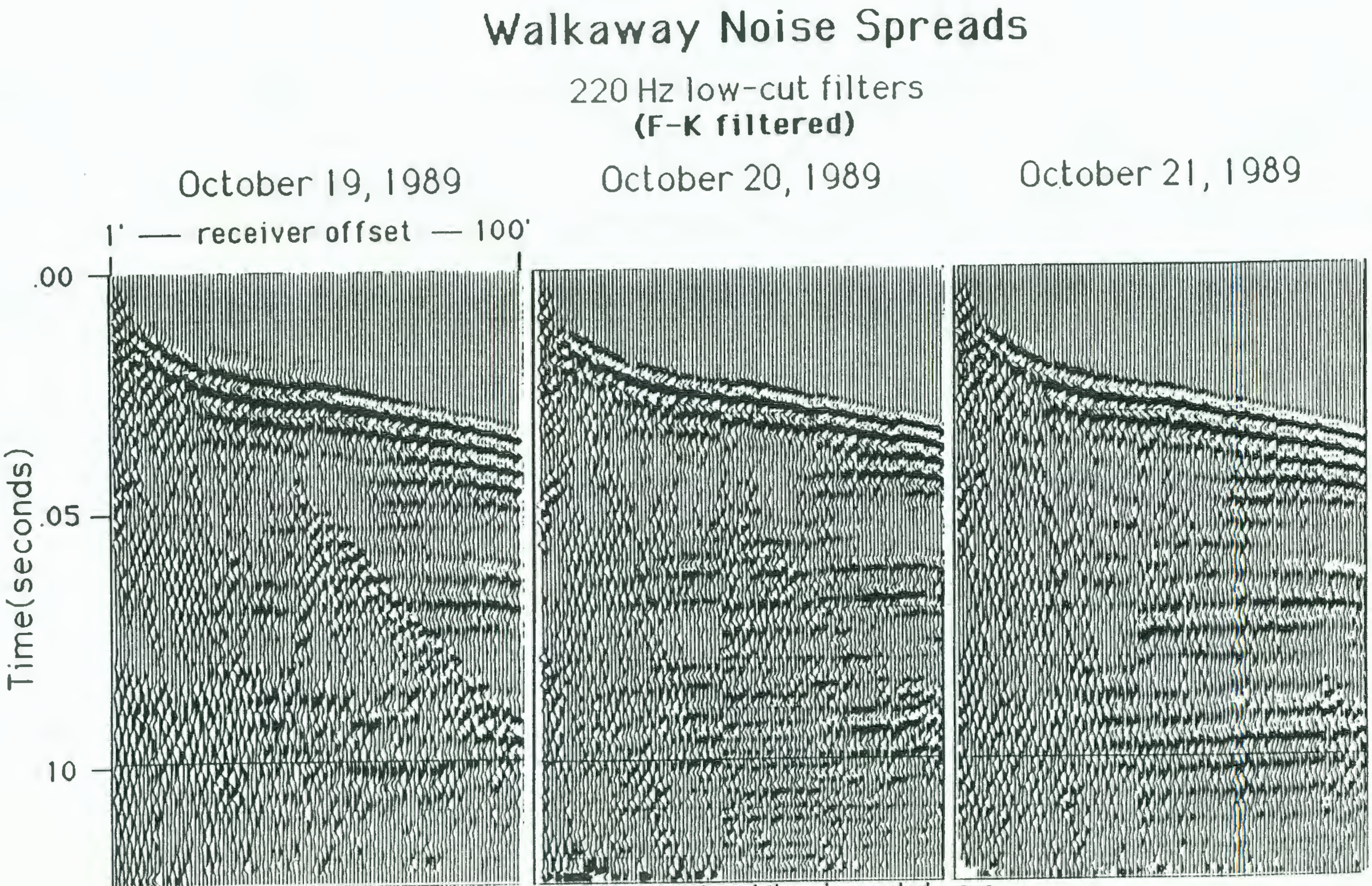

Figure 49. Notice the F-K filter reduced the air-coupled wave interference, but also degraded the reflection character.

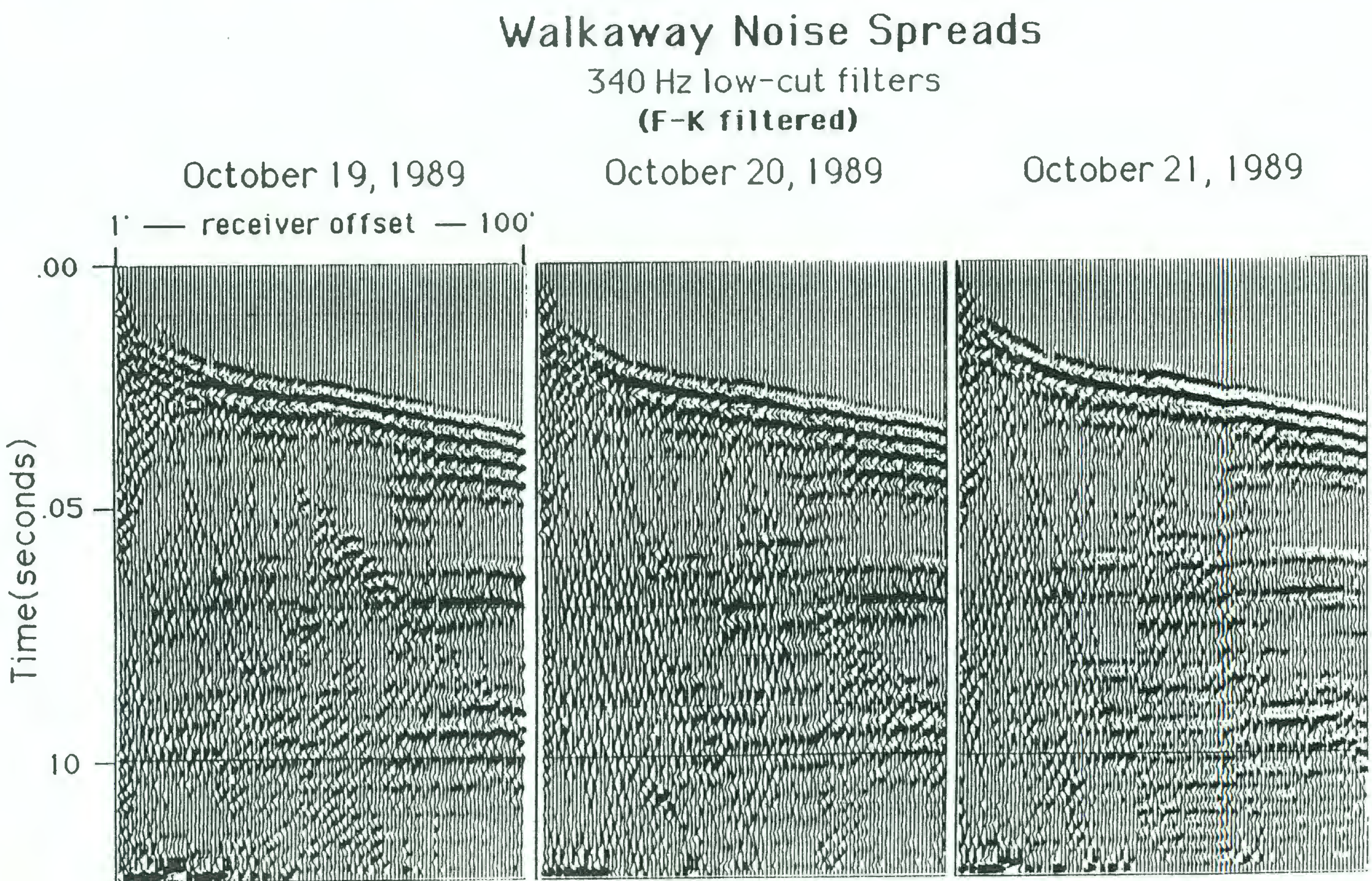

Figure 50. Notice the F-K filter reduced the air-coupled wave interference, but also degraded the reflection character.

walkaways. It is apparent that the filter worked with varying degrees of success.

A comparison of the 220 Hz and 340 Hz reflection data between the data taken after air injection and similar data taken before air injection was made. The quality of the 220 Hz low-cut data taken after the first day of air injection was actually inferior to the data taken before air injection. No arrival time differences were seen in the reflections between 60 ms and 70 ms. No other reflections were consistent enough to compare on the 220 Hz walkaways. Although the quality of the reflection data collected using the 340 Hz low-cut filters were as good as that on the first day, no change in arrival times could be detected when reflections were compared. The data quality increased in both the 220 Hz and 340 Hz low-cut filter walkaways on the second day of seismic testing. However, in both cases little change could be seen in the arrival time of the reflected events. A comparison of the seismic data from the first and last seismic data sets may show a slight time delay in reflection events. When first breaks are carefully aligned a time delay of up to 1 ms can be seen on both the 220 Hz and 340 Hz data sets from the last day of testing (Figures 51 and 52).

In addition to a possible time delay, the reflection data have many other interesting events. One of the most noticeable anomalies in the data is the dip of the reflector toward the source. The dip is most noticeable in the reflection data collected by the first 24 geophones. These receivers cross between well 4-1 and well 4-2. Although the dip could be due to a reflection off a dipping interface, it could also be due to a low velocity anomaly at those receiver locations (Figure 53). This anomaly is seen on

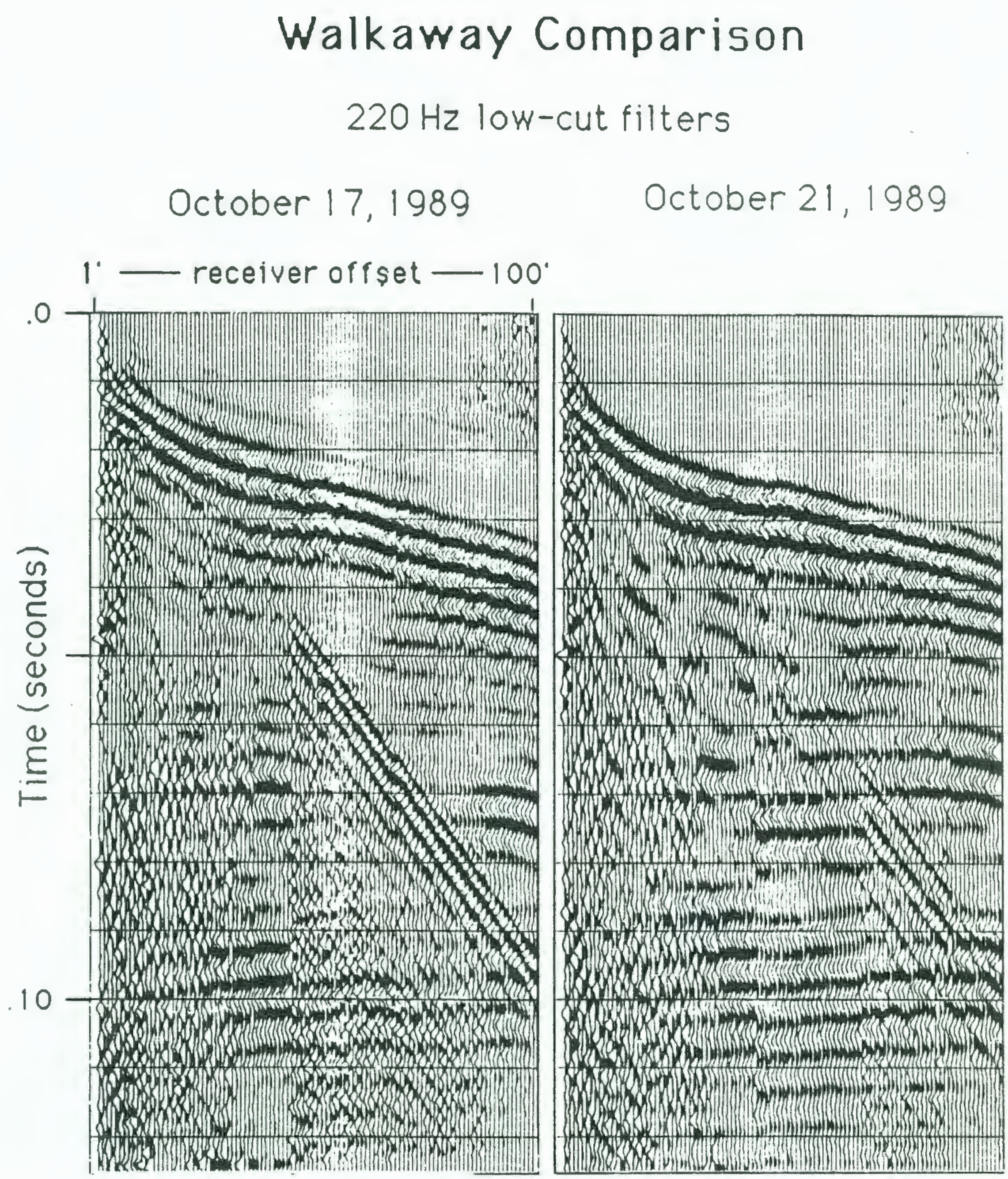

Figure 51. The post-air walkaways have been bulk-shifted to match first arrivals with the pre-air walkaways. Notice a nearly 1ms shift between comparable reflections.

Walkaway Comparison

340 Hz low-cut filters

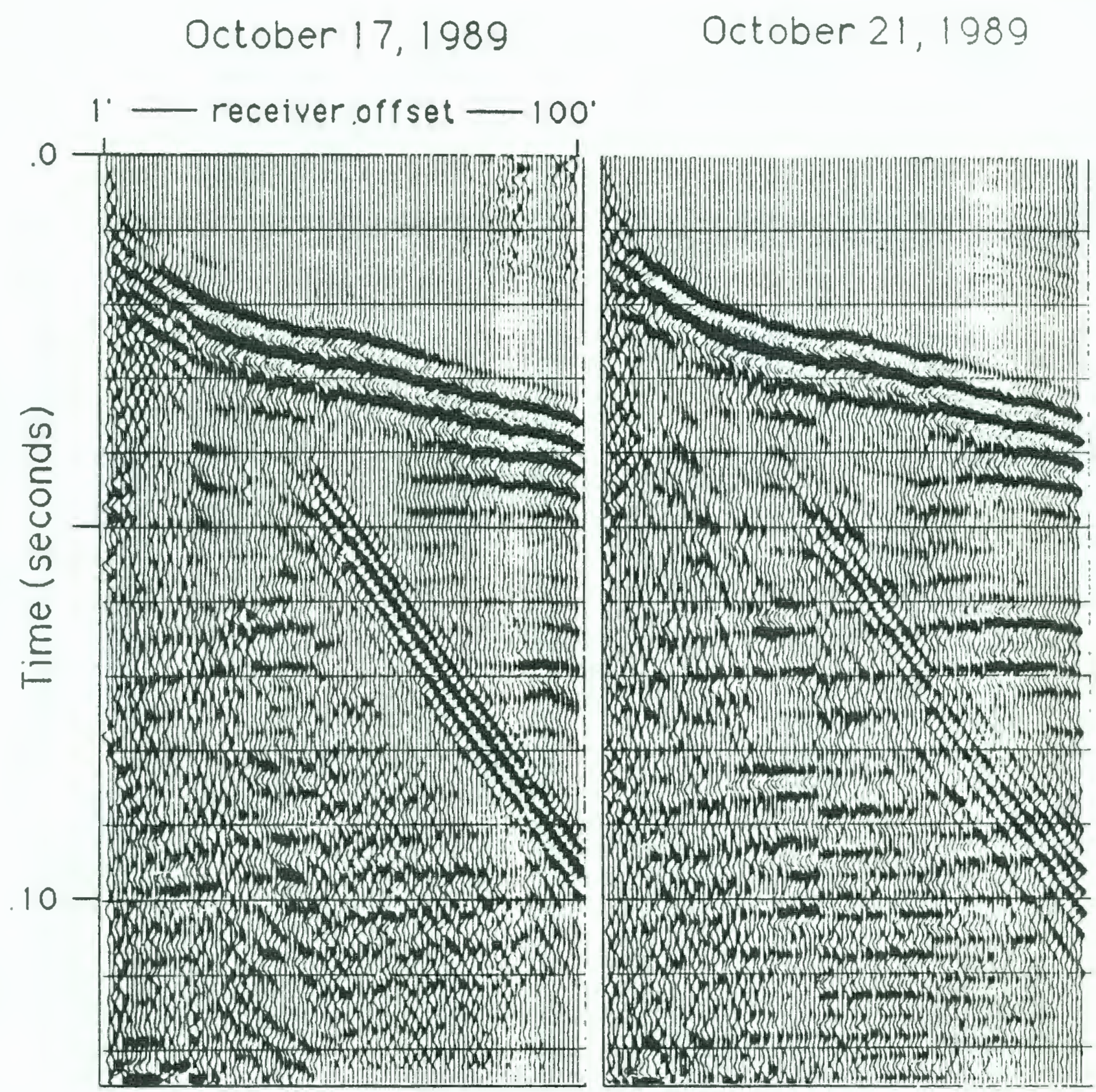

Figure 52. The post-air walkaways have been bulk-shifted to match first arrivals with the pre-air walkaways. Notice a nearly 1ms shift between comparable reflections.

Walkaway Noise Spread

October 19, 1989

340 Hz low-cut filters

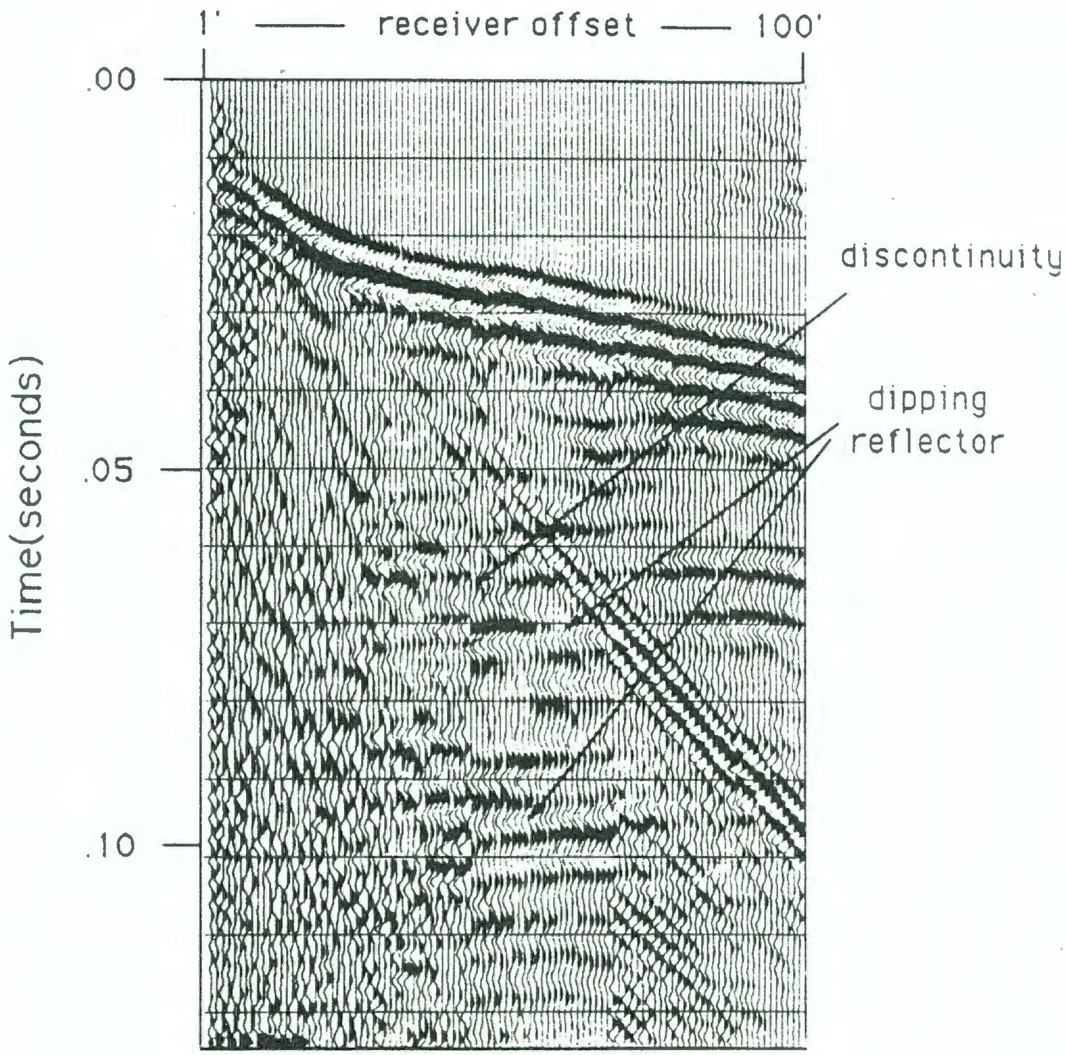

Figure 53. This figure clearly shows a discontinuity within reflected arrivals near the center of the figure. Also seen is the dip of the reflector toward the source.

both the data taken before and after air injection. Another noticeable event seen on these walkaways is seen near the center of the walkaways (Figure 53). This discontinuity is thought to be due to shot static occurring because of a different near-surface velocity structure under the second shot hole.

The refraction data sets were analyzed determine whether there was any time delay among the refracted arrivals. None of the four refraction data sets was significantly different in time arrivals. In fact, the refraction walkaway taken before air injection and the walkaway taken the last day are almost identical (Figure 54). Coherent reflection events were not seen on any of the walkaway files collected during this experiment.

Error Analysis

Because the differences in arrival time between pre-air and post-air data were small or nonexistent, the amount of experimental error in the acquisition of the seismic became important. Time break consistency, consistency of the difference in time between the refracted and reflected arrivals and between reflected events exhibiting frequency and phase changes, were all noted as possible forms of error.

To obtain a statistical base from which to derive these error calculations, another walkaway noise spread was run on November 7 at site 4. The walkaway line consisted of only the first 24 receivers but was otherwise similar to the walkaway used to collect reflection information during the third air experiment (Figure 43). In this experiment, four holes were drilled 2 feet (.6 m) apart, 80 feet (24.3 m) from the first receiver. At each

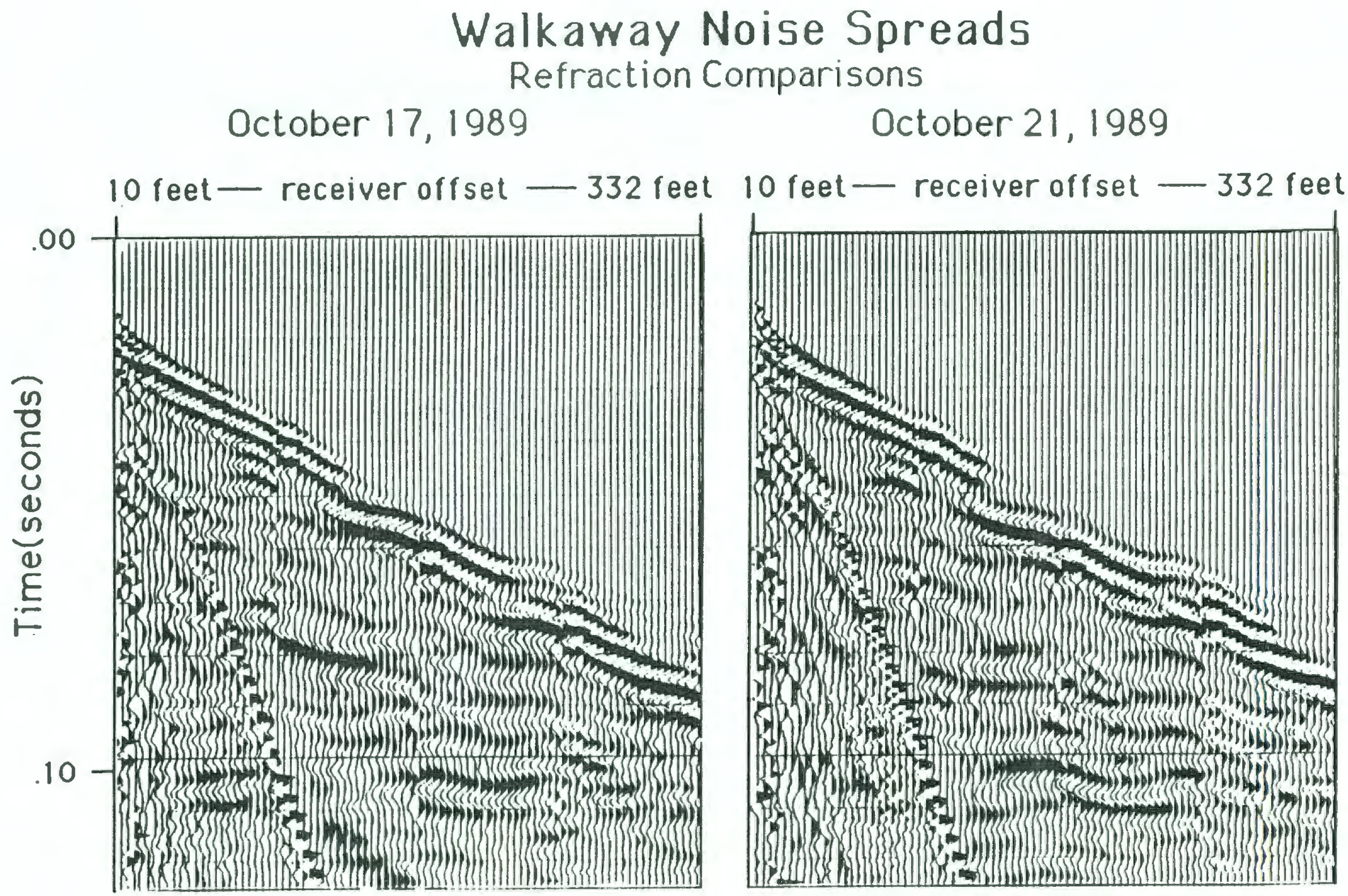

Figure 54. This figure is a comparison of the refraction walkaway taken prior to air injection and the walkaway from the third day of air injection.

location, 30 shots were fired in each hole. Every shot fired was recorded using the same gain and filter settings. Consequently, the only variable between successive shots was the source.

The first error analysis was made to determine error in time break. This was done by looking at the 120 field files collected during the November 7 walkaways and at over 300 other CDP field files taken from all the air experiments from site 4. The data were displayed at the largest scale and in the best possible form to view the air-coupled wave. A consistent phase was picked on each field file. Then a best fit line was sketched in along that phase (Figure 55). Each slope created by the best-fit line was then measured and inverted to find the velocity of the air-coupled wave. The velocities were then averaged with the data set with which they were acquired. Next, the standard deviation was calculated to find points of nonrandom error. Any velocity values found outside the third standard deviation were recalculated. A filter was then applied to account for poorly drawn lines, wind, and small changes in shot and receiver locations in the CDP data collection. One sample, 1/4 ms, was added and subtracted from the arrival time of the air-coupled wave on the field record in each particular data set nearest the average air-coupled wave velocity calculated earlier. The two sloped lines formed using the new arrival times would convert into velocities that were above and below (±) the mean by a certain number of feet per second. Only those field records that had velocities that fell within the range of ± values were kept for analysis. All other field files were assumed to have too much error not associated with the time break arrival to be used. Because

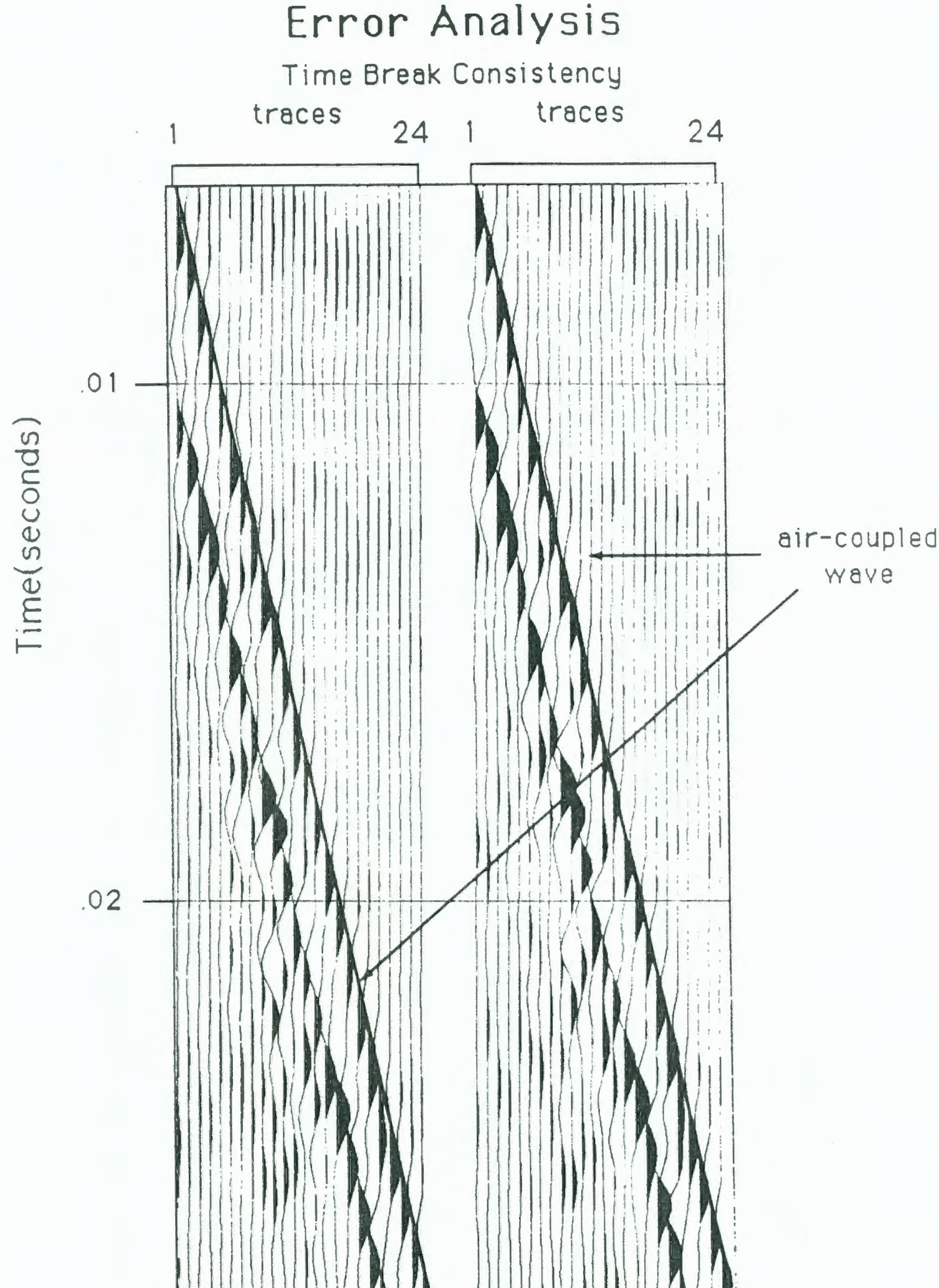

Figure 55. Consistent phase pick for error analysis.

seismic data are discretely sampled and time is continuous, the sample interval, .25 ms, is the minimum error in this experiment regardless of precision of the measurements.

Table 11 shows the results of the air-coupled wave analysis. The time break difference in the CDP data of 1.92 ± .25 ms was much higher than the .96 ± .25 ms found from the stationary hole data. The stationary hole data may in fact be the best measure of time break consistency because the source and receivers were never moved. Even so, the error calculation made from the CDP lines may have merit in measuring consistency of absolute timing of events from CDP field files.

The second error analysis was made to calculate the difference in arrival times between the first-break refracted arrival and a specific phase location of a reflection arriving at a later time. The purpose of this analysis was to substantiate whether refracted arrivals could be used as time references for reflection comparisons. On each of the field files collected on November 7, the eighth and twentieth traces were marked and measured. Table 12 lists the results from this experiment. The eighteenth and successive shots were also calculated separately from all 30 shots because data were not taken for air experiment III until 18 shots had been fired in each hole. The overall difference in time on trace 8 was 1.52 ± .25 ms and the overall difference in time on trace 20 was 1.20 ± .25 ms. Trace 8 and trace 20 have much lower overall differences with only the eighteenth and successive shots averaged, .83 ± .25 ms and .80 ± .25 ms respectively. It was concluded that the eighteenth and successive shots

Time-Break Error

CDP FIELD FILES	# OF FIELD FILES	DIFFERENCE(±.25 ms)
50 CAL 1' SP (before air)	11	1.2 ms
50 CAL 1' SP (after air)	4	1.4 ms
50 CAL 4' SP (before air)	3	.6 ms
30.06 6" SP (before air)	25	1.7 ms
30.06 6" SP (after air)	30	2.1 ms
30.06 1' SP (before air)	18	2.5 ms
30.06 1' SP (after air)	13	2.2 ms
	total 104	average(weighted) 1.92 ms

ERROR ANAL. FF'S	# OF FIELD FILES	DIFFERENCE(±.25 ms)
HOLE #1 1' SP	19	.6 ms
HOLE #2 1' SP	18	.6 ms
HOLE #3 1' SP	17	1.2 ms
HOLE #4 1' SP	21	1.4 ms
	total 75	average(weighted) .96 ms

	# OF FIELD FILES	DIFFERENCE(±.25 ms)
CDP FIELD FILES	104	1.92 ms
ERROR ANALYSIS FF'S	75	.96 ms
	total 179	average(weighted) 1.52 ms

Table 11

Reflection/Refraction Difference

Trace 8

FIELD FILES(all)	# OF FIELD FILES	DIFFERENCE(±.25 ms)
HOLE #1	28	1.8 ms
HOLE #2	28	1.9 ms
HOLE #3	29	1.0 ms
HOLE #4	27	1.4 ms
	total 112	average(weighted) 1.52 ms

FIELD FILES(18&up)	# OF FIELD FILES	DIFFERENCE(±.25 ms)
HOLE #1	13	.5 ms
HOLE #2	13	1.6 ms
HOLE #3	13	.5 ms
HOLE #4	12	.7 ms
	total 51	average(weighted) .83 ms

Trace 20

FIELD FILES(all)	# OF FIELD FILES	DIFFERENCE(±.25 ms)
HOLE #1	28	1.1 ms
HOLE #2	28	1.8 ms
HOLE #3	29	1.0 ms
HOLE #4	27	.9 ms
	total 112	average(weighted) 1.20 ms

FIELD FILES(18&up)	# OF FIELD FILES	DIFFERENCE(±.25 ms)
HOLE #1	13	.6 ms
HOLE #2	13	1.1 ms
HOLE #3	13	.6 ms
HOLE #4	12	.9 ms
	total 51	average(weighted) .80 ms

Table 12

would be used for the total error calculation in order to correlate to air experiment III acquisition procedures.

The decrease in arrival times found in earlier tests was also seen in the November 7 data. A steady decrease in travel time was seen in over half the shots taken from each of the four holes. However, after several shots the arrival times began to oscillate. The first arrivals might drop a few milliseconds over one shot and then slowly rise over many shots only to fall again.

A final error calculation was made in the frequency and phase of the November 7 data. Even if consistent phase is picked between shots, a slight change in frequency can affect the relative timing of an event. An average of all 24 traces over a 22 ms window containing only reflection information was made. A three-dimensional frequency plot of the shot number vs. frequency vs. amplitude plot is shown in Figure 56. The two distinct reflection peaks correspond to a frequency change in the middle of the field file (Figure 57). A change of only .36 ± .25 ms can be seen in the low-frequency event and almost no change in the higher-frequency event. In general, amplitude increased to near equal levels in both the 200 and 300 Hz dominant frequency events with increasing number of shots. The 300 Hz event, however, increased to its peak amplitude at a much slower rate than the 200 Hz event. The periodicity of amplitude in the shot number direction represents small changes in a shot hole when reused consistently (Figure 56). The phase remained constant as a function of frequency. Thus no error analysis was made from the phase values.

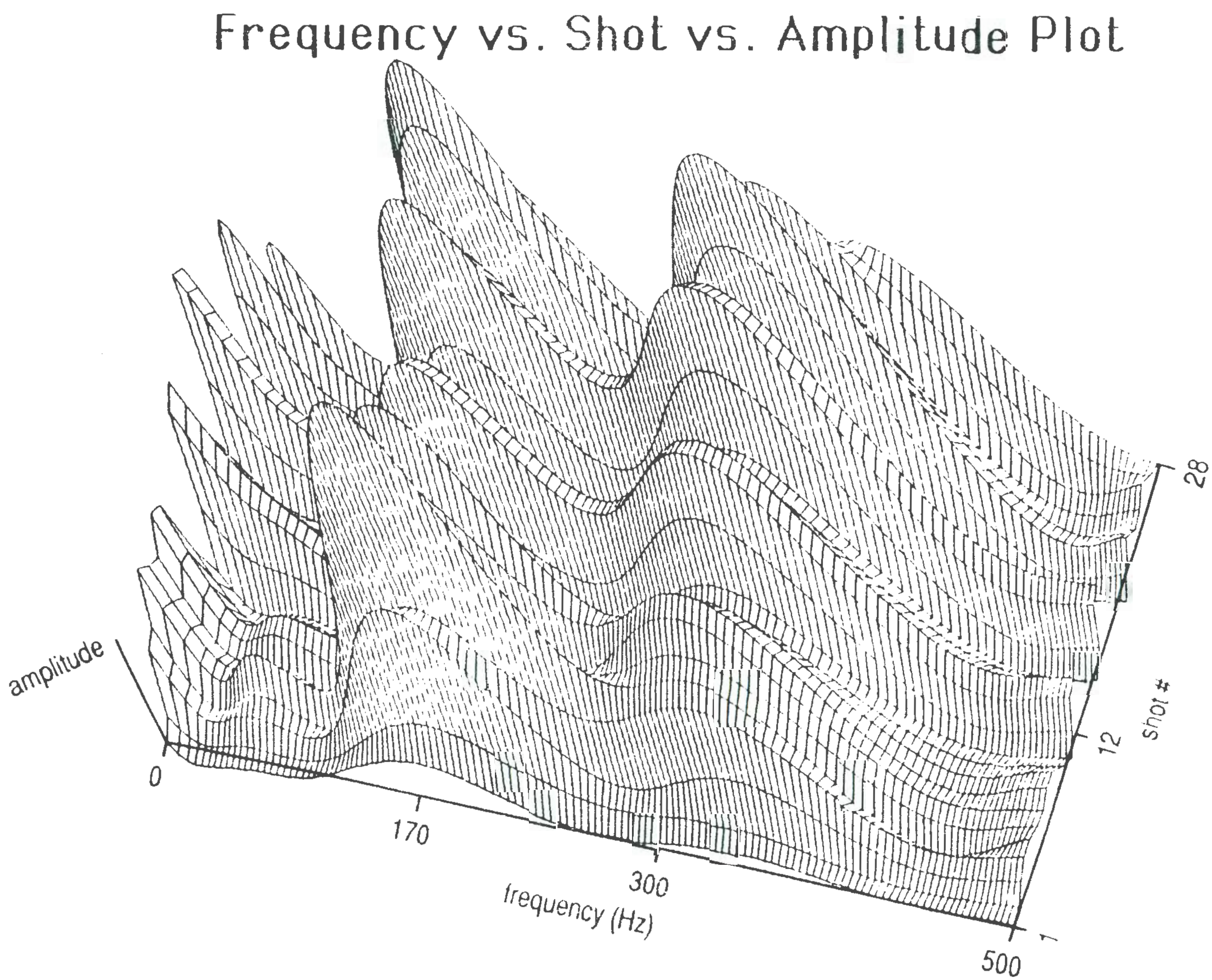

Figure 56. The frequency information below 45 Hz is not usuable.

Field File

November 9, 1989

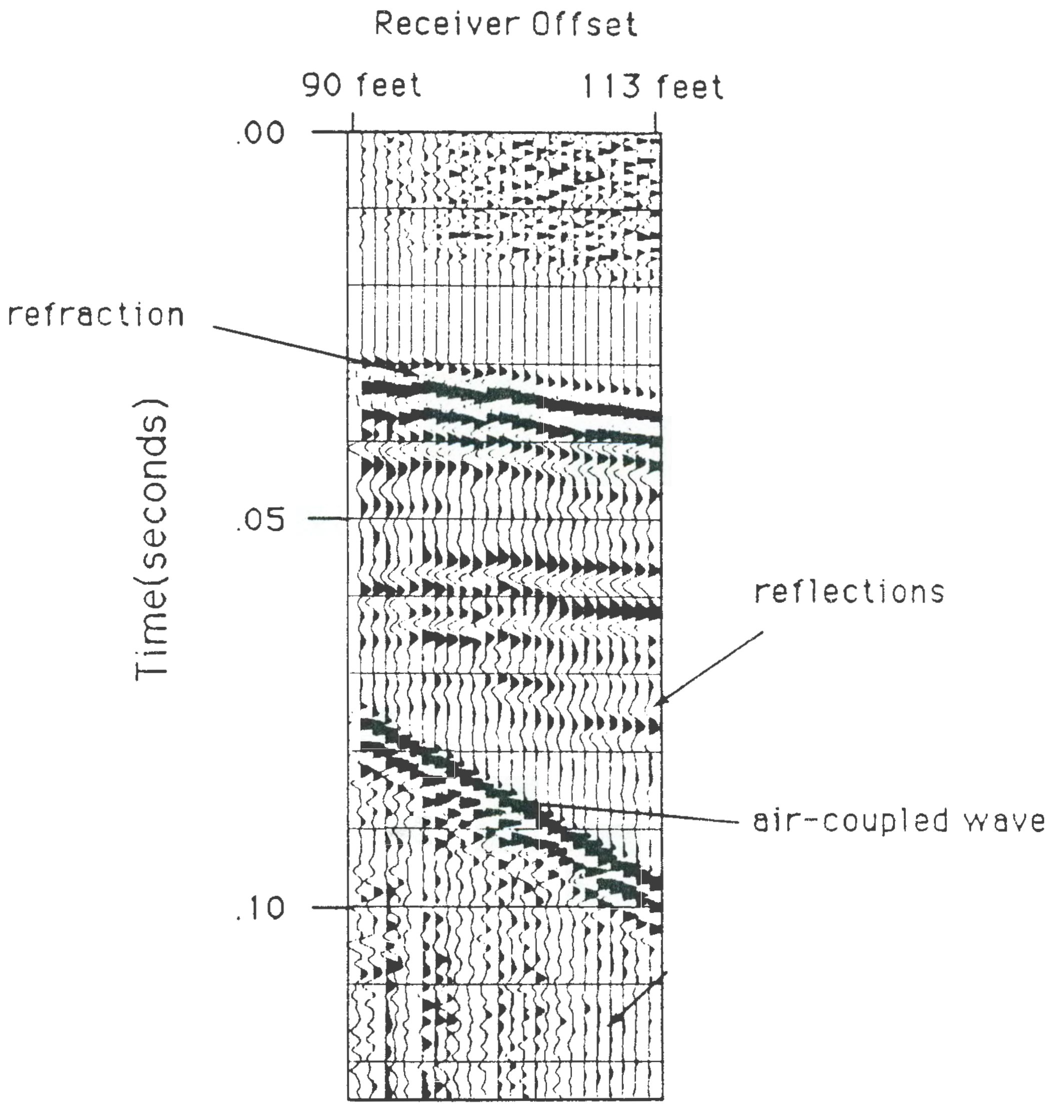

Figure 57. Notice a change from high to low frequency of the reflection wavelet with offset. This field file was recorded on the 24th shot in the same hole.

Results

The total average difference, a sum of difference results from reflection and refraction time arrivals and frequency analysis, that can be expected when comparing like reflection events is 1.16 ± .5 ms. Thus a 1 ms delay may not be due to the presence of air but to experimental error. A minimum delay of 2 ms on stationary walkaway data or nearly twice that much on CDP data would be necessary to ensure detection of air over possible comparison problems. Using the more consistent stationary data, a difference of .96 ± .25 ms can be used as the uncertainty in the time-break.

Several aspects of this experiment support conclusions made from previous experiments in this study. Multiple shots in a single shot hole produce higher quality data. This finding is similar to that in air injection experiment I, which showed that better quality data was recorded when the source was fixed in a used hole. Second, a hole that was fired in many times before data collection was more consistent than a hole that was fired in only a few times. Stationary data sets, such as walkaway noise spreads, appear to be more consistent than CDP data sets. Thus CDP data has problems associated with first break and refraction and reflection time difference problems, in addition to problems created during processing.

CONCLUSIONS

Detection of air at the Robinson tract was not feasible using the shallow reflection techniques and air injection techniques used in this study. Little evidence, quantitative or qualitative, indicated that air was affecting the seismic data. The possible time difference seen in the third air experiment is within the limits of experimental error calculated from the November 17 data set (Figure 58).

Although the purpose of using the shallow reflection technique is often to image the subsurface without detailed well control, in this instance, clear knowledge of the subsurface and how it reacts to the injection of air is necessary to truly understand the seismic results. A better explanation of the nature of the velocity structure of the near-surface and of air expansion within the aquifer is necessary before further work is attempted. Calculations of air thickness and the time difference as a result of the presence of air depend on velocities. Many more questions arise about the nature of the injected air. A few of the more important ones are:

1. Does an air pocket form?
2. If so, what are the dimensions and shape of the air pocket?
3. How does air displace the water?
4. Where does the air go after air injection ceases?
5. How does air affect the aquifer?

It is known that, after the well cap is removed from the well, air continues to return to the surface for quite some time. Therefore it is unlikely that the air is reacting with the water (solubility of air in 100 cc of

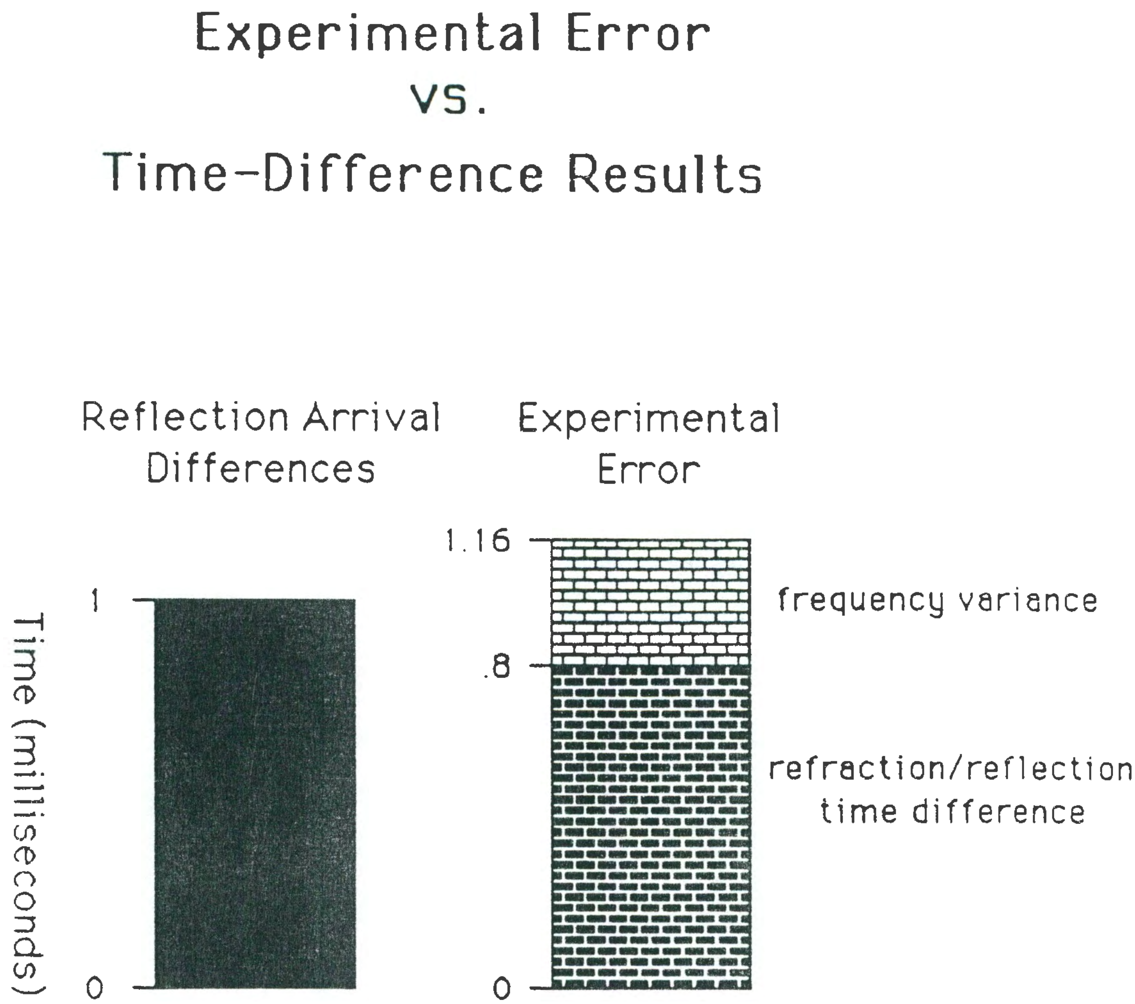

Figure 58. Graphical representation of error analysis with respect to the time-difference results from the third air experiment.

cold water is 4.98 cc). If the air was spreading in any other manner, it should have been detectable with shallow reflection.

A better understanding of many aspects of acquisition, processing, and interpretation of shallow reflection data were developed during this study. The most important are

1. A six-hundred hertz dominant frequency reflection was acquired.
2. Equipment was developed to measure water level and pressure in air-tight monitor wells.
3. Arrival times of reflections and refractions decrease with the number of shots in a hole.
4. Ground roll interference decreases and reflection quality increases with shot hole depth.
5. Surface geophones responded to reflections better than buried receivers.
6. The time break used at the Kansas Geological Survey is good to within 1 ms.
7. Air pressures of 8 PSI were maintained in the Aquifer for at least 3 days after air pumping ceased.

The most prominent result of the seismic study from the Robinson tract is the variability in the data quality. Seismic data collected over an eight month period gave widely varying results. The seismic data acquired in late March were comparable in quality to the data acquired in November. In general, the seismic data quality was best in the wetter months of the spring and fall and worst in the summer. This finding is supports the theory that saturated alluvium is more conducive to acquisition of reflection data.

REFERENCES

Birkelo, B. A., Steeples, D.W., Miller, R.D., and Sophocleous, M.S, 1987, Seismic reflection study of a shallow aquifer during a pumping test. Groundwater, v. 25., pp. 703-709.

Bradley, M.E., 1985, Practical Seismic Interpretation. International Human Resources Development Corporation, 266 pages.

Branham, K.L., and Steeples, D.W., 1988, Cavity detection using high resolution seismic reflection methods. Mining Engineering, v. 40, pp. 115-119.

Domenico, S.N., 1976, Effect of brine gas mixture on velocity in an unconsolidated sand resevoir. Geophysics, v. 41, pp. 882-894.

Fader, S.W., 1974, Ground water in the Kansas River Valley: Junction City to Kansas City, Kansas. Kansas Geological Survey Bulletin 206, map insert.

Gregory, A.R., 1976, Fluid saturation effects on dynamic elastic properties of sedimentary rocks. Geophysics, v. 41, pp. 895-921.

Knapp, R.W. and Steeples, D.W., 1986, High-resolution common-depth-point seismic reflection profiling: instrumentation. Geophyics, v. 51, pp. 276-282.

Knapp, R.W., and Steeples, D.W., 1986, High-resolution common-depth-point seismic reflection profiling: Field acquition parameter design. Geophysics, v. 51, pp. 283-294.

Mayne, W.H., 1962, Common reflection point horizontal data stacking techniques. Geophysics, v. 27, pp. 225-229.

Miller, R.D., Pullen, S.E., Steeples, D.W., and Hunter, J.A., 1990, Field comparison of shallow seismic sources near Chino, CA. Geophysics, in press.

Miller, R.D., Pullen, S.E., Waldner, J.S., and Haeni, F.P., 1986, Field comparison of shallow seismic sources. Geophysics, v. 51, pp. 1067-1092.

Miller, R.D. Steeples, D.W., and Brannan, M., 1989, Mapping a bedrock surface under dry alluvium with shallow seismic reflections. Geophysics, v. 64, pp. 1528-1534.

Myers, P.B., Miller, R.D., and Steeples, D.W., 1987, Shallow seismic reflection of the Meers fault, Commanche County, Oklahoma. Geophysical Research Letters, v. 15, pp. 749-752.

Sorenson, C.W., Sallee, K.H., and Mandel, R.D., Holocene and Pleistocene soils and geomorphic surfaces of the Kansas River Valley. Kansas Geological Survey Guidebook Series 5, pp. 93-102.

Steeples, D.W., 1979, A repeatable impulsive seismic energy source for shallow groundwater exploration. EOS, v. 160, pg. 830.

Stewart, G.F., Hilpman, P.L., Brown, D.T., and Meier, T.J., 1969, Geology of the Robinson farm, in the eastern one-half, section 8 , township 12. A report submitted to the Endowment Association, University of Kansas, 12 pages.

Treadway, J.a., Steeples, D.W., and Miller, R.D., 1985, Seismic reflections within the upper 100 feet near Borah Peak, Idaho, earthquake scarp. Techical Program Abstracts and Biography, SEG Fifty-fifth Annual Meeting, pp. 161-163.

Widess, M.B., 1973, How thin is a thin bed? Geophysics, v.38, pp. 1176-1180.

Yilmaz, O.J., 1987, Seismic Data Processing. Society of Exploration Geophysics, 526 pages.

Yu, G., 1985, Offset-amplitude variation and controlled-amplitude processing. Geophysics, v.50, pp. 2697-2708.

Zeller, D.E., 1968, Stratigraphic Succession in Kansas. Kansas Geological Survey, Bulletin 189, pg. 67.